INVESTIGATION OF MECHANISMS REGULATING LEUKEMOGENESIS USING MOUSE XENOGRAFT MODELS OF HUMAN ACUTE MYELOID LEUKEMIA

Inauguraldissertation

zur

Erlangung der Würde eines Doktors der Philosophie

vorgelegt der

Philosophisch-Naturwissenschaftlichen Fakultät

der Universität Basel

von

Anna Maria Paczulla

Deutschland

Basel, 2018

Genehmigt von der Philosophisch-Naturwissenschaftlichen Fakultät
auf Antrag von

Faculty representative:	Prof. Dr. Markus Affolter
Dissertation supervisor:	Prof. Dr. Claudia Lengerke
Co-Referee:	Prof. Dr. Jürg Schwaller

Basel, 22.05.2018

Prof. Dr. Martin Spiess

Acknowledgements

I want to thank everyone who supported me during all the way from my studies to finally finish my PhD. In particular, I would like to thank:

My supervisor Prof. Dr. Claudia Lengerke, who gave me the opportunity to start my scientific career as a student in her lab, which resulted in this PhD thesis. She always helped, encouraged and motivated me and shared her knowledge and expertise, while at the same time letting me develop my own ideas and way.

Many thanks also to Prof. Jürg Schwaller and Prof. Markus Affolter for being part of my PhD Committee, for giving me input and support during this time and of course for evaluating this work. Prof. Mihaela Zavolan for being the Chair during my defense.

I would like to say 'thank you' to all the collaborators who provided assistance and help: Prof. Helmut Salih and Kathrin Rothfelder at the University of Tuebingen for patient samples and our collaboration work on unraveling the immune escape mechanisms of leukemia stem cells. Prof. Stephan Dirnhofer and Prof. Leticia Quintanilla-Martinez for help with the histopathology, our animal facility team led by Ulrich Schneider and Nicole Meier for the great care-taking of my mice and the flow cytometry team for all the long sorting days at Department of Biomedicine in Basel. Dr. Pontus Lundberg for his help with the Next Generation Sequencing. Prof. Ivan Martin, Paul Bourgine and in particular Thibaut Klein for the great work on the *ex vivo* expansion of hematopoietic stem cells.

All members of Lab 202 at the Department of Biomedicine in Basel who provided a great atmosphere with nice breaks and funny moments in the lab: Marwa, Morgane, Maria, Max, Annaïse and all members of the EXPH and CHLK teams.

Of course, I would like to thank our *Stem Cell and Hematopoiesis* lab for an amazing time and all the support: Hui, Joëlle, Marcelle and Maike, Thorsten, Chris and Pauline. But especially Martina, who was there from the first moment I started. She had always time to discuss my results, she encouraged me, when nothing was working, she gave me new ideas and finally she was also proofreading this thesis.

Meinen besten Freunden Viola und Patrik für die Unterstützung, das Zuhören und die Bestärkung während der gesamten Zeit.

Und natürlich meinem Freund Steffen, der die letzten zwei harten Jahre immer an meiner Seite war, mich unterstützte und so unglaublich viel Verständnis aufbrachte.

Aber besonders auch meinen beiden Schwestern, Alexandra und Agathe, die mich stets ermutigten und aufmunterten, wenn es einmal schwierig wurde und mir immer ein Lächeln auf die Lippen zaubern konnten. Und schließlich geht der größte Dank an meine Eltern – einfach für alles!! Denn ohne sie wäre dies nicht möglich gewesen…

Abbreviations

AGM	Aorto-gonado-mesonephros
ALL	Acute lymphoid leukemia
AML	Acute myeloid leukemia
APL	Acute promyelocytic leukemia
AR	Adrenergic receptor
BM	Bone marrow
BMP	Bone morphogenetic protein
cAMP	Cyclic Adenosine Monophosphate
CB	Cord blood
CD	Cluster of differentiation
CDX	Caudal-type homeobox gene
Ce	Ceramic
CFU	Colony-forming unit
CFSE	Carboxyfluorescin succinimidyl ester
CLL-1	C-type lectin-like molecule 1
CML	Chronic myelogenous leukemia
CSC	Cancer stem cell
CXCR4	C-X-C chemokine receptor type 4
DKK-1	Dickkopf-1
DMSO	Dimethyl sulfoxide
DNA	Deoxyribonucleic acid
DNMT3A	DNA-methyltransferase 3A
ECM	Extracellular matrix
ELISA	Enzyme-linked Immunosorbent Assay
ELN	European Leukemia Net
EMP	Erythroid-myeloid progression
EMT	Epithelial-mesenchymal transition
eN	Engineered niche
ER	Endoplasmatic reticulum

ESC	Embryonic stem cell
EVI-1	Ecotropic virus integration site 1
FAB	French-American-British
FLT3-ITD	Fms-like tyrosine kinase 3
GM-CSF	Granulocyte-mocrophage colony-stimulating factor
GPR56	G protein-coupled receptor 56
GSK3	Glycogen synthase kinase 3
hIPSCs	Human induced pluripotent stem cells
HSC	Hematopoietic stem cells
HSPCs	Hematopoietic stem and progenitor cells
i.f.	Intrafemoral
IFN-γ	Interferon-gamma
IL	Interleukin
Inv	Inversion
ITD	Internal tandem duplication
i.v.	Intravenous
KLF4	Kruppel-like factor 4
LEF	Lymphoid-enhancer factor
LIC	Leukemia-initiating cell
LiCl	Lithium chloride
LSC	Leukemia stem cell
LT-HSC	Long-term hematopoietic stem cell
M-CSF	Macrophage colony-stimulating factor
MHC	Major Histocompatibility complex
MLL	Mixed lineage leukemia
MLP	Multipotent lymphoid progenitor
MPP	Multipotent progenitor
MRD	Minimal residual disease
mRNA	Messenger ribonucleic acid
MSC	Mesenchymal stem cell
NGS	Next generation sequencing

NK cell	Natural killer cell
NKG2DL	NKG2D ligand
NOD	Non-obese diabetic
NSG	NOD/SCID/IL2Rγ^{null}
OM	Osteogenic medium
PARP1	Poly-ADP-ribose polymerase 1
Pax3	Paired box gene 3
PB	Peripheral blood
PBMCs	Peripheral blood mononuclear cells
PD-L1	Programmed death ligand 1
PKA	Protein kinase A
PM	Proliferative medium
PML-RARα	Promyelocytic leukemia-retinoic acid receptor alpha
pNKC	Polyclonal NK cell
qRT-PCR	Quantitative Real-Time polymerase chain reaction
RAS	Rat sarcoma
RNA	Ribonucleic acid
RUNX1	Runt-related transcription factor 1
SCF	Stem cell factor
SCID	Severe combined immunodeficiency
SDF1	Stromal cell-derived factor 1
shRNA	Short-hairpin ribonucleic acid
SOX2	Sex determining region Y-box 2
TPO	Thrombopoietin
Tx	Transplantation
ULBP	UL16 binding protein
ZT	Zeitgeber

Summary

Acute myeloid leukemia (AML) is a malignant neoplasia of the blood system and can occur in people at all ages but more frequently affects people older than 65 years. Although the outlook for patients with AML has improved over the past decades, still more than half of young adult and about 90% of elderly patients die from their disease. The main obstacles to cure are refractoriness to initial induction treatment and, more frequently, relapse after apparent remission. From a cellular perspective, relapse is thought to occur from rare cell populations of so-called "leukemia stem cells" (LSCs) which share molecular and functional features with their healthy counterparts, the hematopoietic stem cells (HSCs). Because they underlie complex regulatory mechanisms, particularly also involving other cell types and niches, LSCs need to be studied *in vivo*. For human LSCs, such studies are confined to xenotransplantation models, which usually are performed in immunosuppressed mice.

In this thesis, a better understanding of human AML was built up by (1) establishing and improving a stable xenotransplantation model, (2) by identifying a novel LSC marker based on the concept of immune escape and (3) by unraveling novel non-cell autonomous pro-leukemogenic mechanisms involving BM niche and healthy hematopoietic stem and progenitor cells (HSPCs) modulation by CDX2 expressing leukemic cells. Lastly, we use an *ex vivo* 3-dimensional niche surrogate for expansion of healthy HSPCs.

Firstly, an improved transplantation protocol of human AML cells into immunosuppressed NOD/SCID/IL2Rγ^{null} (NSG) mice that mimics the clinical course of the disease in patients was established. In this model, the latency of AML cell engraftment in mice depends on molecular risk groups established in patients and xenogeneic leukemic cells show conserved genetic and phenotypic features. Most importantly, the model enables the engraftment of favorable risk AML subtypes previously considered non-engraftable in NSG mice, opening up new perspectives for *in vivo* studies on these disease subtypes. We further optimized this model by observing that transplantation at night or under enhanced catecholamine activity favors homing and adhesion of leukemic cells to BM niches, thereby shortening time-to-leukemia *in vivo*.

Next, this model was used for mechanistic *in vivo* studies on leukemia initiation. In close collaboration with the immunology research group led by Prof. Helmut Salih (University of Tuebingen, Germany), NKG2D-associated immune privilege was identified as a feature of human AML LSCs. These find-

ings offer a novel method for LSC isolation in several subtypes of AML and demonstrate in functional assays an unrecognized and targetable mechanism for sensitizing LSCs to immune control.

Furthermore, our studies on the transcription factor *CDX2*, which is expressed in >80% of AML but not detectable in healthy HSPCs, unraveled a novel non-cell-autonomous role by which *CDX2* promotes leukemogenesis, namely via DKK1 secretion to outcompete resident healthy HSPCs, which indicates treatment with *WNT* agonists as potential strategy to treat incipient AML (e.g. AML at minimal residual disease stage).

Last, as part of a collaborative project with the research group led by Prof. Ivan Martin (Department of Biomedicine, University of Basel), an *ex vivo* BM niche surrogate system was analyzed for its potential to expand and analyze healthy cord-blood derived HSPCs *in vitro*, which could also be adapted to recapitulate pathological situations as leukemia. This could represent a powerful tool with wide range of applications, from the identification of factors deregulating niche or blood functions, to the screening of drugs to predict patient-specific response to defined treatments without using xenotransplantation models.

Table of Contents

Chapter 1.

LIST OF PUBLICATIONS

1.1 For this thesis relevant publications and manuscripts (attached)

1.1.1 Long-term observation reveals high-frequency engraftment of human acute myeloid leukemia in immunodeficient mice

Paczulla A.M., Dirnhofer S., Konantz M., Medinger M., Salih H.R., Rothfelder K., Tsakiris D.A., Passweg J.R., Lundberg P., and Lengerke C. Haematologica 102, 854-864 (2017)

1.1.2 Absence of NKG2D ligands defines human leukaemia stem cells and mediates their immune evasion

Paczulla A.M.*, Rothfelder K.*, Raffel S.*, Konantz M., Steinbacher J., Schaefer T., Wang H, Dörfel D., Falcone M., Nievergall E., Tandler C., Lutz C., Lundberg P., Kanz L., Quintanilla-Martinez L., Steinle A., Trumpp A.*, Salih H.R.,*, and Lengerke C.*, *submitted* in Nature Medicine

1.1.3 Biometric engineering of a functional ex vivo human hematopoietic niche

Bourgine P.E., Klein T., **Paczulla A.M.**, Shimizu T., Kunz L., Kokkalliaris K.D., Coutu D.L., Lengerke C., Skoda R.C., Schroeder T., Martin I., Proc Natl Acad Sci U S A. 2018 Jun 19;115(25)

1.2 More publications (not attached)

1.2.1 Evaluation of stem cell properties in human ovarian carcinoma cells using multi and single cell-based spheres assay

Wang H., **Paczulla A.M**., Lengerke C., J Vis Exp., e52259

1.2.2 Molecular and functional interactions between AKT and SOX2 in breast carcinoma

Schaefer T.*, Wang H.*, Mir P., Konantz M., Pereboom T.C., **Paczulla A.M**., Merz B., Fehm T., Perner S., Rothfuss O.C., Kanz L., Schulze-Osthoff K., Lengerke C. Oncotarget 6, 43540-43556 (2015)

1.2.3 Prominent Oncogenic Roles of EVI1 in Breast Carcinoma

Wang H., Schaefer T., Konantz M., Braun M., Varga Z., **Paczulla A.M.**, Reich S., Jacob F., Perner S., Moch H., Fehm T.N., Kanz L., Schukze-Osthoff K., Lengerke C. Cancer Research 77, 2148-2160 (2017)

1.2.4 *In vitro* Tumorigenic assay: The Tumor Spheres Assay

Wang H., **Paczulla A.M**., Konantz M., and Lengerke C. Methods Mol Biol 1692, 77-87 (2018)

1.3 Manuscript in preparation

Non cell-autonomous pro-leukemogenic roles of CDX2 in AML

Paczulla A.M. *et al,* manuscript in preparation

Chapter 2.

CONTRIBUTION TO PUBLICATIONS

2.1 "Long-term observation reveals high-frequency engraftment of human acute myeloid leukemia in immunodeficient mice"

In this publication, I performed and designed all experiments except for the immunohistochemistry (performed by Stephan Dirnhofer) and the next generation sequencing (performed by P. Lundberg). I analysed the data with the help of Stephan Dirnhofer, Martina Konantz, Pontus Lundberg and Claudia Lengerke. Michael Medinger, Helmut R. Salih, Kathrin Rothfelder, Dimitrios A. Tsakiris and Jakob R. Passweg contributed patient samples or critical reagents. Martina Konantz provided critical input to the manuscript and critical help with the design of the figures. Claudia Lengerke and I conceived and developed the study and methodology and wrote the manuscript.

2.2 "Absence of NKG2D ligands defines human leukaemia stem cells and mediates their immune evasion"

I designed and performed all functional experiments involving *in vitro* and *in vivo* treatments of human AML cells and subsequent analysis of NKG2DL expression (shown in Figures 2 and 4, Extended Data Figures 8, 9, 10, 13, 17 and 19, as well as Supplementary Figures 6-7 of the manuscript), with exception of the *in vitro* 5-azacytidine treatments shown in Extended Data Figure 10a which were performed by Kathrin Rothfelder at the University of Tuebingen. Furthermore, I performed the *in vitro* colony forming assays and the morphological analyses with sorted human AML cells as well as further phenotypic characterization regarding LSC markers (shown in Figures 1, 2 and 3, Extended Data Figures 2, 3, 6 and Supplementary Figure 5) and all *in vivo* experiments shown in Figures 1-4, Extended Data Figures 8, 13 and 19, as well as Supplementary Figure 1 and 5. Of note, NK cells used in the experiments shown in Figures 2 and 4 were generated in Tuebingen by Kathrin Rothfelder and then transported to Basel to be used in experiments. Simon Raffel and Mattia Falcone performed RNAseq analyses shown in Figure 1q and 4a, Simon Raffel, and Eva Nievergall performed the *in vivo* experiments shown in Supplementary Figure 2 and in part in Figure 1i (only for BM). The Western blots were performed by Hui Wang and Thorsten Schaefer after I performed the cell sorting into NKG2DL^{pos} and NKG2DL^{neg} cells. For the microarray analyses AML cells sorted by Julia Steinbacher and me were used and analysis performed by the company IMGM. Kathrin Rothfelder performed analyses

of NKG2DL expression in the AML cohort, performed experiments involving NK cell generation, 5-azacytidine treatments, shedding analysis and collected clinical data on the patients together with Daniela Dörfel and Claudia Tandler and performed statistical analyses on associations between NKG2DL expression and patient' characteristics. Martina Konantz contributed to the bioinformatical analysis on gene expression and RNAseq data sets, performed qRT-PCR experiments together with Hui Wang. Pontus Lundberg performed the next generation sequencing analysis. Helmut R. Salih, Lothar Kanz, Christoph Lutz provided access to clinical samples and purified cells. Leticia Quintanilla-Martinez performed mouse histopathological analyses. Alexander Steinle provided critical reagents for NKG2DL analysis. Data analysis was performed by me, Kathrin Rothfelder, Simon Raffel, Martina Konantz, Julia Steinbacher, Hui Wang, Thorsten Schäfer, Daniela Dörfel, Mattia Falcone, Pontus Lundberg, Leticia Quintanilla-Martinez, Helmut Salih and Claudia Lengerke. The figures were designed by me and Martina Konantz, with the help of Kathrin Rothfelder, Simon Raffel, Helmut Salih and Andreas Trumpp. Andreas Trumpp contributed to the study design and co-supervised the study. The study was conceived and supervised, and the manuscript written by Claudia Lengerke (as led author) and Helmut Salih. All authors critically reviewed the manuscript.

2.3 "Biometric engineering of a functional ex vivo human hematopoietic niche"

In this project I designed, performed as well as analysed the *in vivo* mouse experiments. Paul E. Bourgine, Thibaut Klein and Ivan Martin conceived the study. Paul E. Bourgine, Thibaut Klein, Takafumi Shimizu, Leo Kunz, Konstantinos D. Kokkalliaris, Daniel L. Coutu and I analysed the data. Paul E. Bourgine, Timm Schroeder, Ivan Martin and Thibaut Klein wrote the manuscript and I helped with proofreading. Timm Schroeder, Ivan Martin, Radek C. Skoda and Claudia Lengerke contributed to the resources.

CHAPTER 3.

INTRODUCTION

3.1 Human Acute Myeloid Leukemia

3.1.1 Clinical perspective

Acute myeloid leukemia (AML) is defined as malignant disease of hematopoietic stem and/or progenitor cells (HSPCs) of the myeloid lineage characterized by uncontrolled proliferation and accumulation of leukemic blasts in the bone marrow (BM), peripheral blood (PB) and other organs (Ferrara and Schiffer, 2013; Greim et al., 2014). AML is the most common type of acute leukemia in adults and can occur at all ages but affects more frequently elderly people, where it mainly progresses with an aggressive clinical course (Herrmann et al., 2012; Juliusson et al., 2009; Mrózek et al., 2012). Although the outlook for patients with AML has improved over the past decades, still more than half of young adults and about 90% of elderly patients die from their disease. The main challenges to cure AML are the missing response to initial induction therapy and, more frequently, relapse after first remission (occurring from low numbers of leukemic cells able to survive chemotherapy, the so-called leukemic stem cells) (Ferrara and Schiffer, 2013). If no therapy is given to AML patients, this leads to death which may result from infection, bleeding or organ infiltration (Gutierrez and Romero-Oliva, 2013). From a molecular perspective, AML is a heterogeneous disease, showing a great genetic and phenotypic variety (Faber et al., 2013). Genes found mutated in AML are grouped in three classes: (1) genes that confer growth advantages by activating downstream effectors of various signaling pathways (e.g. RAS), (2) genes that impair differentiation by modulating expression of key transcriptional targets (e.g. RUNX1, MLL) and (3) a third category comprising mutations in genes thought to act via epigenetic mechanisms (e.g. DNMT3A), which has been added more recently. A significant amount of AML cases is associated with nonrandom chromosomal translocations, the most common being t(15;17)/PML-RARα, t(8;21)/AML1-ETO, inv(16)/core binding factor (CBF)b-MYH11, 11q23 and mixed lineage leukemia (MLL)-fusion proteins as well as FLT3-ITD (Mrózek et al., 2012). The molecular background strongly affects outcome and clinical prognosis in AML, which is however furthermore dependent on patient-related factors (e.g. age, fitness and comorbidities affecting treatment choice) (Herrmann et al., 2012).

3.1.2 AML characteristics and classification

Molecular and cytogenetic criteria have been shown to predict AML aggressiveness in patients. The European LeukaemiaNet (ELN) uses these for the classification of adult AML into favorable, intermediate and adverse risk groups (Döhner et al., 2017). The French-British-American (FAB) classification further categorizes AML according to morphological criteria. Analyses correlating molecular characteristics with patient survival resulted in the definition of molecular favorable, intermediate and poor risk groups that can predict survival (Figure 1) (Mrózek et al., 2012). Of note, there are also survival differences between younger and elderly patients of the same ELN molecular risk group (Figure 1A younger and Figure 1B elderly patients) (Mrózek et al., 2012). These are on the one hand due to patient-related factors (e.g. lower tolerance of intensive chemotherapy and higher transplant-related adverse effects in elderly compared to younger patients due to more advanced age and/or comorbidities). But on the other hand perhaps also due to disease-specific differences, since in elderly patients AML initiates in more aged, and perhaps genetically pre-damaged and instable HSPCs, and evolves in close interaction with a more aged microenvironment and immune system (Silva et al., 2017).

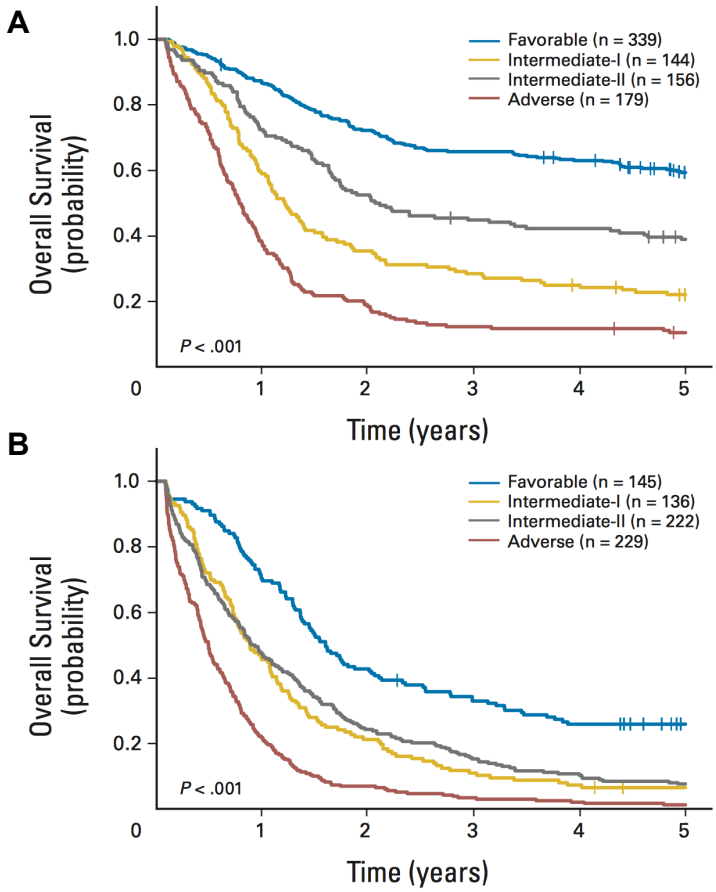

Figure 1: Molecular risk group classification predicts human AML aggressiveness in patients. Probability of patient survival stratified by ELN molecular risk group in younger (<60y; **A**) and elderly (>60y; **B**) patients (Mrózek et al., 2012).

Importantly, this molecular classification directs the treatment choice (Döhner et al., 2017; Medinger et al., 2016a; Medinger et al., 2016b, c; Nagel et al., 2017): to achieve cure, patients with favorable risk AML e.g. receive intensive chemotherapy alone. Intermediate or adverse risk AML patients are at higher risk for relapse with such therapies and, whenever possible, additionally receive stem cell transplantation – which leads to enhanced therapy-related mortality and morbidity.

Although molecular criteria have significantly improved prognostication and therefore also AML patient stratification and risk-based treatment, a full risk prediction is still not available. Further parameters are needed to better stratify patients and personalize treatment towards a targeted therapy for each patient. Especially within the intermediate risk group, which represents ~40-50% of *de novo* AML (Mrózek et al., 2012), there is high variability with respect to clinical course, and additional methods of stratification are urgently sought.

3.1.3 Leukemia stem cells and the hallmarks of cancer

The cancer stem cell (CSC) hypothesis postulates the existence of a subpopulation within each neoplasm, the cancer stem cells, which possess both the ability to undergo self-renewal and to differentiate into all types of cells reconstituting the heterogeneity of the original tumor. Furthermore, CSCs are considered to better survive chemotherapy and lead to subsequent relapse (Hanahan and Weinberg, 2000, 2011). Therefore, further characterization of CSC compartments and identification of targeted therapies capable to kill CSCs, not only mature tumor cells, has been proposed as major research goal. Thus, the oncogenic transformation leading to the generation of malignant self-renewing cells, the so-called leukemic stem cells (LSCs), is one key event in leukemogenesis. In AML, a hierarchical organization was described among malignant cells: on the one hand, there are more mature cells that undergo apoptosis after a variable number of cell divisions and on the other hand, there are immature primitive cells with self-renewing and leukemia propagating capacity (Bonnet and Dick, 1997; Herrmann et al., 2012; Hope et al., 2004; Lapidot et al., 1994; Schulenburg et al., 2010).

3.1.3.1 Classical LSC markers

Several studies focused on the identification of CSC markers in different tumor entities including solid tumors and leukemias. In AML, for example, this is very challenging since most of these antigens are also broadly expressed on various mesenchymal and healthy hematopoietic stem and progenitor cells (HSPCs). While the exact phenotype of LSCs in AML remains still unclear, several studies suggested that the LSC population resides within the $CD34^{+}CD38^{-}$ fraction (Eppert et al., 2011; Herrmann et al., 2012; Lapidot et al., 1994). One of the first studies to further restrict the phenotype identified CD44, an adhesion molecule that binds selectins and hyaluronic acid, as expressed in AML stem cells where it mediates homing, engraftment and LSC maintenance (Jin et al., 2006). Unfortunately, CD44 expression is also found on hematopoietic and non-hematopoietic stem cells, mature blood cells like monocytes, granulocytes and lymphocytes, epithelial cells and melanocytes, making it difficult to specifically distinguish and target LSCs. This is also the case for CD34 expression, which is not only found on HSCs but also on more mature progenitors as well as for example classically on endothelial cells

(Schulenburg et al., 2010). More recently, GPR56 was found to be expressed on LSCs, but not their more differentiated non-LSC counterparts in human AML (Pabst et al., 2016; Saito et al., 2013) and in a murine leukemia model (Daria et al., 2016). More markers proposed to further enrich LSCs within $CD34^{+}CD38^{-}$ populations are CD123 (IL-3 receptor alpha chain) (Jin et al., 2009), CD25 (IL-2 receptor alpha-chain) (Saito et al., 2010), CD96 (Hosen et al., 2007), CD47 (Majeti et al., 2009), CLL-1 (van Rhenen et al., 2007), CD99 (Chung et al., 2017) or TIM3 (Jan et al., 2011). Of note, in these studies markers have been characterized on top of $CD34^{+}CD38^{-}$ populations as pre-enrichment. Importantly, it has also been demonstrated that in CD34 non-expressing AML only subpopulations of leukemic cells have stem cell properties, however in this particular subtype, no reliable marker has been yet identified (Quek et al., 2016; Taussig et al., 2010).

Taken together, no leukemic stem cell specific antigen that holds true for all samples has been identified in AML so far, and especially in CD34 non-expressing AML (which correspond to ~30% of all AML) LSC markers remain elusive.

3.1.3.2 LSCs and immune escape

In their up-dated version from 2011, Hanahan & Weinberg described immune evasion as an emerging hallmark of cancer (Hanahan and Weinberg, 2011). The interactions between cancer stem cells and the immune system are however under-explored although some recent reports indicate that tumor stem cells may possess specific mechanisms of immune escape. For example, activated peripheral blood mononuclear cells (PBMCs) from patients with melanoma were shown to more efficiently inhibit tumor non-stem than stem cells via selective induction of immunosuppressive IL-10 and inhibition of stimulatory IL-2 (Schatton et al., 2010). Glioblastoma stem (but not non-stem) cells likely inhibited T cell proliferation via secretion of IL-2 and IFN-γ (Wei et al., 2010) and enhanced apoptosis of tumor-infiltrating lymphocytes via PD-L1 (programmed death ligand 1) (Dong and Chen, 2003; Hirano et al., 2005; Wei et al., 2010). In colorectal carcinoma, higher resistance towards $\gamma\delta$ T cell lysis was described in stem versus non-stem cells (Todaro et al., 2009). Finally, down-regulation of the MHC class I was reported as a mechanism impairing T cell recognition of melanoma and respectively glioma stem cells (Di Tomaso

et al., 2010; Schatton et al., 2010). According to the so-called "missing self-hypothesis", down-regulation of MHC class I expression would make these cells more amenable to NK (natural killer) cell lysis. However, NK cell activation also requires stimulation via activating NK cell receptors ("induced self") such as NKG2D: NKG2D receptors on NK cells interact with NKG2D ligands (NKG2DL) on target cells that here are induced by exposure to cell stress, viral infection or tumorigenic transformation (Lanier, 2001; Vivier et al., 2008). Expression of NKG2DL on target cells then enables their recognition and subsequent lysis by NK cells. In contrast, down-regulation of NKG2DL allows cells to escape NK cell-mediated immune surveillance. Perhaps reflecting the complex regulatory interactions between tumor (stem) and NK cells, contradictory results have been reported on tumor stem cell recognition by NK cells. Ames *et al*. e.g. report preferential NK cell mediated lysis of cancer cells carrying a stem cell phenotype in a limited number of sarcoma and pancreas carcinoma samples and one breast carcinoma cell line (Ames et al., 2015). However, Reim *et al*. showed preferential survival of $CD44^{(high)}CD24^{(low)}$ putative breast carcinoma stem cells after co-culture with NK cells, suggesting that they selectively escape NK cell attack (Reim et al., 2009).

3.2 Mouse models

3.2.1 Xenotransplantation models of hematopoietic cells

Healthy hematopoietic and also leukemic cells pursue complex interactions with other cell types making their study in an *in vivo* context mandatory. This is particularly evident in the hematopoietic system where HSPCs are tightly regulated by extrinsic signals since they need to rapidly differentiate upon demand in different functional blood cells (Goulard et al., 2018). Furthermore, HSCs need to sustain hematopoiesis throughout the life spam of an organism and therefore suppress excessive differentiation and cycling that can lead to exhaustion and facilitate DNA damage (Rossi et al., 2007). Because of the complex fine-tuned mechanisms regulating their quiescence, self-renewal and differentiation, HSCs – and also their malignant counterparts, the LSCs – are notoriously hard to cultivate and to expand *in vitro* (Morrison and Scadden, 2014; Schofield, 1978, 1983). In fact, most AML cells cultured *in vitro* undergo spontaneous cell death within a few days of culture making *in vivo* studies mandatory for longer-term assays and investigations on LSC identity.

Animal models (e.g. mice) are intensively used for such *in vivo* studies; however, mouse models of AML rely on a limited number of defined genetic events and often do not fully mimic the heterogeneity observed in primary human AML samples. An alternative approach is to study primary human cells *in vivo* by xenotransplantation of these cells into a xenogeneic (e.g. murine) environment (Lapidot et al., 1994). Over the past decades, many efforts have been made to generate most accurate xenotransplantation models in which human HSPCs or leukemic cells are successfully engrafted into immunosuppressed mice (Cosgun et al., 2014; Reinisch et al., 2016; Rongvaux et al., 2014; Sanchez et al., 2009; Shultz et al., 2005; Strowig et al., 2011; Theocharides et al., 2012).

Different animal models have been used as hosts for xenotransplantation of human AML cells. First xenotransplantation studies were performed in SCID (severe combined immunodeficiency) mice, later in NOD/SCID (non-obese diabetic/SCID) lacking B and T cells (Shultz et al., 2005), and finally in NOD/SCID/IL2Rγ^{null} (NSG) strains that additionally lack functional NK cells (Sanchez et al., 2009). Of these, NSG mice appear to enable most robust engraftment rates probably due to their high level of immunosuppression. Although human engraftment is successful, these models are still limited by remaining macrophages, which have been shown to phagocytize transplanted human cells (Theocharides et al., 2012). Additionally, there is only partial cross-reactivity between human and murine proteins (especially of cytokines required for hematopoiesis) and niche components (Mendelson and Frenette, 2014). Therefore, more recently, knock-in mice have been generated for human cytokines ("humanized mice", e.g. M-CSF, GM-CSF, TPO, SCF, IL-3) (Rongvaux et al., 2014) or for the human SIRPA gene, a receptor negatively regulating phagocytosis, in the background of immunosuppressed mouse strains (Strowig et al., 2011). Moreover, Cosgun *et al*. demonstrated in 2014 that introduction of *Kit* receptor mutations in the background of immunosuppressed mouse strains improves the engraftment of human HSPCs by inducing a defect in the endogenous hematopoietic stem cell compartment and therefore creating niche space and offering xenotransplanted cells a competitive advantage over endogenous cells (Cosgun et al., 2014). Humanized niche scaffold elements have been engineered using human stromal cells and revealed enhanced repopulation with human HSPCs when implanted into immunosuppressed mouse strains (e.g. ossicles coated with human mesenchymal stem cells (MSCs), which recently were demonstrated to enhance both

human healthy and malignant hematopoietic engraftment) (Reinisch et al., 2016).

Among others, these xenotransplantation models have indicated a hierarchical organization of human AML with the capacity of leukemia initiation, maintenance and relapse being confined to rare subpopulations of so-called leukemia initiating-cells (LICs) or leukemic stem cells (LSCs) (Eppert et al., 2011; Lapidot et al., 1994). In 1994, Lapidot *et al*. first showed engraftment of human primary AML cells in severe combined immuno-deficient (SCID) mice and described that LSCs reside in the $CD34^+CD38^-$ subpopulations within individual AML samples (Lapidot et al., 1994). More recent comprehensive analyses demonstrate high marker heterogeneity between AML samples and show that LSCs are often also found in the $CD34^+CD38^+$ compartment and also exist as $CD34^-$ cells, in so-called CD34 non-expressing AML subtypes (Quek et al., 2016; Taussig et al., 2010).

3.2.2 Factors influencing engraftment in the NSG xenotransplantation model

Next to differences depending on the used mouse strain, the efficiency of xenotransplantation assays of human healthy hematopoietic stem and progenitor cells as well as primary AML cells depends on several factors:

1. **Age of the recipient mice:** Usually 6 to 10 week old mice are used for xenotransplantation experiments of healthy $CD34^+$ hematopoietic cells. Transplantation into newborn mice (up to 3 days after birth) has been reported to be more efficient but is logistically more difficult (Traggiai et al., 2004).
2. **Gender of recipient mice:** Engraftment of healthy human $CD34^+$ cells (Notta et al., 2010) and also of human acute lymphoblastic leukemia cells (Konantz et al., 2013) is more efficient in female versus male NSG recipients.
3. **Transplanted cell dosage and cell source:** Unselected AML cells are usually transplanted at 0.5-1x10^6 cells per mouse, while LSCs enriched populations are injected at lower numbers (down to 0.5x10^5 cells). Most reports document engraftment from ~40% of transplanted primary AML samples (Eppert et al., 2011) and indicate a clear overrepresenta-

tion of aggressive molecular risk subtypes within the successfully engrafted AML samples. Higher engraftment rates (66%) were reported using increased numbers of transplanted cells ($10x10^6$ per mouse), a lower threshold for the definition of human engraftment (>0.1% human cells within murine bone marrow (BM), peripheral blood (PB) or organs) (Sanchez et al., 2009), and use of high molecular risk (e.g. FLT3-ITD mutated) subtypes (Sanchez et al., 2009).

4. **Transplantation method**: Intrafemoral (i.f.) (Mazurier et al., 2003) and intravenous (i.v.) injections are used for transplantation of human AML cells into mice. When transplanted i.f., AML cells are directly transplanted into vicinity of the BM niches. Direct injection in the liver of newborn mice, a natural site of hematopoiesis amplifying HSCs during development, was shown to further enhance HSC engraftment (Traggiai et al., 2004).
5. **Pre-conditioning of mice (e.g. irradiation)**: Sub-lethal irradiation facilitates engraftment and is commonly used in most protocols (Theocharides et al., 2016). Engraftment without prior irradiation has also been reported (e.g. (Klco et al., 2014)) and might be a better option for studying niche interactions without destroying or disturbing the healthy niche.
6. **Time point of analysis post-transplantation and threshold set to define engraftment**: Mice are mostly considered as successfully engrafted if >1% (in two reports also >0.1% (Sanchez et al., 2009; Shlush et al., 2014)) of human AML cells are detectable in the PB or the BM of mice. Across reports, mice are followed mostly for 12 and no longer than 16 weeks post-transplantation.
7. **Time-point of injection:** Depending on the number of circulating endogenous HSCs, the number of open niches varies, which follows circadian oscillations (Méndez-Ferrer et al., 2008). Correlations between time-point of injection and AML or HSPC cell homing and long-term engraftment are not yet reported and were subject of investigation in the current thesis.

3.2.3 Homing of hematopoietic cells - and the involvement of circadian rhythm and catecholamines

Homing originally describes the ability of HSCs to find their way ("home") into the BM. So far, the SDF1-CXCR4 axis was described as the main molecular regulator of HSC homing. Further analyses of this axis revealed that it follows circadian oscillations. In 2008, Méndez-Ferrer and co-workers showed that after light exposure, SDF1 protein is released from the BM while SDF1 mRNA is down-regulated; this leads to higher HSC mobilization and therefore enhanced levels of circulating HSCs, showing a peak 5 hours after light onset (Méndez-Ferrer et al., 2008). It is possible that enhanced mobilization of endogenous HSCs into the circulation might open up niche space and then facilitate repopulation with transplanted AML cells and/or HSPCs. Moreover, a link between circadian oscillations, SDF1 expression and catecholamines has been described. For example, stimulation of β2-adrenergic receptors (ARs) in osteoblasts was shown to induce clock gene expression whereas β3-AR activation results in acute SDF1 mRNA down-regulation, which are compensatory mechanisms involved in the above-mentioned circadian mechanism of HSC mobilization (Fu et al., 2005; Liu et al., 2007; Méndez-Ferrer et al., 2008).

Furthermore, Katayama and colleagues described that the sympathetic nervous system (SNS) supports normal hematopoiesis by regulating HSC egress from the BM through the action of catecholamines (Katayama et al., 2006), which therefore control the normal BM microenvironment in order to maintain a stem cell pool in the BM (Dar et al., 2011). Taken together, catecholamines play important roles in regulating hematopoietic hemostasis, but their function is not completely understood. In this regard, Spiegel and colleagues studied the interplay of catecholamines with the dynamics of human $CD34^+$ HSPC engraftment and were able to show that treatment with catecholamines indeed enhanced the engraftment in NOD-SCID mice. They explained this phenotype by their observations regarding *Wnt* signaling activation and – at the same time – an increase in endogenous HSC mobilization (Spiegel et al., 2007).

3.3 Healthy hematopoiesis

3.3.1 Blood development and hematopoietic stem cells

Hematopoiesis, the formation of blood cells, occurs during embryonic development, when primitive erythroid and myeloid cells and later on definitive HSCs are established from endothelial cells, and then throughout adulthood when blood cells are produced to maintain the blood system (Jagannathan-Bogdan and Zon, 2013). Since mature blood cells have a limited life-span and progenitor cells an expanded but eventually limited life-span, HSCs are required to sustain life-long hematopoiesis (Orkin and Zon, 2008).

In vertebrates, blood development comprises different waves of hematopoiesis. As mentioned above, the primitive wave occurs first and involves erythroid and myeloid progenitor cells formed during early embryonic development in the extra-embryonic yolk sac (Palis and Yoder, 2001) followed by a transient wave in which the so-called erythroid-myeloid progenitors (EMPs) are produced (McGrath et al., 2011). Finally, definitive hematopoiesis occurs as the last wave of developmental hematopoiesis in which HSCs are formed from endothelial cells in the aorto-gonado-mesonephros (AGM) region of the developing embryo. HSCs then relocate to the fetal liver where they undergo rapid expansion, and then, in mouse and humans, shortly before birth move to the bone marrow (BM) which is the location for HSCs and therefore the main site of hematopoiesis in adults (Cumano and Godin, 2007; Jagannathan-Bogdan and Zon, 2013; Lengerke and Daley, 2012). In each of these sites, HSC properties differ in regard to different niches supporting HSC expansion and differentiation and intrinsic characteristics of HSCs at each stage. For example, HSCs in the fetal liver are in cycle, whereas HSCs present in adult BM are mainly quiescent. In general, HSCs are at the top of the hematological hierarchy and as other stem cells, they are capable of self-renewal, meaning the production of additional HSCs, as well as differentiation into all blood cell lineages (Orkin and Zon, 2008).

A schematic overview of primitive and definitive hematopoiesis is shown in Figure 2 below.

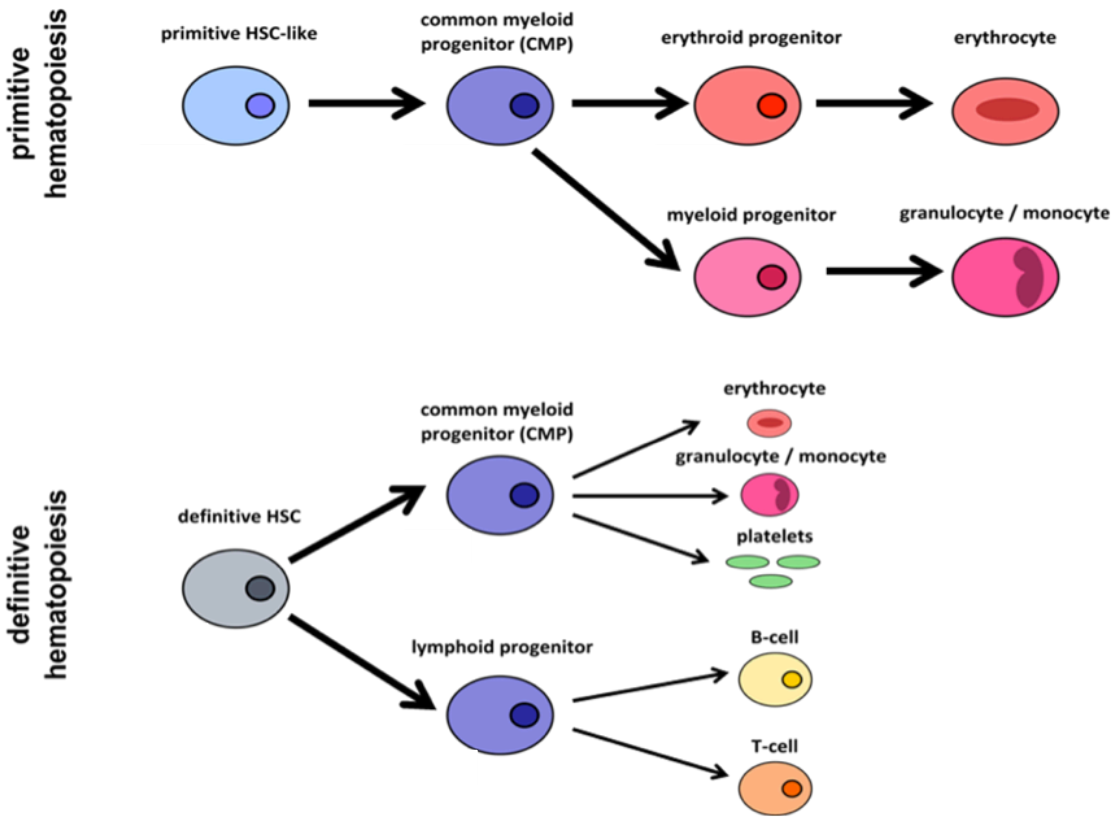

Figure 2: Simplified overview of primitive and definitive hematopoiesis. (adapted from (Jagannathan-Bogdan and Zon, 2013))

3.3.2 The caudal-related homeobox transcription factor family member 2 (CDX2)

3.3.2.1 The Cdx2-Hox axis in embryonic and adult hematopoiesis

The *Cdx* genes, homologues of the Drosophila caudal gene, are a highly conserved family of DNA-binding homeobox transcription factors classically known as regulators of axial elongation and anterior-posterior patterning during early embryogenesis (Chawengsaksophak et al., 2004). In mice and humans, the *Cdx* family consists of three members (*Cdx1*, *Cdx2* and *Cdx4*).

The first link between *cdx* genes and developmental hematopoiesis was made in zebrafish. In this model, the *kugelig (kgg)* mutant displaying defective erythropoiesis was identified as mutated in *cdx4* (Davidson et al., 2003). *cdx* genes were then demonstrated to redundantly regulate embryonic hematopoiesis via activation of downstream *hox* genes (Davidson et al., 2003;

Davidson and Zon, 2006). Furthermore, a conserved *Cdx-Hox* pathway was documented to pattern hemogenic mesoderm and blood cells from *in vitro* differentiating murine embryonic stem cells (ESCs) and human pluripotent stem cells (Lengerke et al., 2009; Lengerke et al., 2007; Lengerke et al., 2008; McKinney-Freeman et al., 2008).

Of note, only very mild decreases in clonogenic capacity were observed in *in vitro* CFU assays performed with differentiating *Cdx1*$^{-/-}$ and *Cdx4*$^{-/-}$ murine ESCs (Wang et al., 2008). Consistently, *Cdx4* knockout mice, as well as *Cdx1* knockout mice show no major defects in hematopoiesis (Jedrusik et al., 2008; Koo et al., 2010; Subramanian et al., 1995), indicating that alone, *Cdx4* and *Cdx1* are dispensable for normal adult HSC functions in mice, possibly because they are compensated by other *Cdx* genes.

In contrast to this, *Cdx2*$^{-/-}$ ESCs show more profound defects leading to perturbed expression of *Hox* genes and other genes involved in signal transduction, cell growth, proliferation and hematopoiesis (Wang et al., 2008). *Cdx2*$^{-/-}$ mice are embryonic lethal due to its essential roles in the trophoblast of the pre-implantation embryo (Chawengsaksophak et al., 1997). Studies using conditional Cre-mediated knockouts of *Cdx1* and *Cdx2* at the same time showed that these double mutants display major defects in primitive hematopoiesis as well as yolk sac vasculature (Brooke-Bisschop et al., 2017).

In the adult hematopoietic system, *Hox* genes are preferentially expressed in immature healthy stem/progenitors and in malignant hematopoietic cells. *Hoxa9*$^{-/-}$ BM cells manifest a severe defect on the level of HSCs and committed progenitors, and constitutive expression of *Hoxb4* increases self-renewal capacity of murine HSCs without initiating leukemic transformation. In contrast to this, aberrant expression of e.g. *Hoxa9* or *Hoxa10* was reported to induce myeloid leukemia in murine experimental models (Rawat et al., 2012).

3.3.2.2 *CDX* genes and their role in leukemia

In the human adult, *CDX2* expression is mainly detectable in epithelial cells of the gastro-intestinal tract, where it regulates proliferation and differentiation (James et al., 1994). In the colon, *CDX2* was involved as tumor suppressor whereas in the stomach and esophagus ectopic *CDX2* expression was linked

to the development of precancerous intestinal metaplasia (Almeida et al., 2003; Eda et al., 2003).

In 2004, Rawat and co-workers detected ectopic *CDX2* expression in t(12;13)(p13;q12) AML, and involved CDX2 as fusion partner for the ETV6 gene in this AML subtype. In a murine model, they then experimentally showed that *Cdx2* overexpression induces myeloid leukemia, as shown in mice transplanted with *Cdx2* overexpressing BM cells which then rapidly developed fatal and transplantable AML. In contrast, co-expression of *ETV6-CDX2* and *Cdx2* in BM cells showed no accelerated AML induction in transplanted mice when compared to *Cdx2* alone (Rawat et al., 2004).

Further investigations concerning the involvement of *Cdx* genes in leukemogenesis revealed *CDX2* expression in 90% of patients with AML, while no *CDX2* expression was detected in HSPCs derived from healthy individuals. In order to characterize the functional role of *CDX2* in human AML, Scholl and colleagues generated a knockdown model of *CDX2* (using shRNA) in several human AML cell lines. These experiments revealed growth inhibition and reduced clonogenicity in *CDX2* knockdown AML cell lines. Furthermore, *Cdx2* overexpression in primary murine BM resulted in an increased serial CFU formation and replating activity. Together these data suggest that activated *CDX2* expression is a frequent event in the pathogenesis of AML promoting proliferation and clonogenicity (Scholl et al., 2007). Previously, *CDX2* was shown to act as positive upstream regulator of several *HOX* genes, which were linked to leukemogenesis in humans and mice, and deregulated *HOX* gene expression characterizes more than every third case of AML. The aberrant expression of *HOXA9* and *HOXA10* is for example strongly associated with certain AML subtypes (Debernardi et al., 2003; Rawat et al., 2008). Thus, several studies examined the crosstalk between *CDX2* expression and expression of *HOX* genes. It was shown that constitutive expression of *Cdx2* dysregulates the expression of several leukemogenic *Hox* genes including *Hoxa10*, *Hoxb8*, *Hoxa6* and *Hoxb6* (Rawat et al., 2008; Scholl et al., 2007). These findings suggest that *CDX2* expression contributes to the altered *HOX* gene expression observed in many AML, and functionally link the leukemogenic potential of *Cdx2* to its ability to dysregulate *Hox* genes. Consistently, expression levels of *CDX2* and *HOX* genes were shown to closely correlate in a cohort of 115 patients with AML. Further confirming this notion, loss of the ability of *Cdx2* to perturb *Hox* gene expression – achieved by deletion of its N-terminal transac-

tivation domain – correlated with the inability of *Cdx2* to induce AML in mice (Rawat et al., 2008).

Notably, aberrant expression of *CDX2* was furthermore reported in ca. 80% of cases with B- or T-lineage acute lymphoblastic leukemia (ALL) in adult as well as pediatric patients, where high *CDX2* gene expression levels associated with poor treatment outcome and inferior overall survival (Thoene et al., 2009) (Riedt et al., 2009). Compatible with these findings, functional analyses showed that overexpression of *Cdx2* in murine BM progenitors perturbed genes involved in lymphoid development (Thoene et al., 2009). *CDX2* expression has also been found in subgroups of patients with myelodysplasia and chronic myelogenous leukemia (CML). Further analyses showed that in a low number of these patients, enhanced *CDX2* expression was associated with transit into secondary AML as well as blast and accelerated phase, respectively (Scholl et al., 2007). In contrast to data published in AML, *CDX2* expression was not found to correlate with deregulation of specific *HOX* genes in pediatric ALL (Lengerke and Daley, 2012). Another study reported *CDX2* expression in 61% of patients with *de novo* adult ALL and decrease of *CDX2* expression with complete remission and increase in relapse (Rawat et al., 2012).

Molecularly, suppression of the transcription factor *KLF4* was reported to be an important feature of the leukemogenic activity of *CDX2* in AML. Furthermore, deregulation of the *PPARγ* signaling pathway was identified as involved in *CDX2*-induced AML. Experiments using a *PPARγ* agonist revealed de-repression of *KLF4* expression to result in toxicity of *CDX2* positive leukemic cells (Faber et al., 2013).

Cdx4 was also shown to activate *Hox* genes and to induce AML in murine models, although with much longer latency. In these experiments, however, leukemia occurred in median after 300 days, suggesting that *Cdx4* by itself is insufficient to drive leukemogenesis and secondary genetic events (which remain yet uncharacterized) needed to be aquired (Bansal et al., 2006). As such, co-expression of *Cdx4* with *Meis1a*, a known *Hox* co-factor, was indeed able to accelerate leukemia induction in mice (Frohling et al., 2007).

3.3.2.3 The link between WNT signaling and CDX genes

Experiments using murine ESCs for the characterization of hematopoietic fate by activation of the *Cdx-Hox* pathway showed a link between *LEF1*, a *Wnt* effector molecule and bone morphogenic protein 4 (BMP4) as up-stream activators of the *Cdx-Hox* pathway. More clearly, when *BMP* signaling was blocked in these studies, this resulted in suppressed *Cdx1* and *Cdx4* expression and hematopoietic development. However, ectopic activation of *CDX* or *HOX* genes was able to restore hematopoietic development in the absence of upstream *BMP* and *WNT* signaling. These findings indicate that *BMP4* and WNT signaling are upstream of the *Cdx-Hox* pathway during hematopoietic development. Consistently, direct activation of the *Cdx1* promoter was reported for the Wnt effector LEF1 (Lengerke et al., 2008). Interestingly, van de Ven *et al.* later showed that in *Cdx* mutants, *Cdx* expression can be restored and phenotypic posterior defects corrected by posterior gain of function of *Lef1* (van de Ven et al., 2011), suggesting that *Wnt* signaling also acts downstream of Cdx proteins. In accordance to this, overexpression of *Cdx1* and *Cdx4* in murine ESCs was shown to induce *Wnt3a* (Lengerke et al., 2008). Furthermore, zebrafish *cdx4* expression was shown to be influenced by *Wnt* levels, however the precise underlying molecular mechanisms are not yet fully elucidated. In 2011, Ro and Dawid suggested that *tcf3* suppresses *cdx4* expression through direct binding to multiple sites in the *cdx4* gene regulatory region (Ro and Dawid, 2011). Sherwood and colleagues investigated the role of *Wnt* signaling in intestinal specification and regionalization. They showed that either genetic or chemical *Wnt* pathway activation leads to induction of *Cdx2* as an intestinal master regulator acting directly on the endoderm, which induces gene expression specific for an intestinal program (Sherwood et al., 2011). In regard to neurogenesis, decrease in *Cdx* expression in mouse *Cdx* mutants leads to progressively more severe posterior vertebral defects, but these defects could be rescued by posterior *Lef1* gain of function, indicating that *Wnt* signaling acts downstream of *Cdx* genes. The observations made by Cesca van de Ven concerning phenotype and transcriptome analysis in early *Cdx* mutants, genetic rescue experiments and gene expression analyses indicated that the *Cdx* family of transcription factors acts via *Wnt* signaling during formation of the uro-rectal mesoderm (van de Ven et al., 2011). Beyond this, in the context of neural crest development, which involves induction of *Pax3* expression by posteriorizing *Wnt* / *β-Catenin* signaling, several reports suggest a role for *Cdx* transcription factors in this process acting as intermediates between *Wnt*-mediated regulation of murine *Pax3* expression. For these experiments,

Sanchez-Ferras used embryonic carcinoma cells cultured in the presence or absence of Wnt3a-conditioned medium, which is known for activating the canonical *Wnt*-pathway (Sanchez-Ferras et al., 2012). Treatment with Wnt3a-conditioned medium resulted in rapid induction of the expression of each *Cdx* member within 2 - 4 hours. In contrast to this, *Pax3* induction was observed considerably delayed (after 18 hours) suggesting an indirect regulation by *Cdx* genes. For further characterization, experiments using the protein synthesis inhibitor CHX were performed for analysis of direct interactions between *Wnt* signaling and *Cdx* genes. *Cdx4* and *Cdx1* are known to be direct targets of the canonical *Wnt* pathway (Pilon et al., 2006; Pilon et al., 2007) and therefore *Cdx1* and *Cdx4* induction by Wnt3a-conditioned medium was not affected by inhibition of *de novo* protein synthesis. Interestingly, *Cdx2* induction was also found to be independent of *de novo* protein synthesis suggesting *Cdx2* as a direct target of *Wnt* / *β-Catenin* signaling in this model (Sanchez-Ferras et al., 2012).

In colon cancer, evidence for a functional crosstalk between *Wnt* and *Cdx* was found, since *Cdx2* was determined to cooperate with *Wnt* signaling to regulate *Claudin-1* expression in this tumor entity. Dysregulation of tight junctions is often associated with carcinogenesis and recent studies also support the role of tight junction integral proteins, such as *Claudin-1*, in the regulation of epithelial-to-mesenchymal transition (EMT). *Claudin-1* expression is highly increased in colon cancer and is associated with tumor growth and progression. In this context, Bhat and colleagues showed key roles of *Cdx1*, *Cdx2* and *Gata4* in the regulation of *claudin-1* expression, with *Cdx2* overexpression resulting in strongest *claudin-1* mRNA induction. Co-expression of activated *β-Catenin* further induced in a *Cdx2*-dependent manner up-regulation of *Claudin-1* promoter activity as measured via luciferase assays (Bhat et al., 2012).

Chapter 4.

AIM OF THIS STUDY

During the last decades the need for personalized targeted therapy in AML treatment became more evident due to further characterization of the disease regarding molecular and cytogenetic variants making their heterogeneity even more obvious. In particular, the characterization and identification of the so-called leukemic stem cells is highly important. These cells are responsible for leukemia initiation, maintenance and further relapse, and therefore have to be eradicated for making a cure possible.

The projects presented in this PhD thesis build up on these features and aim to optimize the xenotransplantation model of human AML cells into NSG mice for its further usage to study mechanistic aspects of leukemia initiation.

The obtained results promise (1) to improve xenotransplantation efficacy and enlarge the use of this model, and (2) to identify key mechanisms regulating the interaction of AML cells with their environment and thus *in vivo* leukemogenesis and (3) also to better understand intrinsic mechanisms of AML cells.

Chapter 5.

RESULTS AND DISCUSSION

5.1 Improvement of the xenotransplantation model of human AML

5.1.1 Long-term observation reveals high-frequency engraftment of human acute myeloid leukemia in immunodeficient mice

Since primary human AML cells are notoriously hard to culture *in vitro* and rely on complex interactions with the microenvironment, *in vivo* mouse models are mandatory to further study the disease. Long-term AML *in vitro* cultures are cumbersome and, besides one individual report performing such cultures (Sontakke et al., 2014), a robust protocol that can be reproducibly used by different research groups and across AML subtypes is still missing. Murine leukemia models are well established and have several advantages such as well-characterized disease and high reproducibility with respect to disease kinetics. Importantly, since these models are mostly generated by a limited number of genetic events, they cannot fully depict the human disease heterogeneity. Xenotransplantation assays into immunosuppressed mice instead enable studies with primary human cells that accommodate a wider range of genetic heterogeneity.

The first successful engraftment of primary human AML cells in mice was reported in SCID mice already in 1994 (Lapidot et al., 1994). Over the past decades, many efforts in optimizing the xenotransplantation model have been made by improving the congenic murine environment for the transplanted cells (e.g. higher immunosuppression (NSG mice), genetic knock-ins of human cytokines ("humanized mice" (Theocharides et al., 2016)) or impairment of the endogenous HSCs (kit mutation (Cosgun et al., 2014))). Nevertheless, most previously published data reported that a wide percentage of human AML (~34-60%) fail to engraft mice (Eppert et al., 2011; Sanchez et al., 2009), and thus cannot be studied *in vivo*. These studies however have pursued a limited follow-up of 12 to maximum 16 weeks post-transplantation, which are time-frames typically used to investigate the engraftment of healthy HSCs (Mazurier et al., 2003; Notta et al., 2010). In these reports, mice were analyzed at these time-points in BM and peripheral blood (PB) and if less than 1% (or respectively 0.1%) of human among murine cells were detected across all transplanted mice, the corresponding AML was scored as non-engraftable (Eppert et al., 2011; Lapidot et al., 1994; Sanchez et al., 2009). Interestingly, using this method, almost only AML samples belonging to aggressive molecular subtypes (intermediate and poor risk AML according to the ELN classification, often showing FLT3-ITD mutations) but not favorable risk AML cases

were shown to engraft (Eppert et al., 2011; Rombouts et al., 2000a; Rombouts et al., 2000b; Sanchez et al., 2009), leaving latter largely understudied *in vivo*.

In our study (Paczulla et al., 2017), we hypothesized that favorable risk AML can also successfully engraft mice, if longer observation time is provided. We transplanted leukemic cells derived from PBMCs of a mixed cohort of primary AML (n=19, among which n=4 favorable risk AML). Cells were transplanted intravenously via the tail vein or intrafemorally in preferentially sublethally irradiated but also in non-irradiated NSG mice. Animals were monitored for signs of disease and human engraftment via flow cytometry of BM biopsies taken routinely every four weeks in one mouse per each experimental group. Experiments were terminated at sickness or detection of >1% human AML among murine cells (Bonnet and Dick, 1997; Eppert et al., 2011; Lapidot et al., 1994).

Indeed, our data indicate that extending post-transplant follow-up to 1 year per se allows robust engraftment and symptomatic leukemia induction from nearly every transplanted AML sample (18/19, ~95%), including also favorable risk subtypes (e.g. inv(16), previously considered mostly non-engraftable in NSG mice). To investigate engraftment at standardized time-points used in previous studies, we additionally screened all transplanted mice for infiltration with human AML cells in the BM by performing BM puncture on anaesthetised animals. At 16 weeks post-transplantation, indeed only 7 out of 19 AML samples (~37%, termed standard engrafters) showed engraftment, confirming observations from previous studies reports (Eppert et al., 2011). However, several mice scored as non-engraftable at this time-point did develop leukemia after longer latency, as shown by analyses performed on the same animals at later time-points. As such, the median time to engraftment in our study was 22 ± 9 weeks; in the majority of cases (11 out of 19 AML, ~58%, termed long-latency engrafters) leukemic repopulation would have been missed using published protocols (Figure 3A and 3B). The fact that BM biopsies taken at 16 weeks failed to detect leukemic cells in these long latency engrafters (11/18, 61%), indicates that leukemic cells can persist *in vivo* over months at undetectable levels without losing disease-initiating properties.

Engraftment was confirmed by multi-parameter flow cytometry, histopathology and next generation sequencing (NGS) showing conserved immune phenotypes and clonal architecture in mouse-derived leukemic cells. Interestingly, time to engraftment and mouse survival were influenced by the AML molecular risk group (Figure 3C) but not by *in vitro* colony forming capacity or percentage of $CD34^{+}(CD38^{-})$ cells which both also did not correlate with *in vivo* leukemia kinetics (Paczulla et al., 2017). One possible explanation for the longer time to *in vivo* leukemia induction in some AML is, as we found, their lower content in LSC and LSC-like cells that can home to the BM (Figure 3D).

In summary, we have developed a model that allows *in vivo* leukemogenesis studies in the vast majority of AML (including favorable risk disease subtypes previously considered non-engraftable). In the following, this model will be used to investigate the effects of genetic or pharmacologic interventions on *in vivo* leukemia progression and LSCs.

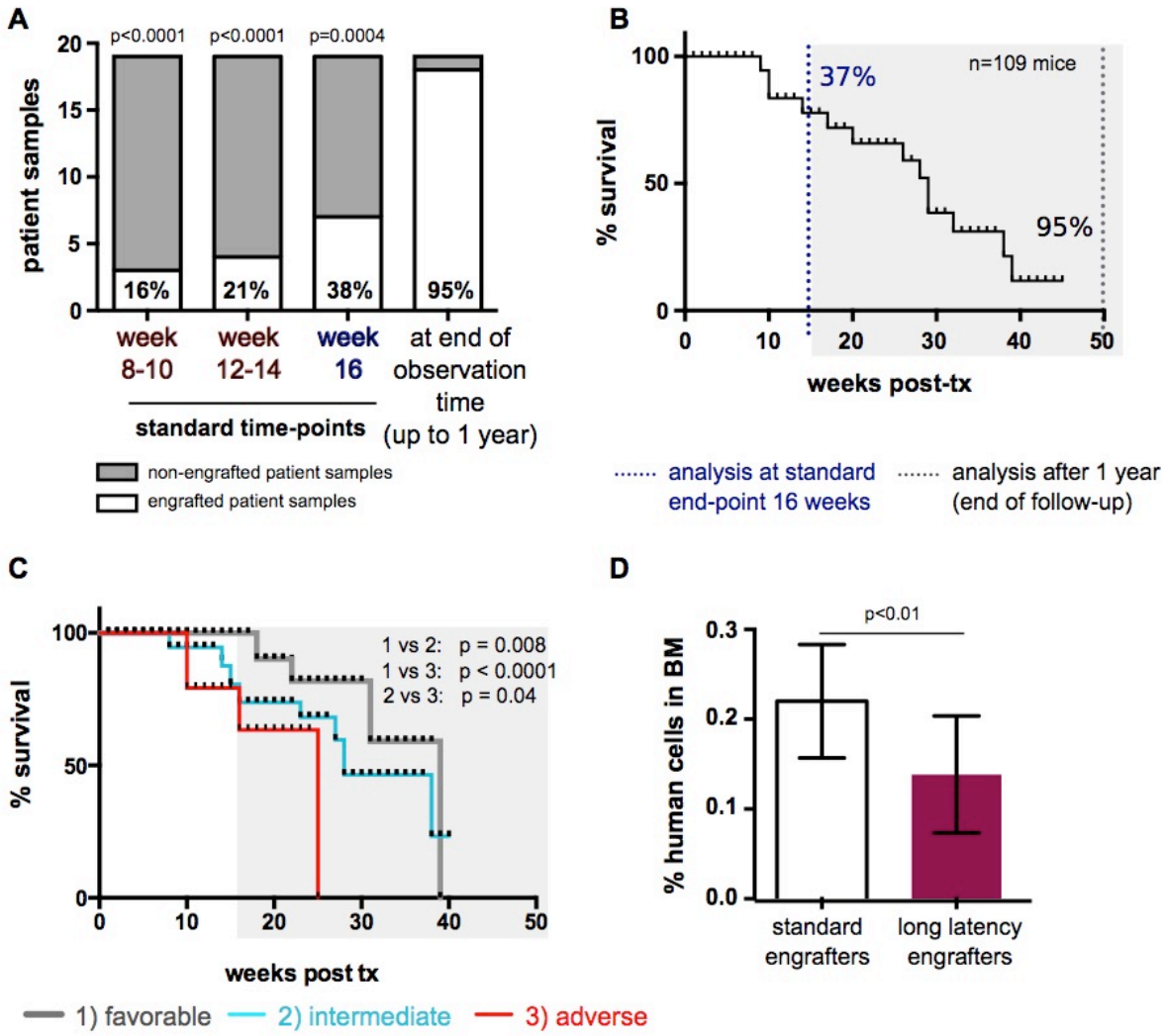

Figure 3: Extended post-transplant follow-up enhances engraftment efficiency of human AML in NSG mice and shows that *in vivo* leukemogenesis correlates with molecular risk group stratification and differences in homing rates. **(A)** Quantification of engrafted samples at 8-10 weeks, 12-14 weeks and 16 weeks versus one year. A Fisher's exact test was used to calculate statistical significance between engrafters and non-engrafters at each analyzed time period to our endpoint of 1-year observation time. **(B)** Kaplan-Meier survival analysis of n=109 mice after xenotransplantation with human primary AML cells showing that ~95% of mice die from leukemia after 1 year of observation time. **(C)** Kaplan-Meier survival analysis of n=99 mice (n=10 mice were transplanted with APL and are therefore not included in this statistic) show that mice transplanted with favorable risk AML showed longest survival when compared to intermediate and respectively adverse risk cases (black: favorable, n=4; blue: intermediate, n=8; red: adverse risk AML, n=3). **(D)** The homing rate of leukemic cells in the BM was higher in standard compared to long-latency engrafters. Data from n=3 AML patients with n=3-5 mice each are shown for each group. (Paczulla et al., 2017)

5.1.2 Investigation of catecholamine-based mechanisms regulating leukemia induction in a xenotransplantation model of human AML

5.1.2.1 Xenotransplantation at night accelerates leukemogenesis

Using the model described above in 5.1.1, we observed that xenotransplantations performed at night (respectively very early in the morning, at 3 am) accelerated engraftment when compared to transplantations performed in the late afternoon (5 pm) (see the experimental time schedule in Figure 4). Therefore, we analyzed this parameter as a method to optimize our AML xenotransplantation model and aimed to investigate the underlying mechanisms, which according to our results so far involve enhanced catecholamine activity in mice transplanted at 3 am.

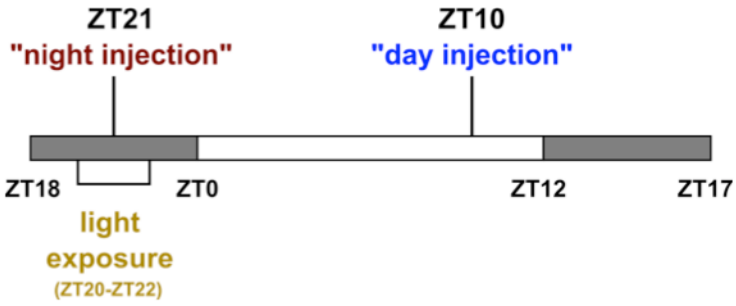

Figure 4. Time schedule of day and night transplantations. Please note that during night, mice were exposed to light one hour prior to and after transplantation. ZT = Zeitgeber time with ZT0 = time-point of light onset and ZT12 = time-point of light offset.

We first transplanted primary AML blasts side-by-side at the two time-points ("night": 3 am and "day": 5 pm) and used the same patient cells for day and night transplantations. Of note, cells were thawed separately and treated equally for the day and the corresponding night experiment. Transplantation at night resulted in higher engraftment when compared to transplantation at daytime (shown for n=5 AML cases transplanted at both time-points, Figure 5A). These findings were further confirmed by histopathology showing micro-leukemic infiltrations in the BM of mice transplanted during day while mice transplanted during night showed very high leukemic infiltration (Figure 5B). When limiting dilution experiments were performed, the results from the long-term assays could be reproduced and even improved, since most of

the mice transplanted during day with the lowest cell dosage did not develop leukemia up to one year after transplantation. In contrast to this, all mice transplanted during night resulted in leukemic engraftment (Figure 5C).

To further investigate the mechanisms underlying this phenomenon, we performed homing assays with CFSE labeled AML cells, since the main physiological process happening directly after xenotransplantation is the migration/homing of the transplanted cells into BM. We therefore hypothesized that this process would be mostly influenced by the time-point of injection. These experiments showed that indeed, cells from the same AML sample show higher homing rates (not only to BM, but also to liver and spleen) upon xenotransplantation via the tail vein at night compared to day time (Figure 5D); in contrast, cells measured in the PB were reduced in mice transplanted at night.

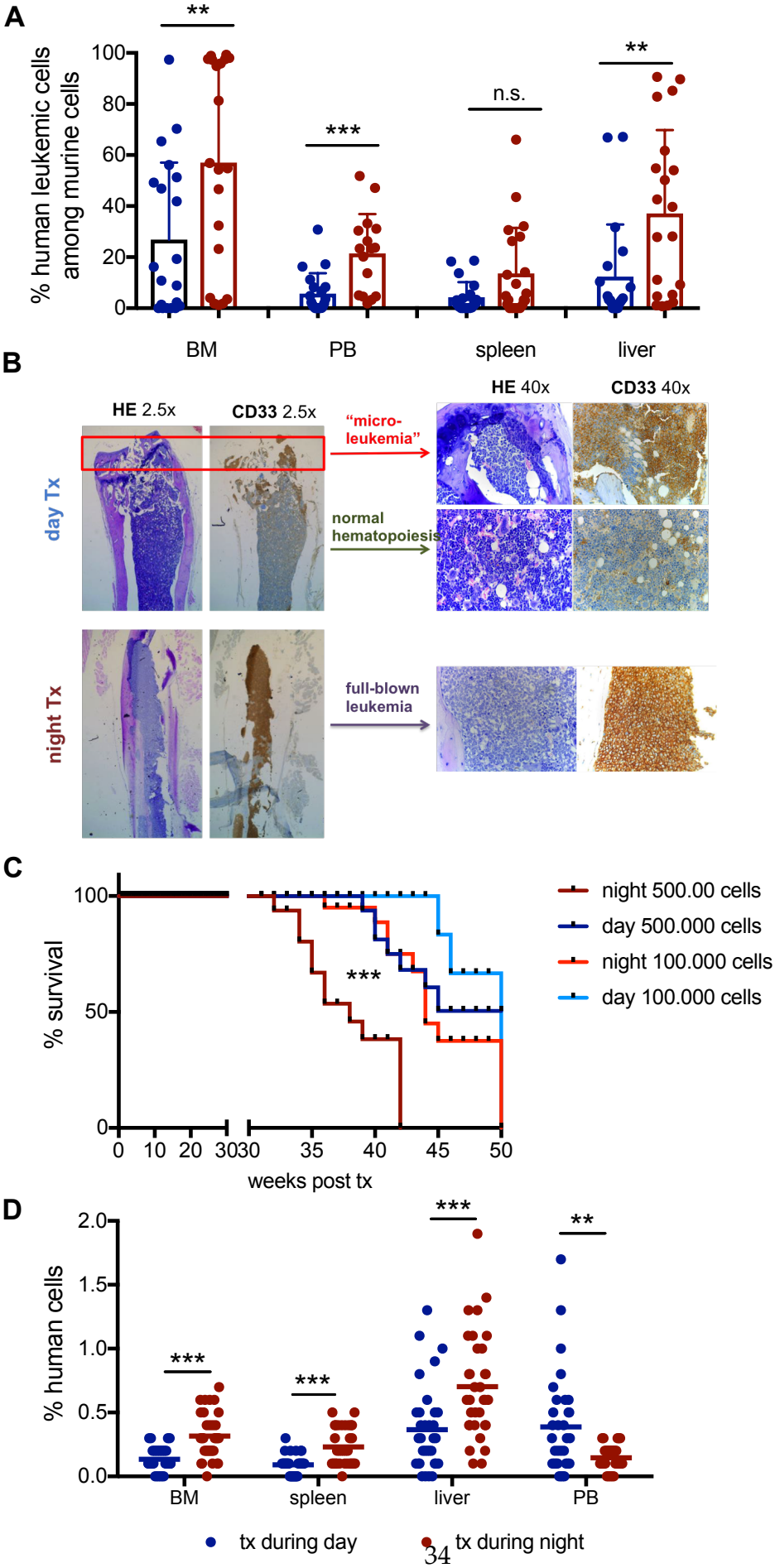
A
% human leukemic cells among murine cells
100
80
60
40
20
0
**
***
n.s.
**
BM
PB
spleen
liver
B
HE 2.5x
CD33 2.5x
HE 40x
CD33 40x
day Tx
"micro-leukemia"
normal hematopoiesis
night Tx
full-blown leukemia
C
% survival
100
50
0
***
0 10 20 30 30 35 40 45 50
weeks post tx
night 500.00 cells
day 500.000 cells
night 100.000 cells
day 100.000 cells
D
% human cells
2.0
1.5
1.0
0.5
0.0
***
***
***
**
BM
spleen
liver
PB
tx during day
tx during night

Figure 5. Transplantation (tx) at night facilitates long-term AML engraftment and enhances homing (in comparison to conventional day-time transplantation). (A) Shown are percentages of engrafted human AML cells as detected by multi-parameter flow cytometry after staining with human antibodies in mice transplanted with cells from the same AML sample at day and respectively night following otherwise exactly similar procedures. Data from n=5 independent experiments using different AML patient samples with n=4-5 mice per group and sample are shown. **(B)** Histopathological confirmation of leukemic infiltration in the BM. Shown are representative H&E as well as anti-human CD33 stainings. **(C)** Kaplan-Meier analysis of limiting dilution assays (using $5x10^5$ and $1x10^5$ cells/mouse) with n=2 patient samples and n=10 mice per arm in total. **(D)** Homing assays showing that night transplantation enhances homing to the BM but also to liver and spleen. Conversely, fewer cells are detectable in the PB. Shown are summarized data from seven independent experiments performed with different AML samples (33 mice per group in total); individual patient-specific analyses also showed the same result. A Mann-Whitney U Test (for not normally distributed data) or students t-test (for normally distributed data) was used for statistical analyses with n.s. = not significant ($p > 0.05$), * = $p < 0.05$, ** = $p < 0.01$ and *** = $p < 0.001$.

So far, the SDF1-CXCR4 axis was described as the main molecular regulator of HSC homing to the BM. The SDF1-CXCR4 axis was indeed shown to follow circadian oscillations. After light exposure, SDF1 is released as chemoattractant from the BM while SDF1 mRNA is down-regulated; this leads to higher HSC mobilization and therefore enhanced levels of circulating HSCs, showing a peak at 5 hours after light onset (Méndez-Ferrer et al., 2008). It is possible that enhanced mobilization of endogenous HSCs into the circulation might open up niche space and then facilitate repopulation with transplanted AML cells. However, in our experimental setting, mice were exposed to light 1 hour prior to transplantation and 1 additional hour after transplantation (Figure 4). Thus, the time-point of transplantation is not corresponding to the peak of HSC mobilization. Consistently, we only detected slight changes in BM-SDF1 (and no changes in PB-SDF-1), when our two transplantation time-points were compared. Furthermore, *in vitro* colony forming assays of PBMCs derived from mice at these two experimental time-points (3 am, 5 pm) showed no significant difference, suggesting that the numbers of circulating HSPCs are comparable. These data overall indicate that alternative mechanisms (e.g. induction of adhesion molecules) are responsible for the engraftment advantage observed at night. In support of this hypothesis, we also observed that night transplantation enhanced AML cell homing to liver and spleen (Figure 5D).

5.1.2.2 Increased catecholamine levels mediate – in part – the “night effect”

Notably, we observed that mice - which are naturally more active at night - showed more distress when they were disturbed by light exposure and transplantation during night when compared to day time.

In our fast society and everyday life stress becomes an important factor affecting our health, since it broadly influences our body by e.g. deregulating circadian rhythms, blood pressure, the cardiac cycle up to panic attacks (Esler et al., 2008). Links between stress levels and cancer development were investigated and some associations reported. In 2016, Weberpals and co-workers published a meta-analysis of 88.026 cancer patients from 30 different studies. They showed that patients receiving beta-blockers had a significantly higher overall and cancer-specific survival (Weberpals et al., 2016) indicating a role of beta-adrenergic signaling in cancer progression. Shortly after this study, a report in line with this notion was published, showing that activation of beta-adrenergic signaling in several human tumor cells and entities results in higher invasiveness and cell deformability (shown in breast, ovarian, prostate and melanoma cancer cells as well as for leukemic cells) (Kim et al., 2016). Moreover the authors postulate a scheme of the putative mechanisms behind these observations suggesting that catecholamines induce beta-adrenergic signaling in cancer cells leading to an internal cascade starting from production of cAMP, in the following activation of the PKA signaling, which in terms results in higher Ca^{2+} efflux from the endoplasmatic reticulum (ER), finally leading to an increase in cortical actin and cytoplasmic F-actin for leukemic cells (Figure 6) (Kim et al., 2016). These cortical actin dynamics have furthermore been linked to cadherin adhesion (de Rooij, 2014) indicating cadherin induction as a possible downstream effector of catecholamine activation in this setting.

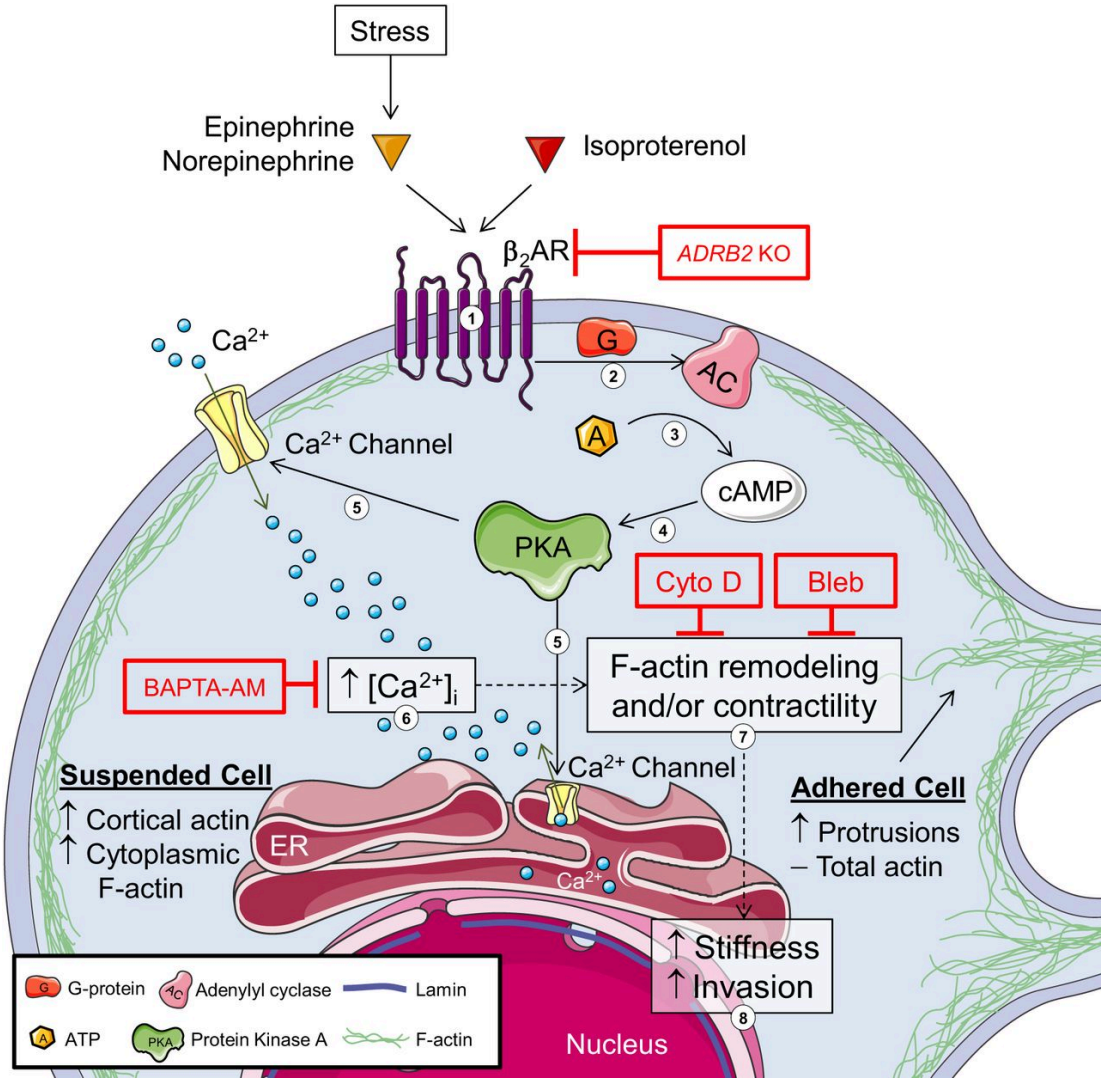

Figure 6: Scheme of putative mechanisms how β-adrenergic signaling activation may influence invasiveness of cancer cells (from (Kim et al., 2016)).

Moreover, also a link between circadian oscillations, SDF1 expression and catecholamines, as known activators of beta-adrenergic signaling, has been reported. For example, stimulation of β2-adrenergic receptors (ARs) in osteoblasts was shown to induce clock gene expression, whereas β3-AR activation results in acute SDF1 mRNA down-regulation, which are compensatory mechanisms involved in the above-mentioned circadian mobilization of HSCs (Fu et al., 2005; Liu et al., 2007; Méndez-Ferrer et al., 2008). Until now, no functional relevance of circadian oscillations and catecholamines influencing leukemogenesis were shown *in vivo*. Therefore, we were wondering if the observed increase in homing and leukemia initiation was mediated by higher

catecholamine (epinephrine and/or nor-epinephrine) levels affecting the BM niche, healthy murine HSCs and/or the transplanted human AML cells.

To further explore this hypothesis, we measured epinephrine and nor-epinephrine levels in the plasma and crushed femurs of mice at day and night (n=3 each group) by using ELISAs as previously described (Heidt et al., 2014). These experiments showed especially enhanced epinephrine levels in mice analyzed at night (and after light exposure) compared to daytime in both, plasma and femur extracts (Figure 7A). We therefore performed additional *in vivo* assays during daytime by pre-treatment of mice with either epinephrine or carrier control (PBS) and subsequent intravenous AML cell injection for long-term (Figure 7B) or Homing (Figure 7C) assays. We observed that indeed epinephrine injection accelerated long-term engraftment (Figure 7B) and resulted in increased homing rates (Figure 7C). This was in part counter-acted by pre-treatment of mice with the beta-blocker propranolol (Figure 7C) with respect to both long-term leukemia induction (Figure 7D) and homing (Figure 7E).

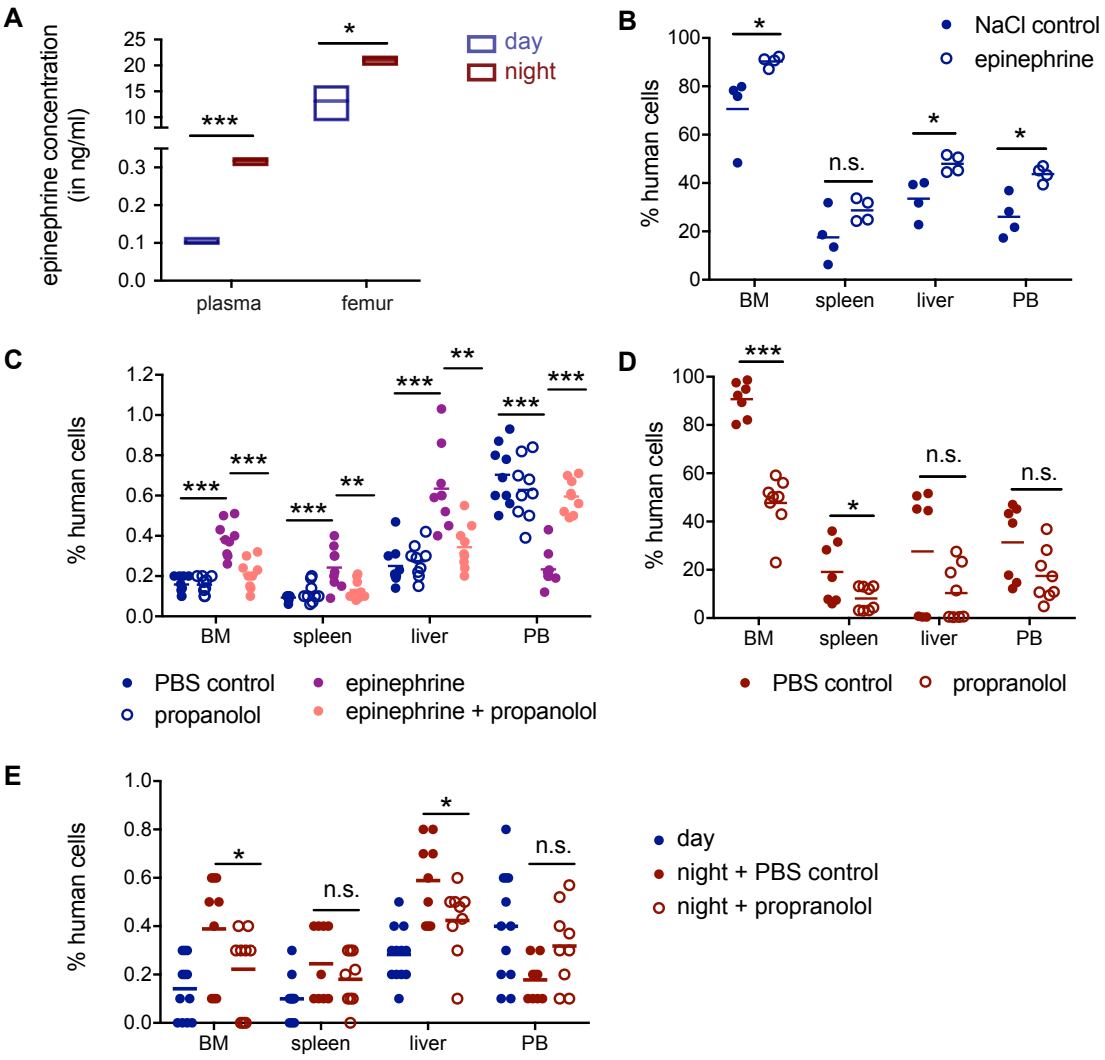
A
epinephrine concentration (in ng/ml)
day
night
plasma
femur
B
% human cells
NaCl control
epinephrine
BM
spleen
liver
PB
n.s.
C
% human cells
PBS control
propanolol
epinephrine
epinephrine + propanolol
D
% human cells
PBS control
propranolol
E
% human cells
day
night + PBS control
night + propranolol

Figure 7. Epinephrine levels influence homing to the BM and long-term engraftment. **(A)** Epinephrine levels are higher in the plasma, when cells are transplanted at night versus daytime (n=5 mice per group) as measured by ELISA. **(B)** Mice were treated with PBS or epinephrine one hour before intravenous AML cell transplantation at daytime for long-term leukemia induction leading to accelerated leukemia development. Shown are data from n=1 patient sample with n=4 mice per group. **(C)** Mice were treated with PBS, propranolol, epinephrine and a combination of both one hour prior to transplantation at daytime. Note that epinephrine treatment increased homing to the BM, while this effect can be blocked by simultaneous administration of propranolol. Shown are summarized data from three different patient samples with n=3 mice per group. **(D-E)** Mice were treated with the β1/2-AR blocker propranolol one hour prior to transplantation at night after which **(D)** long-term leukemia induction and **(E)** homing were analyzed. Indeed, long-term leukemia engraftment was reduced in mice that were treated with propranolol one hour before cells were transplanted at night. Shown are summarized data from n=3 independent experiments with n=4-5 mice per group **(D)**. Also homing properties were lower at daytime when compared to night transplantations without prior propranolol treatment. Shown are summarized data from three different AML samples, transplanted during day and night (+/- propranolol) with n=3 mice/patient and condition **(E)**. A Mann-Whitney U Test (for not normally distributed data) or students t-test (for normally distributed data) was used for statistical analyses with n.s. = not significant ($p > 0.05$), * = $p < 0.05$, ** = $p < 0.01$ and *** = $p < 0.001$.

In conclusion, this project part shows that xenotransplantation at night into NSG mice can accelerate engraftment of human AML cells, thereby further optimizing this model. This possibly results from modulation of cell adhesion, which was enhanced upon addition of epinephrine to *in vitro* cultures of AML cells on stroma (Figure 8). This is in line with published data showing that catecholamines increase the invasiveness and cortical actin in cancer cells (Kim et al., 2016), possibly via regulation of cadherins (de Rooij, 2014).

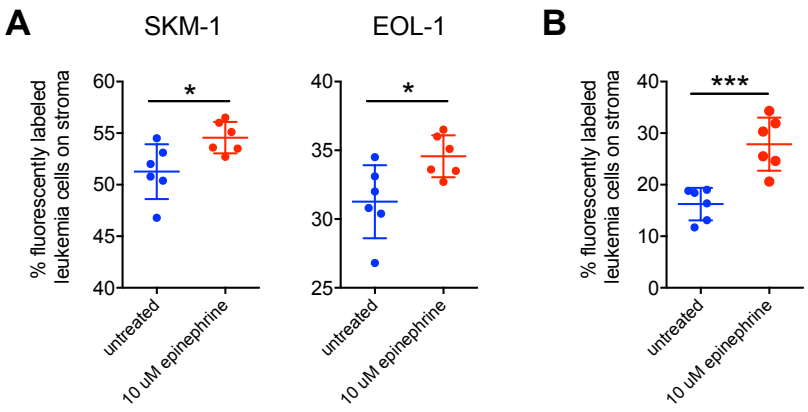

Figure 8. Epinephrine in adhesion assays increases adhesion of human AML cells. Adhesion assays with different CFSE®-labeled cells were performed on MS-5 stroma cells with the addition of 10 µM epinephrine and quantified after 90 min using flow cytometry analyses for fluorescently labeled cells. Shown are data from **(A)** SKM-1 and EOL-1 cell lines and **(B)** primary human AML cells (n=3 patient samples). For experimental setup see also below schematic overview of the procedure in Figure 12B. Data from n=3 independent experiments performed in technical triplicates are shown. A students t-test was used for statistical analyses with * = $p < 0.05$, ** = $p < 0.01$ and *** = $p < 0.001$.

Taken together, with our study we could show for the first time a functional interaction of catecholamines, AML cells and the niche. Our data suggest that disturbing circadian rhythm might have pro-oncogenic effects, and that these are mediated by catecholamines and, importantly, can be partly prevented by beta-blocker treatment. These findings might be of general significance for tumor initiation processes, but however further investigations are required. Finally, if the role of catecholamines and associated adhesion molecules (most likely cadherins) is however conserved in healthy HSPCs, this knowledge might be used to improve their homing and engraftment in clinically employed stem cell transplantations in patients after induction therapy. Facilitating engraftment after stem cell transplantation promises to shorten the period until recovery of the blood system is achieved, and potentially allows transplantation with lower cell doses, which might make it easier to find matching donors by enabling transplantation of individual cord blood samples (which currently cannot be used for adult transplantation because they contain low HSPC numbers). Overall this knowledge might have an important beneficiary impact for clinical treatment of patients.

Follow-up work outside of the scope of the current thesis is planned and will further elucidate the mechanisms underlying enhanced homing and engraftment of leukemic (and perhaps also of healthy HSPCs) observed after transplantation at night-time and respectively in the presence of stimulated catecholamine activity.

5.2 Leukemia stem cells – Absence of NKG2D ligands defines human leukaemia stem cells and mediates their immune evasion

(see also manuscript attached: Paczulla*, Rothfelder*, Raffel* *et al*., in revision in *Nature*)

AML is considered to emerge from subpopulations of LSCs (Lapidot et al., 1994). These cells in parts resemble HSCs, meaning that they can self-renew and show some degree of differentiation into more mature blasts (that themselves cannot initiate leukemia). Next to this, LSCs also show disease initiating properties, enhanced resistance to conventional chemotherapies and are thus thought to be responsible for relapse (Hanahan and Weinberg, 2000). Here we proposed that LSCs also selectively escape immune surveillance, when compared to more differentiated leukemic cells. The study of interactions between human LSCs and the immune system have been hampered by the fact that immunosuppressed animals are used for xenotransplantation assays (as reviewed by Theocharides et al., 2016); thus, possible differences in response of LSCs and non-LSCs to immune cells remain elusive.

LSCs were reported to preferentially reside among $CD34^{+}CD38^{-}$ leukemic subpopulations (Bonnet and Dick, 1997; Lapidot et al., 1994), but were also identified among $CD34^{-}$ cells in CD34 non-expressing AML (Taussig et al., 2010). Further markers have been reported to enrich LSCs in CD34 expressing AML (mostly within the previously described $CD34^{+}CD38^{-}$ subpopulation), among these GPR56 (Daria et al., 2016; Pabst et al., 2016; Saito et al., 2013), CD123 (IL-3 receptor alpha chain) (Jin et al., 2009), CD25 (IL-2 receptor alpha-chain) (Saito et al., 2010), CD96 (Hosen et al., 2007), CD47 (Majeti et al., 2009), CLL-1 (van Rhenen et al., 2007), CD44 (Jin et al., 2006), CD99 (Chung et al., 2017) or TIM3 (Jan et al., 2011). Of note, AML cases show high heterogeneity regarding these markers and do not routinely express all of them in one sample hampering their routine use for LSC identification.

Surface expression of NKG2D ligands (NKG2DL) represents an activating signal for recognition and lysis through NKG2D receptor expressing NK cells. NKG2DL are not expressed on healthy cells but induced upon cellular stress, for example in response to infection or malignant transformation. In this project, we demonstrate that LSCs selectively evade NKG2D-mediated immunosurveillance and clearance by suppressing NKG2DL. NKG2DL comprise different molecules of the MIC and ULBP protein families (Guerra et al., 2008). In cooperation with the Immunology & NK cells laboratory led by Professor Helmut Salih at the University of Tuebingen, Germany, we found that NKG2DL are heterogeneously expressed on AML cells in a cohort of 175 AML patients as analyzed by flow cytometry (Figure 9A).

Analyses of sorted NKG2DL^{pos} and NKG2DL^{neg} subpopulations of the same patients revealed that NKG2DL^{neg} cells display stemness characteristics such as immature morphology (Figure 9B), stemness-associated gene expression signatures (Eppert et al., 2011; Ng et al., 2016) and enhanced *in vitro* clonogenicity (Figure 9C). Upon transplantation into NSG mice, we observed leukemia initiation only from NKG2DL^{neg} cells (Figure 9D) that *in vivo* however were able to differentiate into NKG2DL^{pos} cells, reconstituting the heterogeneous NKG2DL distribution observed in the pre-transplant sample. However, no leukemia induction was observed from corresponding NKG2DL^{pos} cells (Figure 9D). *In vivo* chemoresistance assays using cytarabine injections at the stage of disease showed that NKG2DL^{neg} cells significantly better survive the treatment, which preferentially diminishes NKG2DL^{pos} subpopulations. Moreover, co-culture experiments of bulk AML cells with polyclonal NK cells (pNKCs) enriched for AML cells with functional LSC properties as shown by higher colony-forming capacity and increased *in vivo* leukemogenesis, which could be blocked by addition of specific NKG2D blocking fragments during the co-culture.

These data show that LSCs are selectively protected from NK cell mediated lysis. Dulphy *et al*. recently summarized the current knowledge on the role of NK cells in AML (Dulphy et al., 2016). The fact that AML blasts are sensitive to NK cell-mediated immune response *in vivo* is also highlighted by studies in patients receiving an allogeneic HSC transplantation, in particular when using haplo-identical donors, who showed lower incidence of AML relapse if transplanted with stem cell concentrates containing allo-reactive NK cell clones against recipient cells (Ruggeri et al., 2002). By contrast, in patients who do not receive transplantation, NK cells are not activated via these

mechanisms. Actually, autologous NK cells of patients with overt AML display severe defects (e.g. reduced expression of activating NK receptors, cytotoxicity and IFN-γ release), which are induced by AML cells via production of soluble immunosuppressive molecules, modification of the microenvironment and direct cell-cell interactions leading to defective immunological synapses (Dulphy et al., 2016). Interestingly however, NK cells appear to normalize their function after induction of morphologic remission through chemotherapy (Fauriat et al., 2007; Khaznadar et al., 2015). Taken together, these data reinforce that AML cells actively hamper NK cell function at stages of overt disease, but also suggest that additional mechanisms are responsible for AML cell escape from NK immune surveillance at the stages of minimal residual disease, when leukemia initiation and relapse happen, making our new insights highly important.

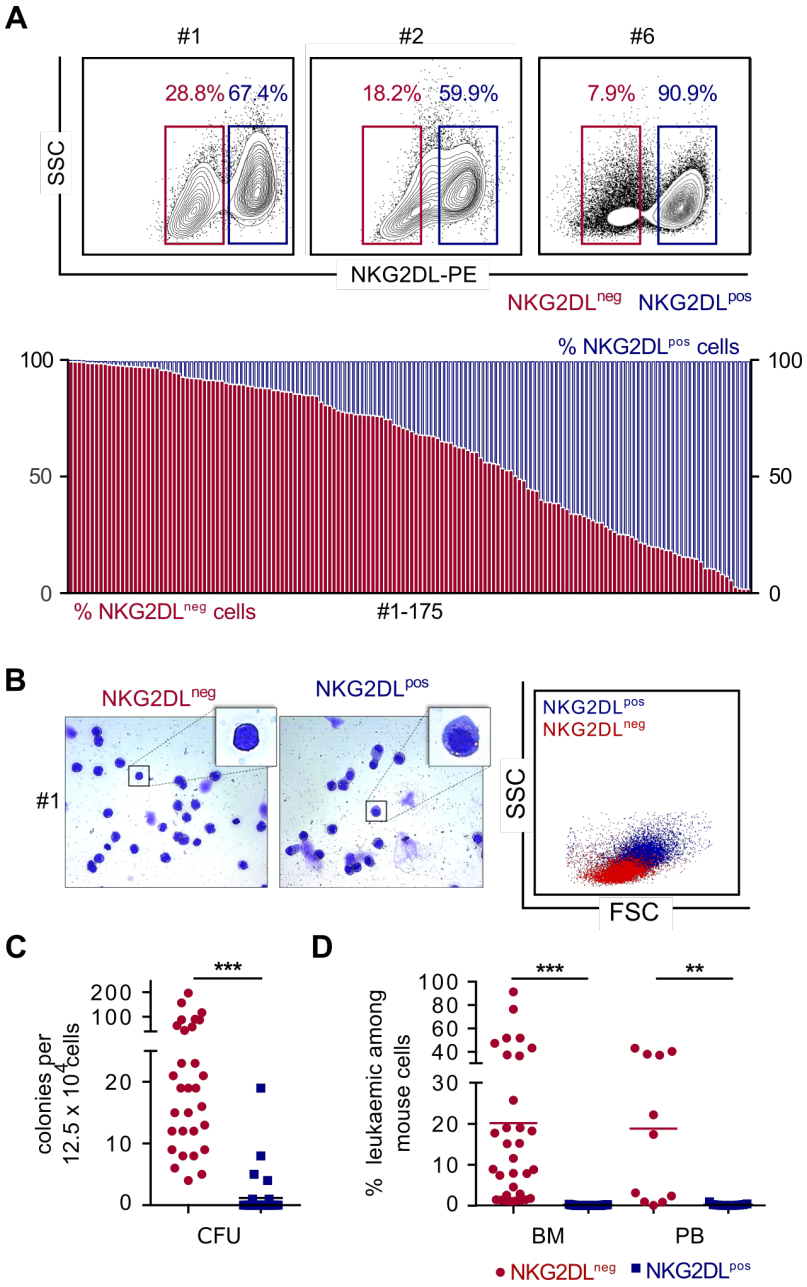

Figure 9. Absence of immunostimulatory NKG2DL enriches for LSCs. (A) upper panel: Representative NKG2DL staining. Lower panel: FACS analysis using NKG2D-Fc chimera showed heterogeneous percentages of NKG2DL^{neg} (red) and NKG2DL^{pos} (blue) AML cells within individual patients. **(B-D)** NKG2DL^{neg} and NKG2DL^{pos} subpopulations were sorted from a given AML patient and analyzed side-by-side at equal numbers. **(B)** Representative May-Grünwald-Giemsa staining (left) and corresponding flow cytometry scatter plots (right). **(C)** Colony formation (data from n=32 patients performed in technical triplicates each). **(D)** Transplantation of NKG2DL^{neg} and corresponding NKG2DL^{pos} AML fractions from the same AML patient sample in NSG mice: summarized results on human leukemic infiltration in mouse BM and PB as detected by flow cytometry (n=10 patient samples and n=3-5 mice per patient and group). A Mann-Whitney U Test (for not normally distributed data) or students t-test (for normally distributed data) was used for statistical analyses with n.s. = not significant ($p > 0.05$), * = $p < 0.05$, ** = $p < 0.01$ and *** = $p < 0.001$.

Around 30% of AML cases show no CD34 expression (termed CD34 non-expressing AML) (Taussig et al., 2010). Although functional analyses indicate that the LSC concept holds true also in this subtype, a robust LSC marker has not yet been reported for this subgroup in which LSCs are thus understudied. In our study, we additionally analyzed 55 cases with CD34 non-expressing AML and also here observed heterogeneous distribution of NKG2DL among leukemic cells of individual patients (Figure 10A), with $CD34^{-}NKG2DL^{neg}$ subpopulations being more clonogenic than their corresponding $CD34^{-}NKG2DL^{pos}$ counterparts (Figure 10B) and showing unique *in vivo* leukemia induction properties in NSG mice (Figure 10C). More detailed investigations on the relationship between CD34 and NKG2DL expression in CD34 expressing AMLs demonstrated that the $CD34^{+}$ subpopulations displayed lower NKG2DL expression when compared to $CD34^{-}$ AML cells of the same patient (Figure 10D-E). Samples with >90% $NKG2DL^{neg}$ AML cells were enriched in $CD34^{+}CD38^{-}$ compared to $CD34^{+}CD38^{+}$ and $CD34^{-}$ fractions (Figure 10F-G) confirming the inverse correlation between NKG2DL expression and stemness. Consistent with the notion that not all $CD34^{+}$ AML cells are LSCs, $CD34^{+}NKG2DL^{pos}$ populations were also detected. This observation indicates that NKG2DL might be acquired during AML cell differentiation.

These data provide molecular and functional evidence that absence of NKG2DL surface expression identifies LSCs in patients suffering from CD34 expressing but also from CD34 non-expressing AML and demonstrate that absence of NKG2DL can be used as putative marker to enrich for LSCs in this AML subgroup.

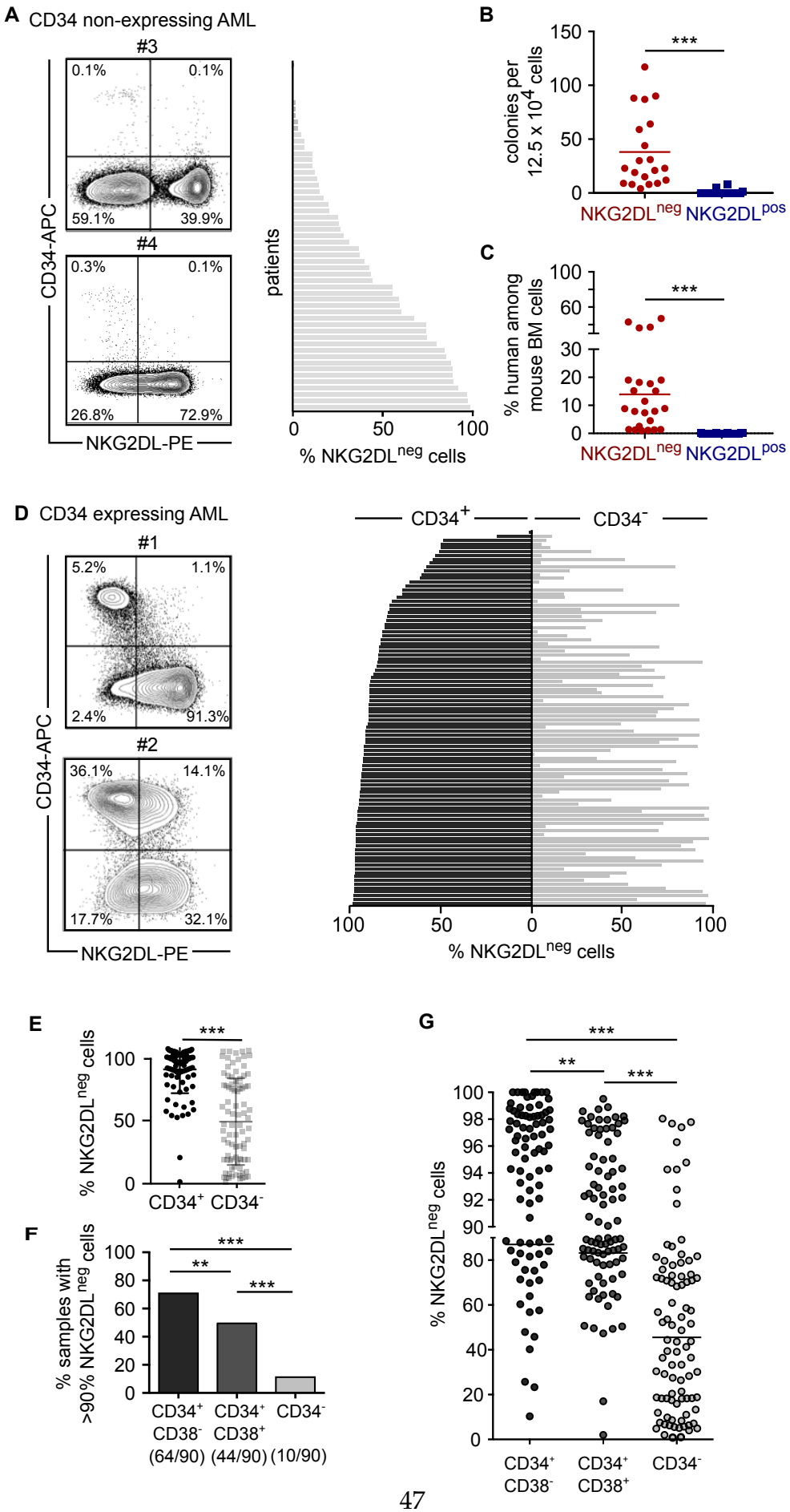
A CD34 non-expressing AML
#3
0.1%
0.1%
59.1%
39.9%
#4
0.3%
0.1%
26.8%
72.9%
CD34-APC
NKG2DL-PE
patients
0
50
100
% NKG2DL^neg cells
B
colonies per 12.5 x 10^4 cells
150
100
50
0
***
NKG2DL^neg
NKG2DL^pos
C
% human among mouse BM cells
100
60
30
20
10
0
***
NKG2DL^neg
NKG2DL^pos
D CD34 expressing AML
#1
5.2%
1.1%
2.4%
91.3%
#2
36.1%
14.1%
17.7%
32.1%
CD34-APC
NKG2DL-PE
CD34+
CD34-
100
50
0
50
100
% NKG2DL^neg cells
E
% NKG2DL^neg cells
100
50
0
***
CD34+
CD34-
F
% samples with >90% NKG2DL^neg cells
100
80
60
40
20
0
***
**
***
CD34+ CD38- (64/90)
CD34+ CD38+ (44/90)
CD34- (10/90)
G
% NKG2DL^neg cells
100
98
96
94
92
90
80
60
40
20
0
***
**
***
CD34+ CD38-
CD34+ CD38+
CD34-

Figure 10. Absence of NKG2DL identifies LSCs independently of CD34 expression. (A-C) CD34 non-expressing AML: **(A)** NKG2D-Fc flow cytometry analysis (left panel: representative plots; right panel: results from n=55 patients); **(B-C)** comparison of sorted NKG2DL^{neg} versus corresponding NKG2DL^{pos} AML cells showed **(B)** enhanced colony formation (data from n=10 patients in technical triplicates each) and **(C)** *in vivo* engraftment in NSG mice (data from n=5 patients in n=3-5 mice per patient and condition). **(D-G)** CD34 expressing AML: **(D-E)** NKG2D-Fc flow cytometry analysis (left panel: representative plots; right panel: results from n=98 patients. **(E)** Shown is the summarized quantification of NKG2DL of 98 patients subdivided into CD34^{+} and CD34^{-} populations. **(F-G)** NKG2D-Fc, anti-human CD34 and anti-human CD38 co-staining: quantification of %NKG2DL^{neg} cells among different AML subpopulations, CD34^{+}CD38^{-}→CD34^{+}CD38^{+}→CD34^{-} subsets, $p<0.001$; **(F)** quantification of samples with >90% NKG2DL^{neg} cells per subpopulation among CD34^{+}, CD34^{+}CD38^{-} and CD34^{-} compartments. A Mann-Whitney U Test (for not normally distributed data) or students t-test (for normally distributed data) was used for statistical analyses with n.s. = not significant ($p > 0.05$), * = $p < 0.05$, ** = $p < 0.01$ and *** = $p < 0.001$.

More detailed molecular analyses using RNAseq and gene expression arrays retrieved poly-ADP-ribose polymerase 1 (PARP1) as significantly up-regulated gene in NKG2DL^{neg} versus NKG2DL^{pos} AML cells across several genetic subtypes (Figure 11A). Interestingly, treatment with PARP1 siRNA (Figure 11B) or alternatively with a PARP1 inhibitor (AG-14361, Figure 11C, left panel) was able to induce NKG2DL expression in CD34^{+} LSCs sensitizing these to NK cell mediated attack. Importantly treatment of cord blood derived CD34^{+} HSPCs did not result in NKG2DL induction (Figure 11C, right panel), suggesting that only leukemic but not healthy HSPCs are targeted by this treatment. Ultimately, *in vivo* co-treatment of mice transplanted with human AML cells with the PARP1 inhibitor AG-14361 and functional NK cells significantly reduced leukemia induction (2/16 leukemic/transplanted mice), while single treatments with AG-14361 or NK cells alone did not (Figure 11D-E). Importantly, pre-treatment of NK cells with a NKG2D-blocking agent abrogated these synergistic anti-leukemic effects, indicating NKG2D-dependence (Figure 11E). Together, these data indicate that enhanced PARP1 expression mediates NKG2D dependent immune escape in LSCs, thereby allowing these to grow out and initiate disease, at primary disease manifestation and at relapse.

These findings carry important translational significance since they indicate that LSCs selectively escape immune control and identify a way (PARP1 inhibition) to circumvent this. See also attached manuscript.

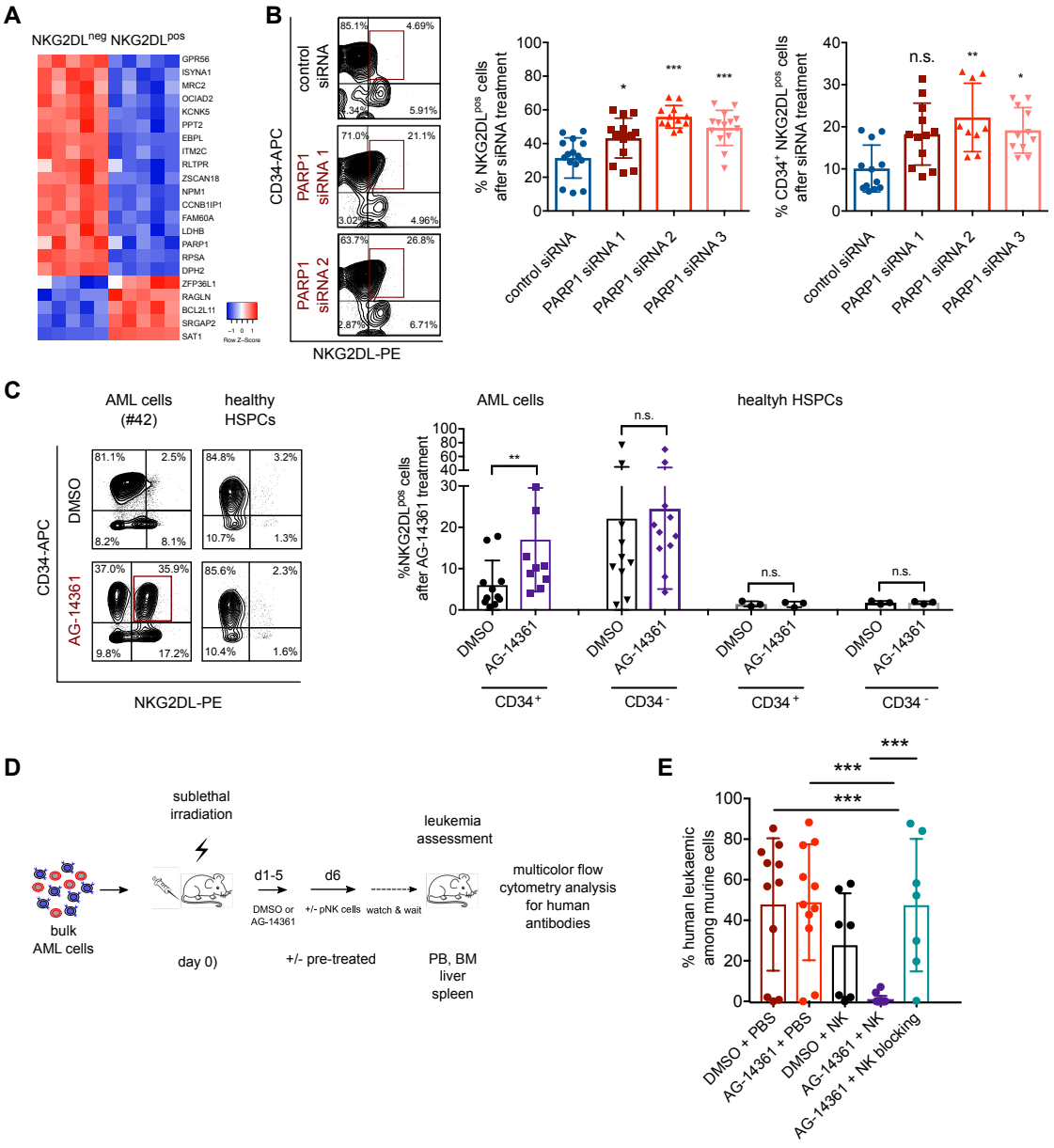
A
NKG2DL^neg NKG2DL^pos
GPR56
ISYNA1
MRC2
OCIAD2
KCNK5
PPT2
EBPL
ITM2C
RLTPR
ZSCAN18
NPM1
CCNB1IP1
FAM60A
LDHB
PARP1
RPSA
DPH2
ZFP36L1
RAGLN
BCL2L11
SRGAP2
SAT1
Row Z-Score
B
control siRNA
PARP1 siRNA 1
PARP1 siRNA 2
CD34-APC
NKG2DL-PE
85.1%
4.69%
34%
5.91%
71.0%
21.1%
3.02%
4.96%
63.7%
26.8%
2.87%
6.71%
% NKG2DL^pos cells after siRNA treatment
% CD34+ NKG2DL^pos cells after siRNA treatment
n.s.
control siRNA
PARP1 siRNA 1
PARP1 siRNA 2
PARP1 siRNA 3
C
AML cells (#42)
healthy HSPCs
DMSO
AG-14361
CD34-APC
NKG2DL-PE
81.1%
2.5%
8.2%
8.1%
84.8%
3.2%
10.7%
1.3%
37.0%
35.9%
9.8%
17.2%
85.6%
2.3%
10.4%
1.6%
AML cells
healtyh HSPCs
%NKG2DL^pos cells after AG-14361 treatment
n.s.
DMSO
AG-14361
CD34+
CD34-
D
sublethal irradiation
leukemia assessment
bulk AML cells
d1-5
d6
DMSO or AG-14361
+/- pNK cells
watch & wait
multicolor flow cytometry analysis for human antibodies
day 0)
+/- pre-treated
PB, BM liver spleen
E
% human leukaemic among murine cells
DMSO + PBS
AG-14361 + PBS
DMSO + NK
AG-14361 + NK
AG-14361 + NK blocking

Figure 11. Increased PARP1 expression in LSCs contributes to their selective escape from NK cell immune surveillance. (A) Overlap of robustly differentially regulated genes in NKG2DL^{neg} versus NKG2DL^{pos} cells isolated from the same AMLs and analysed by gene expression arrays (n=5 AML in biological triplicates each) or RNA sequencing (n=5 AML). **(B-C)** Effects of *in vitro* PARP1 inhibition on NKG2DL expression. **(B)** Flow cytometry analysis for NKG2DL and anti-hCD34 after *in vitro* (24h) treatment of bulk AML cells with 3 different PARP1 siRNAs or scrambled control non-coding siRNAs (n=4 AMLs in technical triplicates each); left panel: exemplary flow cytometry plots, right panel: quantification of NKG2DL^{pos}, and respectively CD34^{+}NKG2DL^{pos}AML cells. **(C)** *In vitro* treatment with the PARP1 inhibitor AG-14361 (20µM) or DMSO carrier control. Left panel: exemplary flow cytometry plots and right panel: quantification of NKG2DL on CD34^{+} and CD34^{-} subpopulations. Shown are data from treatment of AML cells (n=15 AML in technical triplicates each) and of healthy cord blood derived HSPCs (n=3 donors in technical triplicates each). Of note, induction of NKG2DL was only observed on AML cells but not on healthy HSPCs upon AG-14361 treatment. **(D-E)** Leukemia development in NSG mice transplanted with AML cells and treated *in vivo* with AG-14361 or DMSO +/- pNKC (n=7-16 mice per condition. **(D)** Scheme of experimental setup. **(E)** Summarized flow cytometry data of human leukemic engraftment in PB, BM and organs of mice. One dot represents one mouse. A Mann-Whitney U Test (for not normally distributed data) or students t-test (for normally distributed data) was used for statistical analyses with n.s. = not significant ($p > 0.05$), * = $p < 0.05$, ** = $p < 0.01$ and *** = $p < 0.001$.

5.3 Modeling the hematopoietic niche

5.3.1 CDX2-driven non-cell autonomous effects in AML progression (manuscript in preparation: Paczulla *et al*).

5.3.1.1 CDX2 expression regulates WNT signaling in leukemic cells

CDX2 was previously reported to be expressed in a majority of human AML and ALL (see "3.3.2.2 *CDX* genes and their role in leukemia" in the Introduction Chapter 3) but not in healthy hematopoietic cells. *CDX2* knockdown in human AML cells was shown to impair proliferation and clonogenicity in AML cell lines (Scholl et al., 2007). These results were confirmed in additional AML cell lines (EOL-1 and SKM1) as well as primary AML patient samples, which upon lentiviral *CDX2* knockdown all showed reduced clonogenic capacity in *in vitro* colony forming assays (Figure 12A), reduced *in vitro* adhesion to stromal cells (Figure 12B-C), and reduced *in vivo* homing to the BM and leukemia initiation capacities upon transplantation in NSG mice (Figure 12D-G). In contrast, no major effects were observed on growth, apoptosis, proliferation or cell cycle in these cells (data not shown). The majority of these data was collected during my master thesis and are shown there in more detail.

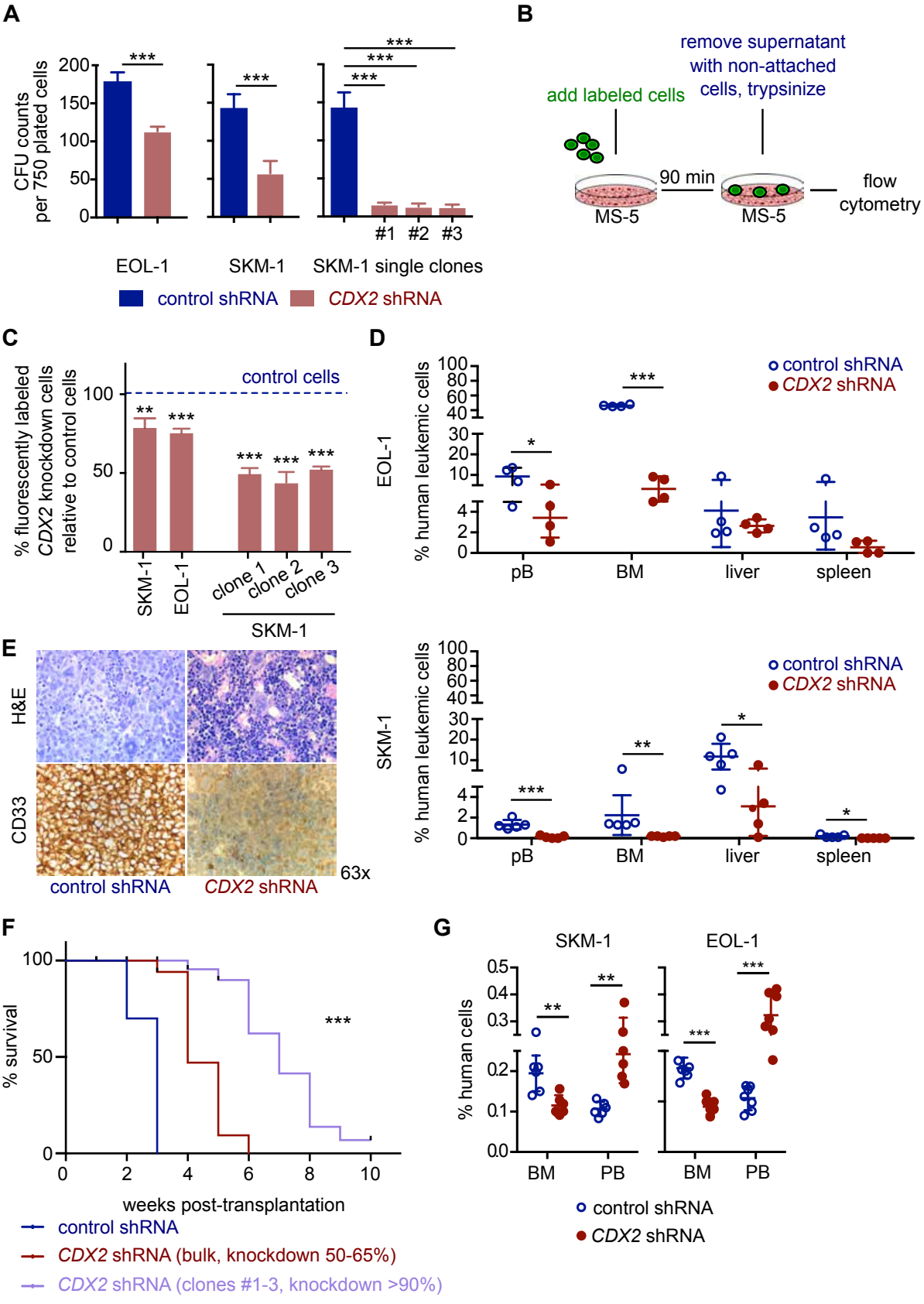
A
CFU counts per 750 plated cells
200
150
100
50
0
***
EOL-1
SKM-1
SKM-1 single clones
#1 #2 #3
control shRNA
CDX2 shRNA
B
remove supernatant with non-attached cells, trypsinize
add labeled cells
90 min
MS-5
MS-5
flow cytometry
C
% fluorescently labeled CDX2 knockdown cells relative to control cells
control cells
100
50
0
**
***
SKM-1
EOL-1
clone 1
clone 2
clone 3
SKM-1
D
% human leukemic cells
EOL-1
control shRNA
CDX2 shRNA
pB
BM
liver
spleen
SKM-1
E
H&E
CD33
control shRNA
CDX2 shRNA
63x
F
% survival
weeks post-transplantation
control shRNA
CDX2 shRNA (bulk, knockdown 50-65%)
CDX2 shRNA (clones #1-3, knockdown >90%)
G
SKM-1
EOL-1
% human cells
BM
PB
control shRNA
CDX2 shRNA

Figure 12. *CDX2* knockdown in AML cells reduces their *in vitro* clonogenic and adhesive capacity as well as their *in vivo* leukemogenic potential. (A) Cells were plated in methylcellulose and scored after 14 days showing decreased CFU formation in *CDX2* knockdown cells. **(B)** Schematic overview of the adhesion assay and **(C)** quantification of fluorescently labeled adherent leukemic cells on stoma monolayer. In **(A-C)** summarized data from n=5 independent experiments performed in technical triplicates are shown. **(D-F)** *In vivo* leukemia induction assay. NSG mice were transplanted with control or *CDX2* knockdown EOL-1 and SKM-1 cells and monitored for engraftment. **(D)** Quantification of leukemic burden using multi-color flow cytometry after 3-4 weeks in mice transplanted with $5x10^4$ AML cells (n=5 mice per group and experiment); **(E)** Histopathological analyses of BM sections of transplanted mice and **(F)** Kaplan-Meier survival analysis. **(G)** Homing assay using control and *CDX2* knockdown EOL-1 and SKM-1 cells. $1x10^6$ cells/mouse were injected via the tail vein and mice were sacrificed after 16h and analyzed for leukemic cells in BM and PB by flow cytometry. A Mann-Whitney U Test (for not normally distributed data) or students t-test (for normally distributed data) was used for statistical analyses with n.s. = not significant ($p > 0.05$), * = $p < 0.05$, ** = $p < 0.01$ and *** = $p < 0.001$.

5.3.1.2 *CDX2* regulates *WNT* signaling and DKK1 secretion in human AML cells

On the molecular level, microarray and qRT-PCR gene expression analyses on *CDX2* modified versus control AML cells confirmed cellular adhesion as one of the main pathways regulated in response to *CDX2* modulation, consistent with our functional results reported above. Furthermore, in line with the published role of *CDX* genes in regulation of *WNT* and *HOX* genes during development (Davidson et al., 2003; Lengerke and Daley, 2012; McKinney-Freeman et al., 2008; Rawat et al., 2012), genes belonging to these categories were found to be modulated in response to *CDX2* modification. Several studies have described a crosstalk between *Cdx* genes and *Wnt* signaling, which was also reported to be involved in leukemogenesis. Lengerke and colleagues for example showed that *Lef1*, a *Wnt* effector molecule, mediates *Bmp4* activation of *Cdx* genes (Lengerke et al., 2008), indicating that *Wnt* signaling acts upstream of *Cdx* genes. Surprisingly, van de Ven and co-workers showed that in *Cdx* mutants phenotypic defects can be corrected by posterior gain of function of *Lef1*. Consistently, overexpression of *Cdx1* and *Cdx4* in murine ESCs was shown to induce *Wnt3a* (Lengerke et al., 2008), suggesting that *Wnt* signaling also acts downstream of *Cdx* genes. Unexpectedly however, since in development *CDX* genes are mostly reported as positive regulators of *WNT* signaling, in our study *CDX2* induction enhanced not only the expression of *β-Catenin* but also the expression of the *WNT*-inhibitory molecule *DKK-1*, while

CDX2 suppression showed opposite effects for both genes. Flow cytometric analysis for activated *β*-Catenin confirmed lower levels in *CDX2* knockdown compared to control cells and correspondingly enhanced levels in *CDX2* overexpressing cells. Furthermore, ELISAs revealed that the secretion of DKK1 protein was modulated in response to *CDX2* expression. Therefore, we hypothesized that *CDX2* positive AML cells may secrete DKK1 to modulate their interaction with the BM niche and thereby obtain competitive advantages over healthy HSPCs for niche occupation. It is known that the number of osteoblasts directly affects the number of long-term repopulating HSCs (Calvi et al., 2003; Zhang et al., 2003). Supporting our hypothesis, Fleming and co-workers (Fleming et al., 2008) showed that Wnt / *β*-Catenin signaling plays an essential role in maintaining HSCs in a quiescent state (Fleming et al., 2008) by showing that constitutive overexpression of Dkk1 on murine osteoblasts leads to exhaustion of LT-HSCs (Fleming et al., 2008).

Here we showed that supplementation of DKK-1 indeed reduced levels of activated *β*-Catenin (Figure 13A), colony formation (Figure 13B) and adhesion to stroma (Figure 13C) in healthy cord blood derived HSPCs cultured *in vitro*, and, when administered *in vivo* (Figure 13D), decreased colony forming capacity in BM cells (Figure 13E). In contrast, DKK-1 supplementation did not alter levels of activated *β*-Catenin (Figure 13F), colony formation (Figure 13G) and adhesion to stroma (Figure 13H) in AML cells which themselves, although they actively secrete DKK-1, are apparently less sensitive themselves to DKK-1 mediated WNT inhibition. This suggests *CDX2* as a guard of WNT signaling in AML, which additionally, by DKK-1 secretion, confers leukemic cells competitive advantages over healthy HSPCs with respect to BM niche occupation (Figure 13I).

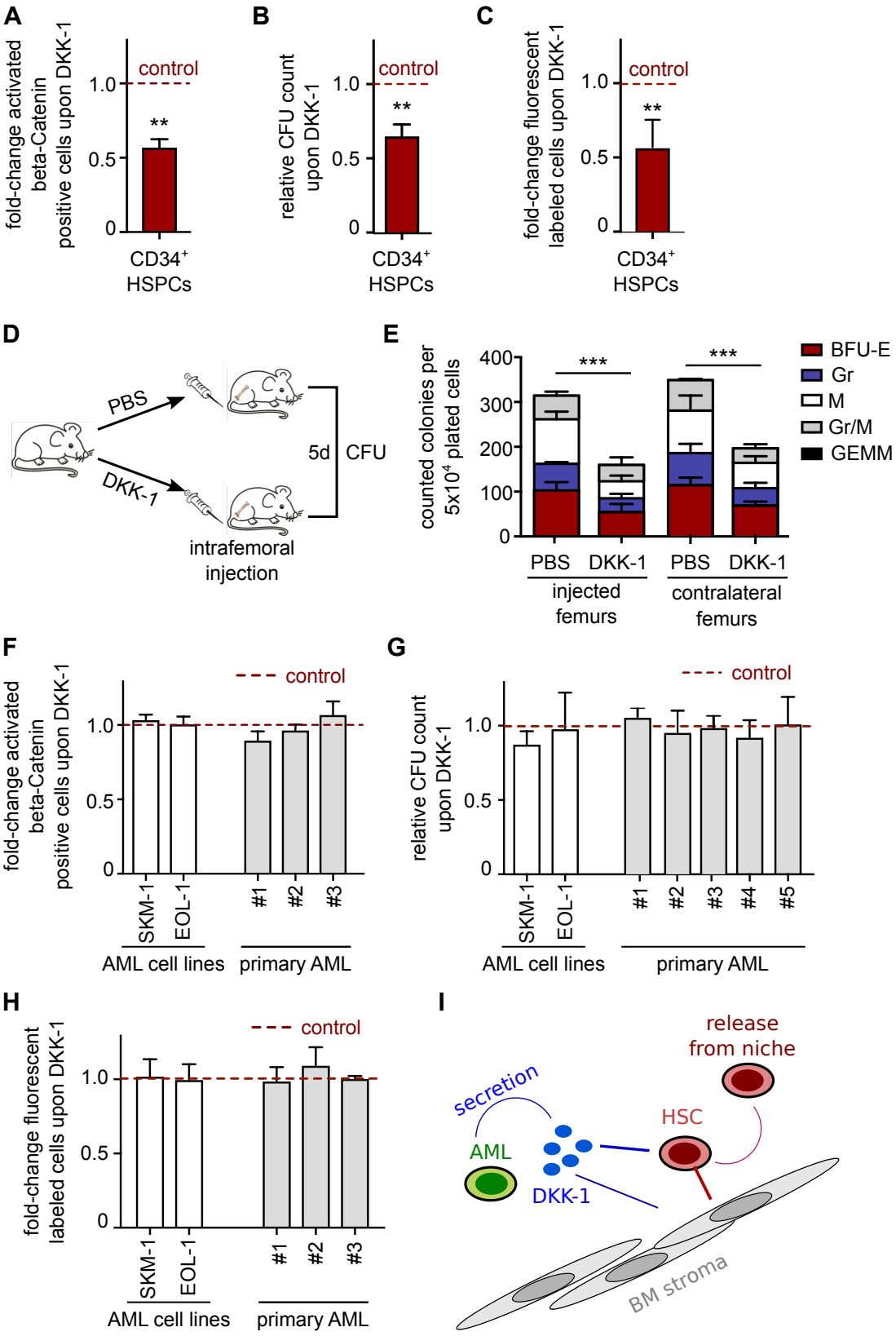
A
fold-change activated beta-Catenin positive cells upon DKK-1
control
1.0
0.5
0
**
CD34+ HSPCs
B
relative CFU count upon DKK-1
control
1.0
0.5
0
**
CD34+ HSPCs
C
fold-change fluorescent labeled cells upon DKK-1
control
1.0
0.5
0
**
CD34+ HSPCs
D
PBS
DKK-1
5d
CFU
intrafemoral injection
E
counted colonies per 5x10^4 plated cells
400
300
200
100
0
***
***
BFU-E
Gr
M
Gr/M
GEMM
PBS
DKK-1
PBS
DKK-1
injected femurs
contralateral femurs
F
fold-change activated beta-Catenin positive cells upon DKK-1
control
1.0
0.5
0
SKM-1
EOL-1
#1
#2
#3
AML cell lines
primary AML
G
relative CFU count upon DKK-1
control
1.0
0.5
0
SKM-1
EOL-1
#1
#2
#3
#4
#5
AML cell lines
primary AML
H
fold-change fluorescent labeled cells upon DKK-1
control
1.0
0.5
0
SKM-1
EOL-1
#1
#2
#3
AML cell lines
primary AML
I
release from niche
secretion
HSC
AML
DKK-1
BM stroma

Figure 13. DKK-1 impairs HSPC but not AML function. (A-C) DKK-1 treatment (200 ng/ml) of cord blood (CB) derived $CD34^+$ HSPCs in regard to **(A)** level of activated beta-Catenin, **(B)** colony formation and **(C)** adhesion capacity. **(D-E)** *In vivo* treatment of murine BM with human recombinant DKK-1 protein. **(D)** Schematic overview of the experimental set-up. In brief, mice were treated via intrafemoral injection with either PBS control or DKK-1 (n=3 mice per group) and after 5 days sacrificed and analyzed for colony forming capacity **(E)**. Quantification of scored CFU assays at day 14 performed in technical triplicates per femur and mouse. **(F-H)** DKK-1 treatment of AML cell lines (EOL-1 and SKM-1) and primary AML cells in regard to **(F)** level of activated beta-Catenin, **(G)** colony formation and **(H)** adhesion capacity. **(I)** Suggested scheme of mechanisms indicating *CDX2* as a guard of WNT signaling in AML cells using DKK-1 secretion to out-compete healthy HSPCs. A Mann-Whitney U Test (for not normally distributed data) or students t-test (for normally distributed data) was used for statistical analyses with n.s. = not significant ($p > 0.05$), * = $p < 0.05$, ** = $p < 0.01$ and *** = $p < 0.001$.

5.3.1.3 Treatment with WNT activators protects healthy HSPCs from leukemic cell derived CDX2-DKK1-mediated WNT inhibition

Building up on these findings, we hypothesized that in contrast to the notion of WNT inhibition in AML treatment, activation of WNT signaling could strengthen the healthy HSPCs in order to gain a competitive and protective advantage against DKK-1 secretion of AML cells and their subsequent niche occupation. A report from 2005 showed that both bone formation and bone mass were increased upon treatment with the known WNT agonist lithium chloride (LiCl) in mice (Clément-Lacroix et al., 2005). Therefore we postulated that *WNT* activation might on the one hand protect the healthy HSPCs against secreted DKK-1 by AML cells and on the other hand might strengthen the bone and subsequently also the hematopoietic niche. For further investigations, we first treated both AML cells and healthy HSPCs *in vitro* with LiCl and the GSK3 inhibitor SB216763 and observed - as expected - increased activated β-Catenin levels in both AML cells and healthy HSPCs (Figure 14A+D). In contrast to the results obtained with DKK-1 supplementation (Figure 13), healthy HSPCs showed slightly improved colony formation (Figure 14B) and enhanced adhesion to stroma (Figure 14C). However upon this treatment, AML cells showed impaired clonogenicity (Figure 14E), decreased adhesion (Figure 14F) and in co-cultures disadvantages regarding competitive adhesion resembling the *CDX2* knockdown phenotype. In order to analyze the functional effect of WNT activation *in vivo*, NSG mice were transplanted with AML cells and treated with LiCl or the respective vehicle control (Figure

14G). Engraftment data indicate impaired leukemic infiltration in mice in which LiCl was administered in the water compared to control treated mice with AML cell lines and primary cells (Figure 14H).

In summary, our data unravels a novel non-cell-autonomous role by which the transcriptional regulator *CDX2* promotes leukemogenesis, namely via DKK1 secretion to modify the hematopoietic BM niche and outcompete resident healthy HSPCs. We propose that *CDX2* positive leukemic cells use *CDX2* to sustain their own β-Catenin activity despite the expression and allow secretion of DKK1, which in turn is used to disturb the *WNT* levels in surrounding *CDX2* negative healthy HSPCs thereby inducing their differentiation and release from protective BM niches – that then can be seeded by AML cells. Treatment with *WNT* agonists counteracting the *WNT* inhibition induced by AML cells in healthy HSPCs and the niche might be a promising strategy to impair leukemogenesis, among others via the restoration of healthy competitor cells and impairment of leukemic cells at the same time. Future studies are needed to follow-up and further solidify these observations.

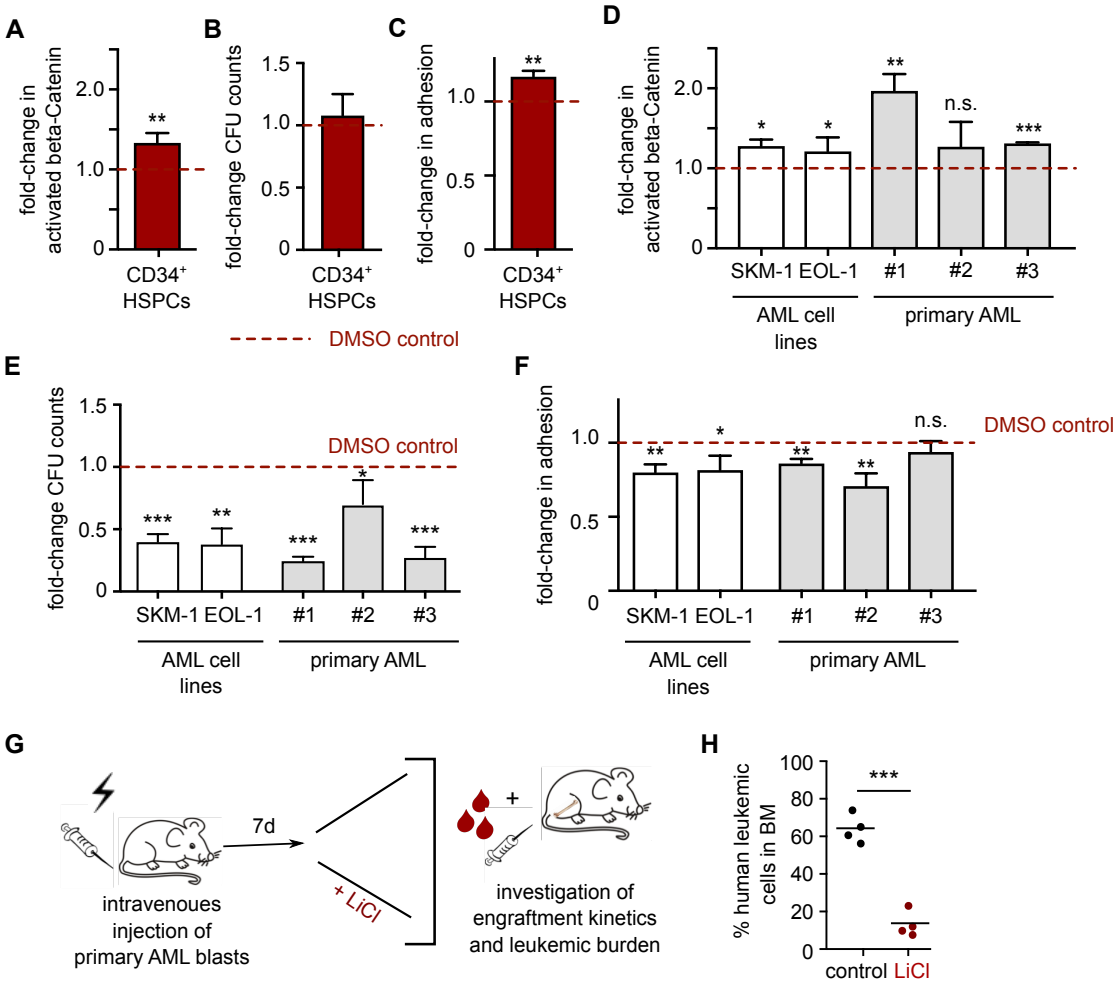

Figure 14. Treatment with the WNT agonist lithium chloride (LiCl) strengthens healthy HSPCs while impairing AML function. (A-C) *In vitro* LiCl treatment of cord blood derived CD34+ HSPCs in regard to **(A)** level of activated *β*-Catenin, **(B)** colony formation and **(C)** adhesion capacity. **(D-F)** LiCl treatment of AML cell lines (EOL-1 and SKM-1) and primary AML cells in regard to **(D)** level of activated beta-Catenin, **(E)** colony formation and **(F)** adhesion capacity. **(G-H)** *In vivo* treatment with LiCl. **(G)** Schematic overview of the experimental set-up. In brief, mice were transplanted via intravenous injection with primary AML samples (n=1 patient) and after one week treated with LiCl or control vehicle in drinking water until engraftment was detected. **(H)** Quantification of engrafted human leukemic cells in murine BM in control compared to LiCl mice (n=4 mice per group). A Mann-Whitney U Test (for not normally distributed data) or students t-test (for normally distributed data) was used for statistical analyses with n.s. = not significant ($p > 0.05$), * = $p < 0.05$, ** = $p < 0.01$ and *** = $p < 0.001$.

5.3.2 Biomimetic engineering of a functional ex vivo human hematopoietic niche

As indicated above, healthy hematopoiesis is dependent on close interactions with the BM niche. Many studies in the last years have focused on unraveling and characterizing the "home" of HSCs in the murine BM (Morrison and Scadden, 2014; Méndez-Ferrer et al., 2010). The hematopoietic niche is very complex and builds a network that enables the regulation of HSC self-renewal and differentiation by cellular (e.g. mesenchymal stem cells (MSCs) with essential roles in maintaining tissue homeostasis in the HSC niche) (Kfoury and Scadden, 2015), molecular (e.g. by cytokines regulating HSC fate) (Rieger et al., 2009; Zhang and Lodish, 2008) and structural components (e.g. interactions with the extracellular matrix) (Guilak et al., 2009) defining the HSC niche. However, the components and interactions of the human HSC niche are poorly understood due to human material accessibility and limits of existing *in vitro* culture models. The development of an *in vitro* human BM surrogate niche system would offer a tunable platform to study hematopoiesis, which may enable unique insights in the regulation of the healthy (and in future also of the leukemic) BM niche. Conventional systems fail at both capturing the complexity of the BM niche while allowing the maintenance of functional HSCs. Previous studies have attempted to maintain human HSPCs *in vitro* by adding different substrates as cytokines or chemoattractants or *in vivo* in humanized mouse models in order to get specific mature blood cells (Rongvaux et al., 2014). However, the complex organization of the BM with all its structures and cellular interactions that are necessary for the functional maintenance of HSCs could not yet be recapitulated *in vitro* so far.

The need for advanced culture systems of higher biological complexity has gained increasing recognition (Vunjak-Novakovic and Scadden, 2011) in order to study the biology of stem cells. The *in vitro* engineering of human BM environments (Dellatore et al., 2008; Di Maggio et al., 2011; Peerani and Zandstra, 2010; Vunjak-Novakovic and Scadden, 2011) capable to sustain HSCs (Peerani and Zandstra, 2010) would enable their study in xeno-free settings similarly to the "organogenesis in a dish" proposed for complex organs using human induced pluripotent stem cells (iPSCs) (e.g. lung (Wilkinson et al., 2017), kidney (Takasato et al., 2015) and liver (Takebe et al., 2013)).

In this study, a human 3D (BM) analogue was established in a perfusion-based bioreactor system, partially recapitulating structural, compositional

and organizational features of the native human osteoblastic niche environment. This approach uses porous hydroxyapatite scaffolds with structural and compositional features of bone as described previously (Porter et al., 2009), functionalized by human MSCs and the extracellular matrix (ECM) components deposited during their progressive maturation into the osteoblastic lineage. The perfusion flow bioreactor system was used for human MSC cultures offering efficient nutrient supply and waste removal at the same time (Wendt et al., 2003), while mimicking interstitial flow and associated shear stress. The blood compartment was introduced into the resulting 3D stromal tissue by perfusion of human purified CB derived $CD34^+$ cells resulting in an engineered organoid capable to mimic structural and functional features of the human BM supporting the maintenance of HSC properties.

This provides an advanced technological platform of broad fundamental and translational relevance, including the study of human HSC biology and interactions with their niche, the expansion of functional human HSCs, or the identification of factors influencing human hematopoiesis.

The generation of the 3D microenvironments was performed by differentiation of primary BM-derived human MSCs on ceramic materials within a perfusion bioreactor. Human MSCs were first cultured one week in proliferative medium (PM) to increase cell number and ensure scaffold colonization, followed by three weeks of osteogenic medium (OM) supplementation to promote cell differentiation while stimulating ECM production. The resulting tissue was defined as “engineered niche” (eN) while naked ceramic (Ce, not containing hMSC but loaded with $CD34^+$ cells) was used as internal 3D culture control.

To characterize the composition of retrieved HSPCs, flow cytometric quantification of cellular distribution regarding stem and progenitor cells was performed (Figure 15A). Moreover, the functionality of retrieved CD34 purified HSPCs was tested *in vitro* by colony formation (Figure 15B) and *in vivo* by xenotransplantation into NSG mice (Figure 15C+D). Indeed, these cells were able to form colonies and to repopulate NSG mice demonstrating as proof of principle their stem/progenitor character.

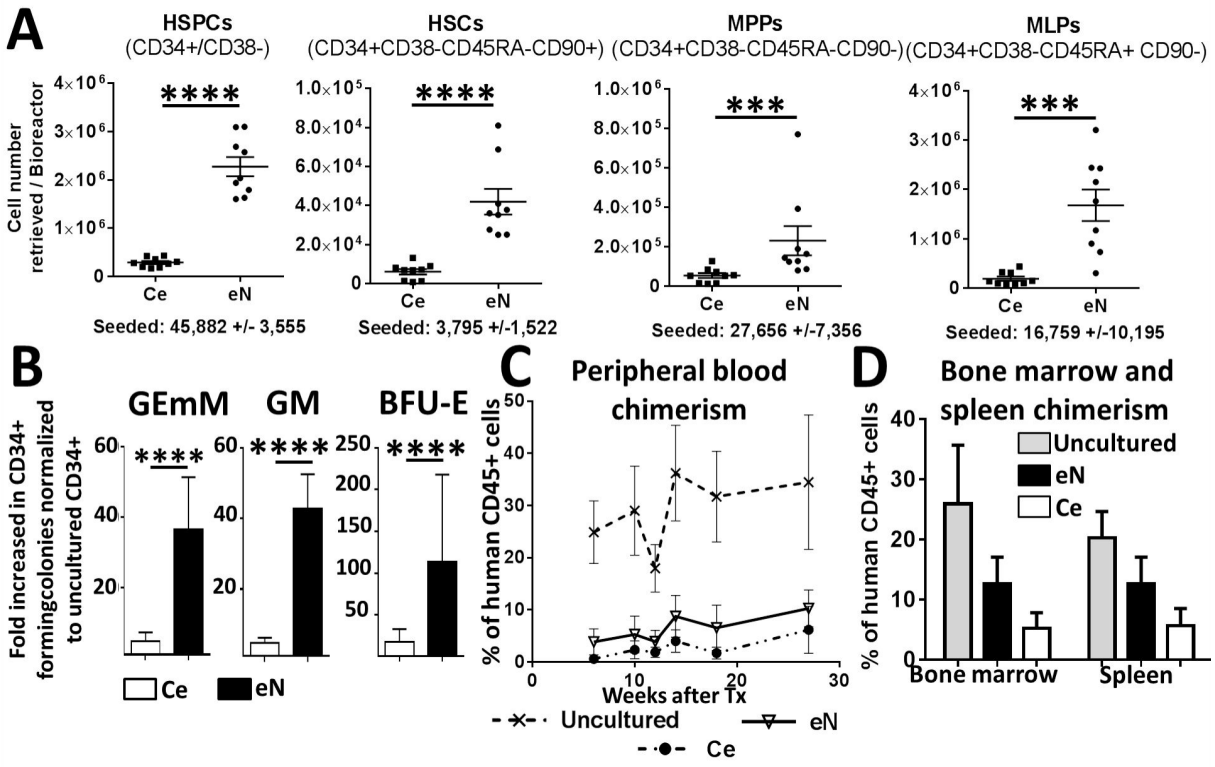

Figure 15. Engineered 3D microenvironments allow the maintenance/expansion of functional HSPCs. (A) The engineered niche (eN) supports the expansion of phenotypic HSPCs, HSCs, multipotent progenitors (MPPs) and multipotent lymphoid progenitors (MLPs), as assessed by quantitative flow cytometry analysis post-3D culture. Data from n≥8 biological replicates are shown. Ce: ceramic only. **(B)** Improved maintenance of colony forming potential of eN versus Ce cultured $CD34^+$ cells. GEmM: Colony-forming unit-Granulocyte, Erythroid, macrophage, Megakaryocyte. GM: Colony-forming unit-granulocyte and macrophage. BFU-E: Burst- forming unit-erythroid. Summarized data from n≥9 biological replicates are presented. **(C-D)** The long-term repopulation capacity of eN and Ce cultured $CD34^+$ cells. Uncultured $CD34^+$ cells served as positive control. Data from n≥4 biological replicates are displayed. **(C)** Reconstitution of the human blood compartment (% of human CD45+ cells in mononuclear cells) in NSG mice is shown by flow cytometry analysis of peripheral blood. **(D)** Human $CD34^+$ cells cultured on eN and Ce also robustly engrafted in the bone marrow and spleen of transplanted mice, as assessed by flow cytometry 28 weeks post- transplantation. A Mann-Whitney U Test (for not normally distributed data) or students t-test (for normally distributed data) was used for statistical analyses.

Taken together, this system can be used to expand and analyze HSPCs *in vitro* and could also be adapted to recapitulate pathological situations such as leukemia. For example, the use of human MSCs and/or HSPCs harvested from patients suffering from leukemia can offer the opportunity to model the disease *in vitro*, in an entirely human and ideally personalized setting with niche-interactions. This could represent a powerful tool with wide range of applications, from the identification of factors deregulating niche or blood functions, to the screening of drugs to predict patient-specific response to defined treatments without the need of an experimental model.

Chapter 6.

OUTLOOK

In summary, we have developed and optimized an *in vivo* xenotransplantation model to study human primary AML samples from different genetic backgrounds, which represents a powerful tool in AML research. This model enables investigations regarding leukemia kinetics in dependency of the special AML subtype and risk group, further characterization of extrinsic (e.g. catecholamines) and intrinsic (e.g. *CDX2*) factors regulating leukemogenesis, and studies on the effects of treatments with chemotherapy, NK cells, PARP1 and WNT modulators on *in vivo* leukemogenesis and LSC subpopulations.

However, this model is still limited e.g. due to the artificial situation of immunosuppression in mice and for example focusing on the niche regulations by *WNT* signaling cannot depict the various possible microenvironmental interplays, but shows at least one mechanism how AML cells conquer the healthy HSC niches. More efforts to understand the far-reaching interconnections of AML cells, healthy HSCs, immune and niche cells are necessary to get more insights and possible targets to develop new therapeutic agents in regard to novel approaches.

Chapter 7.

REFERENCES

Almeida, R., Silva, E., Santos-Silva, F., Silberg, D.G., Wang, J., De Bolos, C., and David, L. (2003). Expression of intestine-specific transcription factors, CDX1 and CDX2, in intestinal metaplasia and gastric carcinomas. J Pathol *199*, 36-40.

Ames, E., Canter, R.J., Grossenbacher, S.K., Mac, S., Chen, M., Smith, R.C., Hagino, T., Perez-Cunningham, J., Sckisel, G.D., Urayama, S., *et al.* (2015). NK Cells Preferentially Target Tumor Cells with a Cancer Stem Cell Phenotype. J Immunol *195*, 4010-4019.

Bansal, D., Scholl, C., Frohling, S., McDowell, E., Lee, B.H., Dohner, K., Ernst, P., Davidson, A.J., Daley, G.Q., Zon, L.I., *et al.* (2006). Cdx4 dysregulates Hox gene expression and generates acute myeloid leukemia alone and in cooperation with Meis1a in a murine model. Proc Natl Acad Sci U S A *103*, 16924-16929.

Bhat, A.A., Sharma, A., Pope, J., Krishnan, M., Washington, M.K., Singh, A.B., and Dhawan, P. (2012). Caudal homeobox protein Cdx-2 cooperates with Wnt pathway to regulate claudin-1 expression in colon cancer cells. PLoS One *7*, e37174.

Bonnet, D., and Dick, J.E. (1997). Human acute myeloid leukemia is organized as a hierarchy that originates from a primitive hematopoietic cell. Nat Med *3*, 730-737.

Brooke-Bisschop, T., Savory, J.G.A., Foley, T., Ringuette, R., and Lohnes, D. (2017). Essential roles for Cdx in murine primitive hematopoiesis. Dev Biol *422*, 115-124.

Calvi, L.M., Adams, G.B., Weibrecht, K.W., Weber, J.M., Olson, D.P., Knight, M.C., Martin, R.P., Schipani, E., Divieti, P., Bringhurst, F.R., *et al.* (2003). Osteoblastic cells regulate the haematopoietic stem cell niche. Nature *425*, 841-846.

Chawengsaksophak, K., de Graaff, W., Rossant, J., Deschamps, J., and Beck, F. (2004). Cdx2 is essential for axial elongation in mouse development. Proc Natl Acad Sci U S A *101*, 7641-7645.

Chawengsaksophak, K., James, R., Hammond, V.E., Köntgen, F., and Beck, F. (1997). Homeosis and intestinal tumours in Cdx2 mutant mice. Nature *386*, 84-87.

Chung, S.S., Eng, W.S., Hu, W., Khalaj, M., Garrett-Bakelman, F.E., Tavakkoli, M., Levine, R.L., Carroll, M., Klimek, V.M., Melnick, A.M., *et al.* (2017). CD99 is a therapeutic target on disease stem cells in myeloid malignancies. Sci Transl Med *9*.

Clément-Lacroix, P., Ai, M., Morvan, F., Roman-Roman, S., Vayssière, B., Belleville, C., Estrera, K., Warman, M.L., Baron, R., and Rawadi, G. (2005). Lrp5-independent activation of Wnt signaling by lithium chloride increases bone formation and bone mass in mice. Proc Natl Acad Sci U S A *102*, 17406-17411.

Cosgun, K.N., Rahmig, S., Mende, N., Reinke, S., Hauber, I., Schäfer, C., Petzold, A., Weisbach, H., Heidkamp, G., Purbojo, A., *et al.* (2014). Kit regulates HSC engraftment across the human-mouse species barrier. Cell Stem Cell *15*, 227-238.

Cumano, A., and Godin, I. (2007). Ontogeny of the hematopoietic system. Annu Rev Immunol *25*, 745-785.

Dar, A., Schajnovitz, A., Lapid, K., Kalinkovich, A., Itkin, T., Ludin, A., Kao, W.M., Battista, M., Tesio, M., Kollet, O., *et al.* (2011). Rapid mobilization of hematopoietic progenitors by AMD3100 and catecholamines is mediated by CXCR4-dependent SDF-1 release from bone marrow stromal cells. Leukemia *25*, 1286-1296.

Daria, D., Kirsten, N., Muranyi, A., Mulaw, M., Ihme, S., Kechter, A., Hollnagel, M., Bullinger, L., Döhner, K., Döhner, H., *et al.* (2016). GPR56 contributes to the development of acute myeloid leukemia in mice. Leukemia *30*, 1734-1741.

Davidson, A.J., Ernst, P., Wang, Y., Dekens, M.P., Kingsley, P.D., Palis, J., Korsmeyer, S.J., Daley, G.Q., and Zon, L.I. (2003). cdx4 mutants fail to specify blood progenitors and can be rescued by multiple hox genes. Nature *425*, 300-306.

Davidson, A.J., and Zon, L.I. (2006). The caudal-related homeobox genes cdx1a and cdx4 act redundantly to regulate hox gene expression and the formation of putative hematopoietic stem cells during zebrafish embryogenesis. Dev Biol *292*, 506-518.

de Rooij, J. (2014). Cadherin adhesion controlled by cortical actin dynamics. Nat Cell Biol *16*, 508-510.

Debernardi, S., Lillington, D.M., Chaplin, T., Tomlinson, S., Amess, J., Rohatiner, A., Lister, T.A., and Young, B.D. (2003). Genome-wide analysis of acute myeloid leukemia with normal karyotype reveals a unique pattern of homeobox gene expression distinct from those with translocation-mediated fusion events. Genes Chromosomes Cancer *37*, 149-158.

Dellatore, S.M., Garcia, A.S., and Miller, W.M. (2008). Mimicking stem cell niches to increase stem cell expansion. Curr Opin Biotechnol *19*, 534-540.

Di Maggio, N., Piccinini, E., Jaworski, M., Trumpp, A., Wendt, D.J., and Martin, I. (2011). Toward modeling the bone marrow niche using scaffold-based 3D culture systems. Biomaterials *32*, 321-329.

Di Tomaso, T., Mazzoleni, S., Wang, E., Sovena, G., Clavenna, D., Franzin, A., Mortini, P., Ferrone, S., Doglioni, C., Marincola, F.M., *et al.* (2010). Immunobiological characterization of cancer stem cells isolated from glioblastoma patients. Clin Cancer Res *16*, 800-813.

Dong, H., and Chen, L. (2003). B7-H1 pathway and its role in the evasion of tumor immunity. J Mol Med (Berl) *81*, 281-287.

Dulphy, N., Chrétien, A.S., Khaznadar, Z., Fauriat, C., Nanbakhsh, A., Caignard, A., Chouaib, S., Olive, D., and Toubert, A. (2016). Underground Adaptation to a Hostile Environment: Acute Myeloid Leukemia vs. Natural Killer Cells. Front Immunol *7*, 94.

Döhner, H., Estey, E., Grimwade, D., Amadori, S., Appelbaum, F.R., Büchner, T., Dombret, H., Ebert, B.L., Fenaux, P., Larson, R.A., *et al.* (2017). Diagnosis and management of AML in adults: 2017 ELN recommendations from an international expert panel. Blood *129*, 424-447.

Eda, A., Osawa, H., Satoh, K., Yanaka, I., Kihira, K., Ishino, Y., Mutoh, H., and Sugano, K. (2003). Aberrant expression of CDX2 in Barrett's epithelium and inflammatory esophageal mucosa. J Gastroenterol *38*, 14-22.

Eppert, K., Takenaka, K., Lechman, E.R., Waldron, L., Nilsson, B., van Galen, P., Metzeler, K.H., Poeppl, A., Ling, V., Beyene, J., *et al.* (2011). Stem cell gene

expression programs influence clinical outcome in human leukemia. Nat Med *17*, 1086-1093.

Esler, M., Eikelis, N., Schlaich, M., Lambert, G., Alvarenga, M., Kaye, D., El-Osta, A., Guo, L., Barton, D., Pier, C., *et al.* (2008). Human sympathetic nerve biology: parallel influences of stress and epigenetics in essential hypertension and panic disorder. Ann N Y Acad Sci *1148*, 338-348.

Faber, K., Bullinger, L., Ragu, C., Garding, A., Mertens, D., Miller, C., Martin, D., Walcher, D., Dohner, K., Dohner, H., *et al.* (2013). CDX2-driven leukemogenesis involves KLF4 repression and deregulated PPARgamma signaling. J Clin Invest *123*, 299-314.

Fauriat, C., Just-Landi, S., Mallet, F., Arnoulet, C., Sainty, D., Olive, D., and Costello, R.T. (2007). Deficient expression of NCR in NK cells from acute myeloid leukemia: Evolution during leukemia treatment and impact of leukemia cells in NCRdull phenotype induction. Blood *109*, 323-330.

Ferrara, F., and Schiffer, C.A. (2013). Acute myeloid leukaemia in adults. Lancet *381*, 484-495.

Fleming, H.E., Janzen, V., Lo Celso, C., Guo, J., Leahy, K.M., Kronenberg, H.M., and Scadden, D.T. (2008). Wnt signaling in the niche enforces hematopoietic stem cell quiescence and is necessary to preserve self-renewal in vivo. Cell Stem Cell *2*, 274-283.

Frohling, S., Scholl, C., Bansal, D., and Huntly, B.J. (2007). HOX gene regulation in acute myeloid leukemia: CDX marks the spot? Cell Cycle *6*, 2241-2245.

Fu, L., Patel, M.S., Bradley, A., Wagner, E.F., and Karsenty, G. (2005). The molecular clock mediates leptin-regulated bone formation. Cell *122*, 803-815.

Goulard, M., Dosquet, C., and Bonnet, D. (2018). Role of the microenvironment in myeloid malignancies. Cell Mol Life Sci *75*, 1377-1391.

Greim, H., Kaden, D.A., Larson, R.A., Palermo, C.M., Rice, J.M., Ross, D., and Snyder, R. (2014). The bone marrow niche, stem cells, and leukemia: impact of drugs, chemicals, and the environment. Ann N Y Acad Sci *1310*, 7-31.

Guerra, N., Tan, Y.X., Joncker, N.T., Choy, A., Gallardo, F., Xiong, N., Knoblaugh, S., Cado, D., Greenberg, N.M., Greenberg, N.R., *et al.* (2008).

NKG2D-deficient mice are defective in tumor surveillance in models of spontaneous malignancy. Immunity *28*, 571-580.

Guilak, F., Cohen, D.M., Estes, B.T., Gimble, J.M., Liedtke, W., and Chen, C.S. (2009). Control of stem cell fate by physical interactions with the extracellular matrix. Cell Stem Cell *5*, 17-26.

Gutierrez, S.E., and Romero-Oliva, F.A. (2013). Epigenetic changes: a common theme in acute myelogenous leukemogenesis. J Hematol Oncol *6*, 57.

Hanahan, D., and Weinberg, R.A. (2000). The hallmarks of cancer. Cell *100*, 57-70.

Hanahan, D., and Weinberg, R.A. (2011). Hallmarks of cancer: the next generation. Cell *144*, 646-674.

Heidt, T., Sager, H.B., Courties, G., Dutta, P., Iwamoto, Y., Zaltsman, A., von Zur Muhlen, C., Bode, C., Fricchione, G.L., Denninger, J., *et al.* (2014). Chronic variable stress activates hematopoietic stem cells. Nat Med *20*, 754-758.

Herrmann, H., Blatt, K., Shi, J., Gleixner, K.V., Cerny-Reiterer, S., Mullauer, L., Vakoc, C.R., Sperr, W.R., Horny, H.P., Bradner, J.E., *et al.* (2012). Small-molecule inhibition of BRD4 as a new potent approach to eliminate leukemic stem- and progenitor cells in acute myeloid leukemia AML. Oncotarget *3*, 1588-1599.

Hirano, F., Kaneko, K., Tamura, H., Dong, H., Wang, S., Ichikawa, M., Rietz, C., Flies, D.B., Lau, J.S., Zhu, G., *et al.* (2005). Blockade of B7-H1 and PD-1 by monoclonal antibodies potentiates cancer therapeutic immunity. Cancer Res *65*, 1089-1096.

Hope, K.J., Jin, L., and Dick, J.E. (2004). Acute myeloid leukemia originates from a hierarchy of leukemic stem cell classes that differ in self-renewal capacity. Nat Immunol *5*, 738-743.

Hosen, N., Park, C.Y., Tatsumi, N., Oji, Y., Sugiyama, H., Gramatzki, M., Krensky, A.M., and Weissman, I.L. (2007). CD96 is a leukemic stem cell-specific marker in human acute myeloid leukemia. Proc Natl Acad Sci U S A *104*, 11008-11013.

Jagannathan-Bogdan, M., and Zon, L.I. (2013). Hematopoiesis. Development *140*, 2463-2467.

James, R., Erler, T., and Kazenwadel, J. (1994). Structure of the murine homeobox gene cdx-2. Expression in embryonic and adult intestinal epithelium. J Biol Chem *269*, 15229-15237.

Jan, M., Chao, M.P., Cha, A.C., Alizadeh, A.A., Gentles, A.J., Weissman, I.L., and Majeti, R. (2011). Prospective separation of normal and leukemic stem cells based on differential expression of TIM3, a human acute myeloid leukemia stem cell marker. Proc Natl Acad Sci U S A *108*, 5009-5014.

Jedrusik, A., Parfitt, D.E., Guo, G., Skamagki, M., Grabarek, J.B., Johnson, M.H., Robson, P., and Zernicka-Goetz, M. (2008). Role of Cdx2 and cell polarity in cell allocation and specification of trophectoderm and inner cell mass in the mouse embryo. Genes Dev *22*, 2692-2706.

Jin, L., Hope, K.J., Zhai, Q., Smadja-Joffe, F., and Dick, J.E. (2006). Targeting of CD44 eradicates human acute myeloid leukemic stem cells. Nat Med *12*, 1167-1174.

Jin, L., Lee, E.M., Ramshaw, H.S., Busfield, S.J., Peoppl, A.G., Wilkinson, L., Guthridge, M.A., Thomas, D., Barry, E.F., Boyd, A., *et al.* (2009). Monoclonal antibody-mediated targeting of CD123, IL-3 receptor alpha chain, eliminates human acute myeloid leukemic stem cells. Cell Stem Cell *5*, 31-42.

Juliusson, G., Antunovic, P., Derolf, A., Lehmann, S., Mollgard, L., Stockelberg, D., Tidefelt, U., Wahlin, A., and Hoglund, M. (2009). Age and acute myeloid leukemia: real world data on decision to treat and outcomes from the Swedish Acute Leukemia Registry. Blood *113*, 4179-4187.

Katayama, Y., Battista, M., Kao, W.M., Hidalgo, A., Peired, A.J., Thomas, S.A., and Frenette, P.S. (2006). Signals from the sympathetic nervous system regulate hematopoietic stem cell egress from bone marrow. Cell *124*, 407-421.

Kfoury, Y., and Scadden, D.T. (2015). Mesenchymal cell contributions to the stem cell niche. Cell Stem Cell *16*, 239-253.

Khaznadar, Z., Boissel, N., Agaugué, S., Henry, G., Cheok, M., Vignon, M., Geromin, D., Cayuela, J.M., Castaigne, S., Pautas, C., *et al.* (2015). Defective NK Cells in Acute Myeloid Leukemia Patients at Diagnosis Are Associated with Blast Transcriptional Signatures of Immune Evasion. J Immunol *195*, 2580-2590.

Kim, T.H., Gill, N.K., Nyberg, K.D., Nguyen, A.V., Hohlbauch, S.V., Geisse, N.A., Nowell, C.J., Sloan, E.K., and Rowat, A.C. (2016). Cancer cells become less deformable and more invasive with activation of β-adrenergic signaling. J Cell Sci *129*, 4563-4575.

Klco, J.M., Spencer, D.H., Miller, C.A., Griffith, M., Lamprecht, T.L., O'Laughlin, M., Fronick, C., Magrini, V., Demeter, R.T., Fulton, R.S., *et al.* (2014). Functional heterogeneity of genetically defined subclones in acute myeloid leukemia. Cancer Cell *25*, 379-392.

Konantz, M., Andre, M.C., Ebinger, M., Grauer, M., Wang, H., Grzywna, S., Rothfuss, O.C., Lehle, S., Kustikova, O.S., Salih, H.R., *et al.* (2013). EVI-1 modulates leukemogenic potential and apoptosis sensitivity in human acute lymphoblastic leukemia. Leukemia *27*, 56-65.

Koo, S., Huntly, B.J., Wang, Y., Chen, J., Brumme, K., Ball, B., McKinney-Freeman, S.L., Yabuuchi, A., Scholl, C., Bansal, D., *et al.* (2010). Cdx4 is dispensable for murine adult hematopoietic stem cells but promotes MLL-AF9-mediated leukemogenesis. Haematologica *95*, 1642-1650.

Lanier, L.L. (2001). A renaissance for the tumor immunosurveillance hypothesis. Nat Med *7*, 1178-1180.

Lapidot, T., Sirard, C., Vormoor, J., Murdoch, B., Hoang, T., Caceres-Cortes, J., Minden, M., Paterson, B., Caligiuri, M.A., and Dick, J.E. (1994). A cell initiating human acute myeloid leukaemia after transplantation into SCID mice. Nature *367*, 645-648.

Lengerke, C., and Daley, G.Q. (2012). Caudal genes in blood development and leukemia. Ann N Y Acad Sci *1266*, 47-54.

Lengerke, C., Grauer, M., Niebuhr, N.I., Riedt, T., Kanz, L., Park, I.H., and Daley, G.Q. (2009). Hematopoietic development from human induced pluripotent stem cells. Ann N Y Acad Sci *1176*, 219-227.

Lengerke, C., McKinney-Freeman, S., Naveiras, O., Yates, F., Wang, Y., Bansal, D., and Daley, G.Q. (2007). The cdx-hox pathway in hematopoietic stem cell formation from embryonic stem cells. Ann N Y Acad Sci *1106*, 197-208.

Lengerke, C., Schmitt, S., Bowman, T.V., Jang, I.H., Maouche-Chretien, L., McKinney-Freeman, S., Davidson, A.J., Hammerschmidt, M., Rentzsch, F., Green, J.B., *et al.* (2008). BMP and Wnt specify hematopoietic fate by activation of the Cdx-Hox pathway. Cell Stem Cell *2*, 72-82.

Liu, A.C., Lewis, W.G., and Kay, S.A. (2007). Mammalian circadian signaling networks and therapeutic targets. Nat Chem Biol *3*, 630-639.

Majeti, R., Chao, M.P., Alizadeh, A.A., Pang, W.W., Jaiswal, S., Gibbs, K.D., van Rooijen, N., and Weissman, I.L. (2009). CD47 is an adverse prognostic factor and therapeutic antibody target on human acute myeloid leukemia stem cells. Cell *138*, 286-299.

Mazurier, F., Doedens, M., Gan, O.I., and Dick, J.E. (2003). Rapid myeloerythroid repopulation after intrafemoral transplantation of NOD-SCID mice reveals a new class of human stem cells. Nat Med *9*, 959-963.

McGrath, K.E., Frame, J.M., Fromm, G.J., Koniski, A.D., Kingsley, P.D., Little, J., Bulger, M., and Palis, J. (2011). A transient definitive erythroid lineage with unique regulation of the beta-globin locus in the mammalian embryo. Blood *117*, 4600-4608.

McKinney-Freeman, S.L., Lengerke, C., Jang, I.H., Schmitt, S., Wang, Y., Philitas, M., Shea, J., and Daley, G.Q. (2008). Modulation of murine embryonic stem cell-derived CD41+c-kit+ hematopoietic progenitors by ectopic expression of Cdx genes. Blood *111*, 4944-4953.

Medinger, M., Halter, J., Heim, D., Buser, A., Gerull, S., Lengerke, C., and Passweg, J. (2016a). Gene-expression Profiling in Patients with Plasma Cell Myeloma Treated with Novel Agents. Cancer Genomics Proteomics *13*, 275-279.

Medinger, M., Lengerke, C., and Passweg, J. (2016b). Novel Prognostic and Therapeutic Mutations in Acute Myeloid Leukemia. Cancer Genomics Proteomics *13*, 317-329.

Medinger, M., Lengerke, C., and Passweg, J. (2016c). Novel therapeutic options in Acute Myeloid Leukemia. Leuk Res Rep *6*, 39-49.

Mendelson, A., and Frenette, P.S. (2014). Hematopoietic stem cell niche maintenance during homeostasis and regeneration. Nat Med *20*, 833-846.

Morrison, S.J., and Scadden, D.T. (2014). The bone marrow niche for haematopoietic stem cells. Nature *505*, 327-334.

Mrózek, K., Marcucci, G., Nicolet, D., Maharry, K.S., Becker, H., Whitman, S.P., Metzeler, K.H., Schwind, S., Wu, Y.Z., Kohlschmidt, J., *et al.* (2012). Prognostic significance of the European LeukemiaNet standardized system for reporting cytogenetic and molecular alterations in adults with acute myeloid leukemia. J Clin Oncol *30*, 4515-4523.

Méndez-Ferrer, S., Lucas, D., Battista, M., and Frenette, P.S. (2008). Haematopoietic stem cell release is regulated by circadian oscillations. Nature *452*, 442-447.

Méndez-Ferrer, S., Michurina, T.V., Ferraro, F., Mazloom, A.R., Macarthur, B.D., Lira, S.A., Scadden, D.T., Ma'ayan, A., Enikolopov, G.N., and Frenette, P.S. (2010). Mesenchymal and haematopoietic stem cells form a unique bone marrow niche. Nature *466*, 829-834.

Nagel, G., Weber, D., Fromm, E., Erhardt, S., Lübbert, M., Fiedler, W., Kindler, T., Krauter, J., Brossart, P., Kündgen, A., *et al.* (2017). Epidemiological, genetic, and clinical characterization by age of newly diagnosed acute myeloid leukemia based on an academic population-based registry study (AMLSG BiO). Ann Hematol *96*, 1993-2003.

Ng, S.W., Mitchell, A., Kennedy, J.A., Chen, W.C., McLeod, J., Ibrahimova, N., Arruda, A., Popescu, A., Gupta, V., Schimmer, A.D., *et al.* (2016). A 17-gene stemness score for rapid determination of risk in acute leukaemia. Nature *540*, 433-437.

Notta, F., Doulatov, S., and Dick, J.E. (2010). Engraftment of human hematopoietic stem cells is more efficient in female NOD/SCID/IL-2Rgc-null recipients. Blood *115*, 3704-3707.

Orkin, S.H., and Zon, L.I. (2008). Hematopoiesis: an evolving paradigm for stem cell biology. Cell *132*, 631-644.

Pabst, C., Bergeron, A., Lavallée, V.P., Yeh, J., Gendron, P., Norddahl, G.L., Krosl, J., Boivin, I., Deneault, E., Simard, J., *et al.* (2016). GPR56 identifies pri-

mary human acute myeloid leukemia cells with high repopulating potential in vivo. Blood *127*, 2018-2027.

Paczulla, A.M., Dirnhofer, S., Konantz, M., Medinger, M., Salih, H.R., Rothfelder, K., Tsakiris, D.A., Passweg, J.R., Lundberg, P., and Lengerke, C. (2017). Long-term observation reveals high-frequency engraftment of human acute myeloid leukemia in immunodeficient mice. Haematologica *102*, 854-864.

Palis, J., and Yoder, M.C. (2001). Yolk-sac hematopoiesis: the first blood cells of mouse and man. Exp Hematol *29*, 927-936.

Peerani, R., and Zandstra, P.W. (2010). Enabling stem cell therapies through synthetic stem cell-niche engineering. J Clin Invest *120*, 60-70.

Pilon, N., Oh, K., Sylvestre, J.R., Bouchard, N., Savory, J., and Lohnes, D. (2006). Cdx4 is a direct target of the canonical Wnt pathway. Dev Biol *289*, 55-63.

Pilon, N., Oh, K., Sylvestre, J.R., Savory, J.G., and Lohnes, D. (2007). Wnt signaling is a key mediator of Cdx1 expression in vivo. Development *134*, 2315-2323.

Porter, J.R., Ruckh, T.T., and Popat, K.C. (2009). Bone tissue engineering: a review in bone biomimetics and drug delivery strategies. Biotechnol Prog *25*, 1539-1560.

Quek, L., Otto, G.W., Garnett, C., Lhermitte, L., Karamitros, D., Stoilova, B., Lau, I.J., Doondeea, J., Usukhbayar, B., Kennedy, A., *et al.* (2016). Genetically distinct leukemic stem cells in human CD34- acute myeloid leukemia are arrested at a hemopoietic precursor-like stage. J Exp Med *213*, 1513-1535.

Rawat, V.P., Cusan, M., Deshpande, A., Hiddemann, W., Quintanilla-Martinez, L., Humphries, R.K., Bohlander, S.K., Feuring-Buske, M., and Buske, C. (2004). Ectopic expression of the homeobox gene Cdx2 is the transforming event in a mouse model of t(12;13)(p13;q12) acute myeloid leukemia. Proc Natl Acad Sci U S A *101*, 817-822.

Rawat, V.P., Humphries, R.K., and Buske, C. (2012). Beyond Hox: the role of ParaHox genes in normal and malignant hematopoiesis. Blood *120*, 519-527.

Rawat, V.P., Thoene, S., Naidu, V.M., Arseni, N., Heilmeier, B., Metzeler, K., Petropoulos, K., Deshpande, A., Quintanilla-Martinez, L., Bohlander, S.K., *et*

al. (2008). Overexpression of CDX2 perturbs HOX gene expression in murine progenitors depending on its N-terminal domain and is closely correlated with deregulated HOX gene expression in human acute myeloid leukemia. Blood *111*, 309-319.

Reim, F., Dombrowski, Y., Ritter, C., Buttmann, M., Häusler, S., Ossadnik, M., Krockenberger, M., Beier, D., Beier, C.P., Dietl, J., *et al.* (2009). Immunoselection of breast and ovarian cancer cells with trastuzumab and natural killer cells: selective escape of CD44high/CD24low/HER2low breast cancer stem cells. Cancer Res *69*, 8058-8066.

Reinisch, A., Thomas, D., Corces, M.R., Zhang, X., Gratzinger, D., Hong, W.J., Schallmoser, K., Strunk, D., and Majeti, R. (2016). A humanized bone marrow ossicle xenotransplantation model enables improved engraftment of healthy and leukemic human hematopoietic cells. Nat Med.

Riedt, T., Ebinger, M., Salih, H.R., Tomiuk, J., Handgretinger, R., Kanz, L., Grunebach, F., and Lengerke, C. (2009). Aberrant expression of the homeobox gene CDX2 in pediatric acute lymphoblastic leukemia. Blood *113*, 4049-4051.

Rieger, M.A., Hoppe, P.S., Smejkal, B.M., Eitelhuber, A.C., and Schroeder, T. (2009). Hematopoietic cytokines can instruct lineage choice. Science *325*, 217-218.

Ro, H., and Dawid, I.B. (2011). Modulation of Tcf3 repressor complex composition regulates cdx4 expression in zebrafish. Embo J *30*, 2894-2907.

Rombouts, W.J., Blokland, I., Löwenberg, B., and Ploemacher, R.E. (2000a). Biological characteristics and prognosis of adult acute myeloid leukemia with internal tandem duplications in the Flt3 gene. Leukemia *14*, 675-683.

Rombouts, W.J., Martens, A.C., and Ploemacher, R.E. (2000b). Identification of variables determining the engraftment potential of human acute myeloid leukemia in the immunodeficient NOD/SCID human chimera model. Leukemia *14*, 889-897.

Rongvaux, A., Willinger, T., Martinek, J., Strowig, T., Gearty, S.V., Teichmann, L.L., Saito, Y., Marches, F., Halene, S., Palucka, A.K., *et al.* (2014). Development and function of human innate immune cells in a humanized mouse model. Nat Biotechnol *32*, 364-372.

Rossi, D.J., Seita, J., Czechowicz, A., Bhattacharya, D., Bryder, D., and Weissman, I.L. (2007). Hematopoietic stem cell quiescence attenuates DNA damage response and permits DNA damage accumulation during aging. Cell Cycle *6*, 2371-2376.

Ruggeri, L., Capanni, M., Urbani, E., Perruccio, K., Shlomchik, W.D., Tosti, A., Posati, S., Rogaia, D., Frassoni, F., Aversa, F., *et al.* (2002). Effectiveness of donor natural killer cell alloreactivity in mismatched hematopoietic transplants. Science *295*, 2097-2100.

Saito, Y., Kaneda, K., Suekane, A., Ichihara, E., Nakahata, S., Yamakawa, N., Nagai, K., Mizuno, N., Kogawa, K., Miura, I., *et al.* (2013). Maintenance of the hematopoietic stem cell pool in bone marrow niches by EVI1-regulated GPR56. Leukemia *27*, 1637-1649.

Saito, Y., Kitamura, H., Hijikata, A., Tomizawa-Murasawa, M., Tanaka, S., Takagi, S., Uchida, N., Suzuki, N., Sone, A., Najima, Y., *et al.* (2010). Identification of therapeutic targets for quiescent, chemotherapy-resistant human leukemia stem cells. Sci Transl Med *2*, 17ra19.

Sanchez, P.V., Perry, R.L., Sarry, J.E., Perl, A.E., Murphy, K., Swider, C.R., Bagg, A., Choi, J.K., Biegel, J.A., Danet-Desnoyers, G., *et al.* (2009). A robust xenotransplantation model for acute myeloid leukemia. Leukemia *23*, 2109-2117.

Sanchez-Ferras, O., Coutaud, B., Djavanbakht Samani, T., Tremblay, I., Souchkova, O., and Pilon, N. (2012). Caudal-related homeobox (Cdx) protein-dependent integration of canonical Wnt signaling on paired-box 3 (Pax3) neural crest enhancer. J Biol Chem *287*, 16623-16635.

Schatton, T., Schutte, U., Frank, N.Y., Zhan, Q., Hoerning, A., Robles, S.C., Zhou, J., Hodi, F.S., Spagnoli, G.C., Murphy, G.F., *et al.* (2010). Modulation of T-cell activation by malignant melanoma initiating cells. Cancer Res *70*, 697-708.

Schofield, R. (1978). The relationship between the spleen colony-forming cell and the haemopoietic stem cell. Blood Cells *4*, 7-25.

Schofield, R. (1983). The stem cell system. Biomed Pharmacother *37*, 375-380.

Scholl, C., Bansal, D., Dohner, K., Eiwen, K., Huntly, B.J., Lee, B.H., Rucker, F.G., Schlenk, R.F., Bullinger, L., Dohner, H., *et al.* (2007). The homeobox gene CDX2 is aberrantly expressed in most cases of acute myeloid leukemia and promotes leukemogenesis. J Clin Invest *117*, 1037-1048.

Schulenburg, A., Bramswig, K., Herrmann, H., Karlic, H., Mirkina, I., Hubmann, R., Laffer, S., Marian, B., Shehata, M., Krepler, C., *et al.* (2010). Neoplastic stem cells: current concepts and clinical perspectives. Crit Rev Oncol Hematol *76*, 79-98.

Sherwood, R.I., Maehr, R., Mazzoni, E.O., and Melton, D.A. (2011). Wnt signaling specifies and patterns intestinal endoderm. Mech Dev *128*, 387-400.

Shlush, L.I., Zandi, S., Mitchell, A., Chen, W.C., Brandwein, J.M., Gupta, V., Kennedy, J.A., Schimmer, A.D., Schuh, A.C., Yee, K.W., *et al.* (2014). Identification of pre-leukaemic haematopoietic stem cells in acute leukaemia. Nature *506*, 328-333.

Shultz, L.D., Lyons, B.L., Burzenski, L.M., Gott, B., Chen, X., Chaleff, S., Kotb, M., Gillies, S.D., King, M., Mangada, J., *et al.* (2005). Human lymphoid and myeloid cell development in NOD/LtSz-scid IL2R gamma null mice engrafted with mobilized human hemopoietic stem cells. J Immunol *174*, 6477-6489.

Silva, P., Neumann, M., Schroeder, M.P., Vosberg, S., Schlee, C., Isaakidis, K., Ortiz-Tanchez, J., Fransecky, L.R., Hartung, T., Türkmen, S., *et al.* (2017). Acute myeloid leukemia in the elderly is characterized by a distinct genetic and epigenetic landscape. Leukemia *31*, 1640-1644.

Sontakke, P., Carretta, M., Capala, M., Schepers, H., and Schuringa, J.J. (2014). Ex vivo assays to study self-renewal, long-term expansion, and leukemic transformation of genetically modified human hematopoietic and patient-derived leukemic stem cells. Methods Mol Biol *1185*, 195-210.

Spiegel, A., Shivtiel, S., Kalinkovich, A., Ludin, A., Netzer, N., Goichberg, P., Azaria, Y., Resnick, I., Hardan, I., Ben-Hur, H., *et al.* (2007). Catecholaminergic neurotransmitters regulate migration and repopulation of immature human CD34+ cells through Wnt signaling. Nat Immunol *8*, 1123-1131.

Strowig, T., Rongvaux, A., Rathinam, C., Takizawa, H., Borsotti, C., Philbrick, W., Eynon, E.E., Manz, M.G., and Flavell, R.A. (2011). Transgenic expression of human signal regulatory protein alpha in Rag2-/-gamma(c)-/- mice im-

proves engraftment of human hematopoietic cells in humanized mice. Proc Natl Acad Sci U S A *108*, 13218-13223.

Subramanian, V., Meyer, B.I., and Gruss, P. (1995). Disruption of the murine homeobox gene Cdx1 affects axial skeletal identities by altering the mesodermal expression domains of Hox genes. Cell *83*, 641-653.

Takasato, M., Er, P.X., Chiu, H.S., Maier, B., Baillie, G.J., Ferguson, C., Parton, R.G., Wolvetang, E.J., Roost, M.S., Chuva de Sousa Lopes, S.M., *et al.* (2015). Kidney organoids from human iPS cells contain multiple lineages and model human nephrogenesis. Nature *526*, 564-568.

Takebe, T., Sekine, K., Enomura, M., Koike, H., Kimura, M., Ogaeri, T., Zhang, R.R., Ueno, Y., Zheng, Y.W., Koike, N., *et al.* (2013). Vascularized and functional human liver from an iPSC-derived organ bud transplant. Nature *499*, 481-484.

Taussig, D.C., Vargaftig, J., Miraki-Moud, F., Griessinger, E., Sharrock, K., Luke, T., Lillington, D., Oakervee, H., Cavenagh, J., Agrawal, S.G., *et al.* (2010). Leukemia-initiating cells from some acute myeloid leukemia patients with mutated nucleophosmin reside in the CD34(-) fraction. Blood *115*, 1976-1984.

Theocharides, A.P., Jin, L., Cheng, P.Y., Prasolava, T.K., Malko, A.V., Ho, J.M., Poeppl, A.G., van Rooijen, N., Minden, M.D., Danska, J.S., *et al.* (2012). Disruption of SIRPα signaling in macrophages eliminates human acute myeloid leukemia stem cells in xenografts. J Exp Med *209*, 1883-1899.

Theocharides, A.P., Rongvaux, A., Fritsch, K., Flavell, R.A., and Manz, M.G. (2016). Humanized hemato-lymphoid system mice. Haematologica *101*, 5-19.

Thoene, S., Rawat, V.P., Heilmeier, B., Hoster, E., Metzeler, K.H., Herold, T., Hiddemann, W., Gokbuget, N., Hoelzer, D., Bohlander, S.K., *et al.* (2009). The homeobox gene CDX2 is aberrantly expressed and associated with an inferior prognosis in patients with acute lymphoblastic leukemia. Leukemia *23*, 649-655.

Todaro, M., D'Asaro, M., Caccamo, N., Iovino, F., Francipane, M.G., Meraviglia, S., Orlando, V., La Mendola, C., Gulotta, G., Salerno, A., *et al.* (2009). Efficient killing of human colon cancer stem cells by gammadelta T lymphocytes. J Immunol *182*, 7287-7296.

Traggiai, E., Chicha, L., Mazzucchelli, L., Bronz, L., Piffaretti, J.C., Lanzavecchia, A., and Manz, M.G. (2004). Development of a human adaptive immune system in cord blood cell-transplanted mice. Science *304*, 104-107.

van de Ven, C., Bialecka, M., Neijts, R., Young, T., Rowland, J.E., Stringer, E.J., Van Rooijen, C., Meijlink, F., Novoa, A., Freund, J.N., *et al.* (2011). Concerted involvement of Cdx/Hox genes and Wnt signaling in morphogenesis of the caudal neural tube and cloacal derivatives from the posterior growth zone. Development *138*, 3451-3462.

van Rhenen, A., van Dongen, G.A., Kelder, A., Rombouts, E.J., Feller, N., Moshaver, B., Stigter-van Walsum, M., Zweegman, S., Ossenkoppele, G.J., and Jan Schuurhuis, G. (2007). The novel AML stem cell associated antigen CLL-1 aids in discrimination between normal and leukemic stem cells. Blood *110*, 2659-2666.

Vivier, E., Tomasello, E., Baratin, M., Walzer, T., and Ugolini, S. (2008). Functions of natural killer cells. Nat Immunol *9*, 503-510.

Vunjak-Novakovic, G., and Scadden, D.T. (2011). Biomimetic platforms for human stem cell research. Cell Stem Cell *8*, 252-261.

Wang, Y., Yabuuchi, A., McKinney-Freeman, S., Ducharme, D.M., Ray, M.K., Chawengsaksophak, K., Archer, T.K., and Daley, G.Q. (2008). Cdx gene deficiency compromises embryonic hematopoiesis in the mouse. Proc Natl Acad Sci U S A *105*, 7756-7761.

Weberpals, J., Jansen, L., Carr, P.R., Hoffmeister, M., and Brenner, H. (2016). Beta blockers and cancer prognosis - The role of immortal time bias: A systematic review and meta-analysis. Cancer Treat Rev *47*, 1-11.

Wei, J., Barr, J., Kong, L.Y., Wang, Y., Wu, A., Sharma, A.K., Gumin, J., Henry, V., Colman, H., Priebe, W., *et al.* (2010). Glioblastoma cancer-initiating cells inhibit T-cell proliferation and effector responses by the signal transducers and activators of transcription 3 pathway. Mol Cancer Ther *9*, 67-78.

Wendt, D., Marsano, A., Jakob, M., Heberer, M., and Martin, I. (2003). Oscillating perfusion of cell suspensions through three-dimensional scaffolds enhances cell seeding efficiency and uniformity. Biotechnol Bioeng *84*, 205-214.

Wilkinson, D.C., Alva-Ornelas, J.A., Sucre, J.M., Vijayaraj, P., Durra, A., Richardson, W., Jonas, S.J., Paul, M.K., Karumbayaram, S., Dunn, B., et al. (2017). Development of a Three-Dimensional Bioengineering Technology to Generate Lung Tissue for Personalized Disease Modeling. Stem Cells Transl Med 6, 622-633.

Zhang, C.C., and Lodish, H.F. (2008). Cytokines regulating hematopoietic stem cell function. Curr Opin Hematol 15, 307-311.

Zhang, J., Niu, C., Ye, L., Huang, H., He, X., Tong, W.G., Ross, J., Haug, J., Johnson, T., Feng, J.Q., et al. (2003). Identification of the haematopoietic stem cell niche and control of the niche size. Nature 425, 836-841.

Chapter 8.

ATTACHMENTS

“Absence of NKG2D ligands defines human leukaemia stem cells and mediates their immune evasion”

Paczulla A.M.*, Rothfelder K.*, Raffel S.*, Konantz M., Steinbacher J., Schaefer T., Dörfel D., Falcone M., Nievergall E., Tandler C., Lutz C., Lundberg P., Kanz L., Quintanilla-Martinez L., Steinle A., Trumpp A.*, Salih H.R.,*, and Lengerke C.*

in revision in Nature Medicine

Absence of NKG2D ligands defines human leukaemia stem cells and mediates their immune evasion

Anna M. Paczulla[1]*, Kathrin Rothfelder[2]*, Simon Raffel[3,4,5]*, Martina Konantz[1], Julia Steinbacher[2], Hui Wang[1], Thorsten Schäfer[1], Daniela Dörfel[2,6], Mattia Falcone[3], Eva Nievergall[3], Claudia Tandler[2], Christoph Lutz[6], Pontus Lundberg[7], Lothar Kanz[6], Leticia Quintanilla-Martinez[8], Alexander Steinle[9], Andreas Trumpp[3,4,10]*, Helmut R. Salih[2,6]*, Claudia Lengerke[1,11]*

(*equally shared co-authorships)

[1]University of Basel and University Hospital Basel, Department of Biomedicine, Switzerland

[2]Clinical Collaboration Unit Translational Immunology, German Cancer Consortium (DKTK), partner site Tuebingen, University Hospital Tuebingen, Germany

[3]Division of Stem Cells and Cancer, Deutsches Krebsforschungszentrum (DKFZ), Heidelberg, Germany

[4]Heidelberg Institute for Stem Cell Technology and Experimental Medicine (HI-STEM gGmbH), Heidelberg, Germany

[5]Department of Medicine V, Heidelberg University, Germany

[6]Department of Hematology and Oncology, Eberhard-Karls-University, Tuebingen, Germany

[7]Diagnostic Hematology, Department of Laboratory Medicine, University Hospital Basel, Basel, Switzerland

[8]Institute for Pathology, University of Tuebingen, Tuebingen, Germany

[9]Institute for Molecular Medicine, Goethe University, Frankfurt am Main, Germany

[10]German Cancer Consortium (DKTK), DKFZ, Heidelberg, Germany

[11]Division of Clinical Hematology, University Hospital Basel, Basel, Switzerland

Running title: Absence of immunostimulatory NKG2D ligands defines stem cells in human leukaemia

Key words: acute myeloid leukaemia, leukaemia stem cells, leukaemia-initiating cells, NK cells, immune escape, immunosurveillance, NKG2D, NKG2D ligands, MICA, MICB, PARP1

Abstract

Patients with acute myeloid leukaemia (AML) often achieve remission yet subsequently die of relapse[1]. Disease is driven by therapy resistant leukaemic stem cells (LSCs)[2-4,5] which, to induce cancer, must also escape immune surveillance [6]. Interactions between patient LSCs and immune cells are poorly understood because human LSCs are studied upon transplantation into mice that lack a competent immune system.[7] Here we demonstrate that stemness and immune escape are closely intertwined. Ligands of the danger detector NKG2D, a critical mediator of anti-tumour immunity by cytotoxic lymphocytes such as natural killer (NK) cells, are generally expressed on bulk AML cells but not on LSCs. NKG2D ligand (NKG2DL) expressing AML subpopulations are efficiently cleared by NK cells *in vitro* and in NOD/SCID/IL2Rγ^{null} (NSG) mice co-transplanted with NK cells, whereas NKG2DL negative counterparts isolated from the same patients escape NK cell killing. These NKG2DL^{neg} AML subpopulations furthermore display stemness characteristics including immature morphology, stem cell specific gene signatures, enhanced *in vitro* clonogenicity and selective abilities to initiate leukaemia and to survive chemotherapy in NSG mice. Mechanistically, enhanced levels of poly-ADP-ribose polymerase 1 (PARP1) suppress NKG2DL surface expression in LSCs, which in turn can be induced upon PARP1 inhibition (PARPi). Co-treatment with PARPi and NK cells, but not with PARPi or NK cells alone, suppresses leukaemogenesis in patient-derived xenotransplantation models. In patients with AML, low surface NKG2DL as well as high PARP1 expression associate with inferior clinical outcome.

In summary, our findings that LSCs benefit from NKG2D-associated immune privilege driven by PARP1 uncover a novel method for LSC isolation and an unrecognised and targetable mechanism for sensitizing LSCs to immune control. They also provide a conceptual framework for the integration of two central hypotheses of cancer development – the concepts of cancer stem cells and immune escape.

Manuscript

Despite decades of research, AML still shows high mortality rates dependent on genetic drivers and patient age. Different types of LSCs have been identified and were shown to mediate chemotherapy-resistance and disease recurrence, known as the main obstacles to cure in AML.[1,2-4,5]

Here we demonstrate that LSCs also selectively evade immune surveillance mediated by NKG2D[8]. This danger detector is expressed by cytotoxic lymphocytes including NK cells and recognizes stress-induced ligands (NKG2DL) of the MIC and ULBP protein families on target cells[9]. We screened 175 AML patients (Supplementary Table 1) for individual NKG2DL expression (MICA, MICB, ULBP1 and ULBP2/5/6, Extended Data Fig. 1). In addition, we used an NKG2D-Fc chimeric protein for simultaneous detection of these and potentially yet unknown NKG2DL[9]. Beyond the reported variation in NKG2DL patterns among different AML cases[10], we detected profound heterogeneity in NKG2DL expression on AML cells from individual patients (Fig. 1a and Extended Data Fig. 1). Analyses of $NKG2DL^{pos}$ and $NKG2DL^{neg}$ AML subpopulations sorted from the same patient (Fig. 1b-c) revealed that $NKG2DL^{neg}$ AML cells were smaller with less granularity and lower cell to nucleus size ratio (Fig. 1d-f and Extended Data Fig. 2a-b). Furthermore, they showed enhanced *in vitro* clonogenicity when compared to $NKG2DL^{pos}$ counterparts (39±47 colonies vs. 1±4, $p<0.001$, Fig. 1g and Extended Data Fig. 3). Supporting their stem cell-like properties, only $NKG2DL^{neg}$ AML subpopulations, but not corresponding $NKG2DL^{pos}$ cells isolated from the same samples, induced leukaemia in NSG mice. These leukaemias manifested by infiltration of bone marrow (BM) and other organs with human AML cells as detected by multicolour flow cytometry ($NKG2DL^{neg}$, 33/35, 94%; $NKG2DL^{pos}$, 0/35, 0%; $p<0.001$, Fig. 1h) and immunohistochemistry (Fig. 1i), and displayed variable degrees of associated illness and survival ($p<0.001$, Fig. 1j). Notably, $NKG2DL^{neg}$ cells generated both $NKG2DL^{neg}$ and $NKG2DL^{pos}$ progeny in engrafted mice (Fig. 1k-l), and sorted $NKG2DL^{pos}$ progeny again failed to induce leukaemia upon re-transplantation (Supplementary Fig. 1). $NKG2DL^{pos}$ AML cells showed a 10-fold reduced ability to home to the BM compared to $NKG2DL^{neg}$ cells (0.001±0.002% vs. 0.01±0.009 leukaemic among mouse BM cells, $p<0.001$, Fig. 1m), but also failed to engraft when transplanted directly into the BM by intra-femoral injection (Supplementary Fig. 2). Finally, *in vivo* treatment of mice engrafted with human AML cells with cytarabine (Fig. 1n) reduced mouse BM infiltration with $NKG2DL^{pos}$ ($p<0.001$) but not with

NKG2DL^{neg} AML cells (Fig. 1o-p), which indicates that latter are more resistant to chemotherapy. Molecularly, comparative gene expression array and qRT-PCR analyses revealed enrichment of established hematopoietic stem cell (HSC) LSC[11] and 17-gene stemness signatures[12] in NKG2DL^{neg} versus NKG2DL^{pos} AML subpopulations, whereas the common lineage-committed progenitor signature[11] was instead enriched in NKG2DL^{pos} fractions (Fig. 1q and Supplementary Fig. 3). As revealed by next generation sequencing, these differences did not result from intra-patient variation in leukaemia-specific mutations in NKG2DL^{neg} versus NKG2DL^{pos} AML cells (Fig. 1r). Together, these data collected in experimental systems devoid of NK cell interactions demonstrate that functionally defined primary human AML LSCs lack NKG2DL surface expression, display resistance to chemotherapy and can be prospectively isolated from patients using an NKG2D-Fc chimeric protein. Moreover, most if not all leukaemia-initiating activity within primary human AML samples is contained in the NKG2DL^{neg} subpopulation.

Next, we hypothesized that the absence of NKG2DL may allow LSCs to preferentially evade NK cell immunosurveillance. Indeed, co-cultivation of bulk AML cells with polyclonal NK cells (pNKC+Mock condition) selectively reduced NKG2DL^{pos} subpopulations, thereby enriching for NKG2DL^{neg} cells. Importantly, this effect was abrogated by NKG2D-blockade (pNKC+anti-NKG2D condition) (Fig. 2a-c, 7±3% vs. 82±9% compared to pre-culture conditions, $p<0.001$). Consistently, exposure to pNKC alone or pNKC+mock resulted in enrichment of AML cells with increased clonogenicity (Fig. 2d, 1.7 ± 0.20-fold versus 1.091 ± 0.15-fold, $p<0.001$). To confirm enriched LSC activity *in vivo*, identical numbers of AML cells retrieved from *in vitro* pNKC+mock or pNKC+anti-NKG2D co-cultures were transplanted into NSG mice, which lack endogenous NK cell activity[13,14] and thus allow assessment of *in vivo* leukaemia development in an environment devoid of NK cell immune surveillance. At the time when leukaemic engraftment was uniformly detected in the BM and peripheral blood (PB) of mice transplanted with pNKC+mock derived AML cells (18/18 mice engrafted/transplanted mice, 6/6 AML cases), no (15/18 mice, 5/6 AML) or clearly lower (3/18 mice, 1/6 AML) engraftment was observed in mice receiving AML cells derived from pNKC+anti-NKG2D conditions (Fig. 2e). These data indicate that, within the transplanted population of fixed size, cells derived from pNKC+mock conditions contain higher numbers of LSCs due to elimination of non-leukaemogenic NKG2DL^{pos} cells by the

functional NK cells. This effect is prevented in the pNKC+anti-NKG2D setting in which NKG2DL^{pos} without LSC activity survive and dilute the NKG2DL^{neg} LSCs. As expected[15], some LSCs were also present in pNKC+anti-NKG2D conditions, from which leukaemia developed after 10±1.5 weeks longer latency (Fig. 2e-f). In line, mice transplanted with pNKC+anti-NKG2D AML cells showed better survival than those receiving pNKC+mock AML cells (Fig. 2g). Together, these data demonstrate that LSCs in fact are immune-privileged and not eliminated by NK cells, which preferentially target non-LSCs in a NKG2D-dependent manner.

LSCs were reported to reside predominantly within CD34$^+$ AML cell subpopulations[11], among which they can be further enriched based on CD38 negativity and surface markers such as TIM-3, CD44, CD47, CD99, CD25 or CD123[3,16-25]. However, LSCs show immunophenotypic heterogeneity and profound variation among patients was documented by several studies[3,16-25]. LSCs are particularly understudied in AML cases with low or absent CD34 expression (<5% CD34$^+$ among total AML cells, termed CD34 non-expressing AML) which comprise about ~30% of AMLs [26,27]. We analysed 55 such CD34 non-expressing AMLs and again observed heterogeneous intra-patient distribution of NKG2DL expression on AML cells (Fig. 3a-b, Extended Data Figs. 4a and 5a and Supplementary Fig. 4). As in CD34 expressing AMLs (Fig. 1g-j), also in CD34 non-expressing AMLs NKG2DL^{neg} subpopulations showed higher clonogenicity (38±34 colonies versus 0.7±2, $p<0.001$, Fig. 3c) and selective *in vivo* AML engraftment (33/35 versus 0/35 engrafted/transplanted mice, $p<0.001$, Fig. 3d) when compared to corresponding CD34$^-$NKG2DL^{pos} AML cells isolated from the same patient. RNAseq analyses revealed enrichment for HSC and LSC signatures and the 17-genes AML stemness score in CD34$^-$NKG2DL^{neg} subpopulations ($p<0.001$, Fig. 3e)[11,12]. These data provide molecular and functional evidence that absence of NKG2DL surface expression identifies LSCs in patients suffering from CD34 non-expressing AML and highlight NKG2D-Fc staining as a method to prospectively isolate LSCs irrespective whether they express CD34 or not.

Next, we explored the absence of NKG2DL as LSC marker in the subgroup of CD34 expressing AMLs. The CD34$^+$ subpopulations containing LSCs (Supplementary Fig. 5) displayed lower NKG2DL expression when compared to

$CD34^-$ (non-stem) AML subpopulations of the same patients (Fig. 3f-h and Extended Data Figs. 4b and 5b). Moreover, higher numbers of samples containing >90% $NKG2DL^{neg}$ AML cells and higher percentages of $NKG2DL^{neg}$ AML cells in general were detected in $CD34^+CD38^-$ compared to $CD34^+CD38^+$ and $CD34^-$ subpopulations ($p<0.001$, Fig. 3i-j), confirming the inverse correlation between NKG2DL expression and stemness. Consistent with the notion that not all $CD34^+$ AML cells are LSCs, $CD34^+NKG2DL^{pos}$ populations were also detected (Fig. 3f-g and Extended Data Fig. 4b and 5b). In AML samples displaying ubiquitous CD34 expression (Fig. 3k-l), lack of NKG2DL separated stem-like immature $CD34^+NKG2DL^{neg}$ subpopulations with clonogenic and *in vivo* leukemogenic properties from non-clonogenic, non-leukemogenic $CD34^+NKG2DL^{pos}$ cells (Fig. 3m-n and Extended Data Fig. 2c). Similar associations were observed for other markers reported to identify LSCs in CD34 expressing AML (e.g. GPR56, CD133[3,16-25]) (Extended Data Fig. 6).

To gain mechanistic insights into the cellular pathways associated with absence of NKG2DL expression in LSCs, we compared $NKG2DL^{neg}$ and corresponding $NKG2DL^{pos}$ subpopulations isolated from ten genetically and phenotypically heterogeneous AML patients by gene expression arrays and RNAseq (see Supplementary Tables 2-4). We identified 22 commonly differentially regulated genes, among which the recently reported LSC and HSC molecule GPR56[28-30] and PARP1 were higher expressed in $NKG2DL^{neg}$ cells (Fig. 4a and Supplementary Table 5). PARP1 was further analysed because of its known involvement in the DNA damage response, which is a process (i) linked to NKG2DL induction[31] and (ii) influenced by differentiation state[32]. Furthermore, PARP1 was shown to regulate transcription, chromatin remodelling and stem cell pluripotency[33,34]. Finally, PARP1 is a pharmacologically tractable candidate, and respective inhibitors were reported to influence apoptosis, senescence, cell cycle and differentiation in AML cells[35], especially when applied together with chemotherapy[36], hypomethylating agents[37-40], temozolamide[41,42] or vitamin C[43].

Immunoblotting confirmed increased PARP1 protein expression in $NKG2DL^{neg}$ versus $NKG2DL^{pos}$ and $CD34^+$ versus $CD34^-$ AML subpopulations within the same patients (Fig. 4b, Extended data Fig. 7 and Supplementary Table 6). PARP1 inhibition (PARPi) using three different PARP1 siRNAs (Fig.

4c-d and Supplementary Fig. 6) or the PARP1 inhibitor AG-14361[44] (Fig. 4e-f, Supplementary Table 7 and Extended Data Fig. 8a-b) induced NKG2DL surface expression on *in vitro* cultured AML cells, specifically fostering the emergence of $CD34^{+}NKG2DL^{pos}$ but not $CD34^{-}NKG2DL^{pos}$ cells. These effects are unlikely to result from selective survival of $CD34^{+}NKG2DL^{pos}$ compared to $CD34^{-}NKG2DL^{pos}$ counterparts within the same AML sample, since no consistent differences in viability, growth and apoptotic responses were observed when sorted populations were treated separately (Extended Data Fig. 9). Furthermore, treatment with AG-14361 or the alternative PARP1 inhibitor veliparib also induced NKG2DL surface expression on purified, separately treated $NKG2DL^{neg}$ AML cells (Fig. 4g-h and Extended Data Fig. 10 c). In contrast, treatment with 5-azacytidine, a clinically used DNA methyltransferases inhibitor previously reported to up-regulate NKG2DL[45], only enhanced $CD34^{-}NKG2DL^{pos}$ non-LSCs but not $CD34^{+}NKG2DL^{pos}$ subpopulations (Extended Data Fig. 10a). Other drugs associated with NKG2DL induction including all-trans retinoic acid, or valproic acid showed no significant effects on NKG2DL expression in our analyses (Extended Data Fig. 10b).

NKG2DL are regulated both transcriptionally and post-transcriptionally (e.g. by shedding from the cell surface[46]). Although differential *in vivo* shedding cannot be excluded, similar NKG2DL release was observed with cultured $CD34^{+}$ LSC-enriched subpopulations versus corresponding $CD34^{-}$ non-LSCs sorted from the same patient samples (Extended Data Fig. 11). In contrast, increased NKG2DL mRNA expression was detected by qRT-PCR in sorted $NKG2DL^{pos}$ AML cells versus $NKG2DL^{neg}$ subpopulations (Extended Data Fig. 12), suggesting differential transcriptional regulation of NKG2DL in LSC compared to non-LSCs. Importantly, treatment with either PARP1 siRNAs or AG-14361 robustly induced NKG2DL mRNA expression between 6 and >50 fold (Fig. 4i and Supplementary Fig. 7). Moreover, PARP1 binding sites were identified by *in silico* analysis in NKG2DL promoters (Supplementary Fig. 8), and binding was confirmed by chromatin immunoprecipitation in the promoters of MICA and MICB (Fig. 4j). Together, these data suggest selective repressive effects of PARP1 on NKG2DL mRNA in LSCs that can be reverted by PARPi.

Given that NKG2DL expression on non-stem AML cells sensitizes these AML subpopulations to NK cell attack, and that PARPi can induce NKG2DL on LSCs, we hypothesized that PARPi should sensitize LSCs to *in vivo* lysis by co-transplanted NK cells. Indeed, when AML cells were pre-treated with AG-14361 and co-transplanted together with pNKCs into NSG mice (Extended Data Fig. 13a-b), co-treatment with AG-14361 and pNKC strongly reduced leukemic cell burden at all analysed sites when compared to control settings. This suggests that indeed PARPi exposed AML cells are better lysed by NK cells. The modest reduction observed in cells treated with AG-14361 alone (Extended Data Fig. 13b) points to potential cytotoxic (NK cell/NKG2D-independent) effects of PARPi, consistent with the reported single agent anti-leukemic activity reported for PARP inhibitors[35]. Next, NSG mice were transplanted with human AML cells and then treated *in vivo* with AG-14361 followed by transfer of pNKCs. We found that both the leukemic burden and the number of mice showing long-term AML engraftment were strongly reduced in mice co-treated with AG-14361 plus pNKCs, but not in animals receiving AG-14361 or pNKCs alone (Fig. 4k-l). The anti-leukemic effects in the co-treatment group were mediated via NKG2D, since they were abrogated by NKG2D blockade (AG-14361 + blocked pNKCs, Fig. 4l). These data unravel that the combination of PARPi and NK cells mediate synergistic anti-leukemic effects. Of note, in our experimental settings the treatment of AML cells with AG-14361 was performed before pNKC transfer. The reported results are thus independent of reported stimulatory effects of PARPi on NK cells themselves[47]. In conclusion, our data strongly suggest that PARP1 expression on AML stem cells represses NKG2DL expression mediating their NKG2D dependent immune escape thereby promoting LSC survival, disease progression and relapse.

Indeed, in the patient cohort analysed in our study, NKG2DL surface expression inversely associated with clinical AML aggressiveness as documented (i) by molecular characteristics (ELN risk group AML[48]: p=0.01, inv(16) versus other: p=0.028), (ii) by rate of complete remission after induction chemotherapy (all patients: p=0.002, patients <65 years: p=0.004) and (iii) by overall survival rates (patients <65 year: p=0.028)[48] (Fig. 4m-o and Extended Data Figs. 14-16), while no associations were observed with age or leukaemic cell counts (Supplementary Fig. 9). Furthermore, high PARP1 expression in leukaemic cells associated with poor clinical outcome in a cohort of 179 AML patients

(p=0.0038, Fig. 4p) as revealed upon retrospective analysis of the TCGA database (http://cancergenome.nih.gov)[49].

Extensive work particularly on NKG2D pointed out that beyond infections, immune surveillance indeed extends to cancer[8,50]. The mechanisms allowing cancer cells to thrive despite the existence of NKG2D and other immune surveillance systems include defects in NK cells[51,52] and adaptations to the tumour microenvironment[53]. Tumour cell-intrinsic immune escape mechanisms such as inhibitory microRNAs e.g. down-regulating NKG2DL[54] or shedding of NKG2DL[46] also play a role, but selective effects in subpopulations of malignant cells are still elusive. Here we provide molecular, cellular and functional *in vivo* evidence that LSC activity associates with immune evasion. Our data demonstrate that LSCs escape immune-surveillance due to an intrinsic lack of NKG2DL expression. Thus, NKG2DL^{neg} LSCs selectively survive and can cause leukaemia relapse even when NK cell functionality is restored (e.g. upon allogeneic stem cell transplantation, SCT). This is of particular relevance since adoptive transfer of NK cells for AML treatment is currently intensively evaluated for the treatment of AML in clinical trials (see https://clinicaltrials.gov/ct2/results?cond=Acute+Myeloid+Leukemia&term=NK&cntry1). Therapies aiming at installing NKG2DL expression on LSCs, like PARPi identified in our study, may thus represent a novel therapeutic strategy to target LSCs *in vivo*.

While the existence of LSCs is well documented, a precise and generally applicable immune phenotypic profile of this cellular subpopulation remains elusive. For example, LSCs were reported to reside in CD34^{+}CD38^{-} AML subpopulations, but CD34^{+}CD38^{+} and CD34^{-} LSCs were also documented[3,26,27]. Within CD34^{+}CD38^{-} subpopulations, additional markers were reported to enrich LSCs but however are not robustly expressed in all AML cases and were not further tested in combination. Absence of NKG2DL expression may constitute a universal novel LSC marker because it reflects a major functional property of LSCs, namely the newly identified capacity to preferentially evade immune surveillance. As shown by our data collected in 175 patient samples, the vast majority of analysed AML cases (n=175 AML, Fig. 1a) do contain NKG2DL^{neg} AML subpopulations and absence of NKG2DL expression indeed identifies functionally and molecularly defined LSCs in AMLs of various genetic and phenotypic background. Future studies will elucidate

whether co-staining with NKG2D-Fc chimeric protein and previously reported LSC markers can even more precisely define LSCs. Notably, reduced NK cell lysis was observed for $CD44^{(high)}CD24^{(low)}$ stem-like ovarian carcinoma cells[55,56], and down-regulation of NKG2DL was described for metastatic breast carcinoma cells[57] and in a glioma cell line model[58]. Stemness-associated immune privilege may thus extend to other cancers and very well involve multiple mechanisms beyond NKG2D. Follow-up studies will investigate whether stemness-associated immune escape may be a general principle in neoplasia and whether absence of NKG2DL expression can identify cancer stem cells also in other types of leukaemia and solid tumours.

The selective suppression of NKG2DL expression on LSCs may reflect their resemblance to their cells of origin, the healthy hematopoietic stem and early progenitor cells (HSPCs). Although non-malignant hematopoietic cells in general lack NKG2DL expression, NKG2DL are particularly absent on the surface of $CD34^+$ HSPCs[59] (Fig. 4e-f and Extended Data Fig. 17) whereas low percentages of $NKG2DL^{pos}$ cells can be detected within more differentiated subpopulations, particularly upon activation or exposure to cellular stress[60-62]. In line, a gradual inverse correlation between NKG2DL expression and stemness is also noted in AML, as indicated by the intermediate clonogenicity observed in $NKG2DL^{interm}$ AML cells when compared to corresponding $NKG2DL^{neg}$ and $NKG2DL^{pos}$ subpopulations (Extended Data Fig. 3), and the reduced percentages of $NKG2DL^{neg}$ AML cells in $CD34^+CD38^-$ subpopulations versus $CD34^+CD38^+$ and $CD34^-$ AML subpopulations (Fig. 3i-j).

Our findings that PARP1 expression precludes NKG2DL expression in LSCs are of particular interest as PARP1 inhibitors are under clinical investigation[63] and appear to be well-tolerated in patients[42,64-66]. This is consistent with our data showing that short-term *in vivo* treatment with AG-14361, while sufficient to up-regulate NKG2DL on engrafted human AML cells (Extended Data Fig. 8c-d), did not cause overt hematopoietic toxicity nor lead to cell death or NKG2DL induction on healthy hematopoietic cells (Extended data Fig. 18). At advanced disease stages of AML, immune surveillance is disturbed by multiple mechanisms beyond those affecting NKG2DL expression. Thus, the immune-sensitizing effect of PARPi on LSCs unravelled by our study may be particularly well exploited when respective drugs are applied in the context

of a functionally restored immune system, e.g. at minimal residual disease stage and/or in conjunction with SCT or allogeneic NK cell therapies. In conclusion, PARP1 inhibition indeed holds promise to specifically target LSCs and to facilitate immune-mediated long-term cure in AML.

Acknowledgements:

This study was supported by grants from the DFG (Deutsche Forschungsgemeinschaft, LE 2483/7-1 to C.L., SA1360/9-1 and SA1360/7-3 to H.R.S. and FOR2033 to A.T.), the Schweizerischer Nationalfonds, 310030_179239, and the Foundation for Fight Against Cancer (Zürich, Switzerland) to C.L., and the SyTASC consortium funded by the Deutsche Krebshilfe and the Dietmar Hopp Foundation to A.T. We thank Ursula Kohlhofer (Institute of Pathology, University of Tübingen) for her help with mouse sections and immunohistochemistry, Mergim Maraj Martinez and Marcelle Mbarga (Department of Biomedicine, University and University Hospital Basel) for assistance with qRT-PCR analyses, the members of the Animal Facilities at the Department of Biomedicine (Basel) and the Central Animal Laboratory at DKFZ (Heidelberg) for animal husbandry, the members of the flow cytometry facility at the University Hospital Tübingen, the Department of Biomedicine (Basel), and the DKFZ (Heidelberg, especially S. Schmitt) for expertise and support, the high throughput sequencing unit of the Genomics & Proteomics Core Facility, DKFZ, for providing excellent RNA sequencing as well as Z. Gu for processing of raw sequencing data, and Verdon Taylor (Department of Biomedicine, University Hospital Basel, Basel, Switzerland) and George Q. Daley (Harvard Medical School, Boston, USA) for critical review of the manuscript.

Author Contributions:

A.M.P. designed and performed experiments, analyzed data and generated figures and tables. K.R. designed and performed experiments, analyzed data and generated figures and tables. S.R. designed and performed experiments, analyzed data and generated figures on bioinformatics data. M.K. designed and performed experiments, analyzed data, generated figures and tables. J.S. designed and performed experiments and analyzed data. T.S. and H.W. per-

formed experiments and analyzed data. D.D. collected clinical samples and provided patient data. M.F. performed bioinformatic analyses of RNAseq and microarray data. E.N. performed experiments. C.T. characterized AML samples. C.L. (Heidelberg) provided AML samples and purified cells. P.L. molecularly characterized AML patient samples. L.K. provided clinical samples. L.Q-M performed mouse histopathological analyses. A.S. provided critical reagents. A.T. contributed to the study design, performed data analysis, wrote the manuscript and supervised the study. H.R.S. conceived the study, analyzed the data, wrote the manuscript and supervised the study. C.L. (Basel) conceived the study, analyzed the data, wrote the manuscript as lead author and supervised the study. All authors critically reviewed the manuscript.

Author information:

The authors declare no competing financial interests. Correspondence and requests for materials should be addressed to Helmut R. Salih, MD, Clinical collaboration unit Translational Immunology, German Cancer Consortium (DKTK), partner site Tuebingen, University Hospital Tuebingen, Otfried-Müller-Str. 10, D-72076 Tuebingen, Germany, Tel.: +49 7071 2983275, Fax: +49 7071 294391, Email: helmut.salih@med.uni-tuebingen.de

References:

1 Ferrara, F. & Schiffer, C. A. Acute myeloid leukaemia in adults. *Lancet* **381**, 484-495, doi:10.1016/S0140-6736(12)61727-9 (2013).

2 Lapidot, T. *et al.* A cell initiating human acute myeloid leukaemia after transplantation into SCID mice. *Nature* **367**, 645-648, doi:10.1038/367645a0 (1994).

3 Bonnet, D. & Dick, J. E. Human acute myeloid leukemia is organized as a hierarchy that originates from a primitive hematopoietic cell. *Nat Med* **3**, 730-737 (1997).

4 Shlush, L. I. *et al.* Tracing the origins of relapse in acute myeloid leukaemia to stem cells. *Nature* **547**, 104-108, doi:10.1038/nature22993 (2017).

5 Bahr, C., Correia, N. C. & Trumpp, A. Stem cells make leukemia grow again. *EMBO J*, doi:10.15252/embj.201797773 (2017).

6 Hanahan, D. & Weinberg, R. A. Hallmarks of cancer: the next generation. *Cell* **144**, 646-674, doi:S0092-8674(11)00127-9 [pii]

10.1016/j.cell.2011.02.013 (2011).

7 Theocharides, A. P., Rongvaux, A., Fritsch, K., Flavell, R. A. & Manz, M. G. Humanized hemato-lymphoid system mice. *Haematologica* **101**, 5-19, doi:10.3324/haematol.2014.115212 (2016).

8 Guerra, N. *et al.* NKG2D-deficient mice are defective in tumor surveillance in models of spontaneous malignancy. *Immunity* **28**, 571-580, doi:10.1016/j.immuni.2008.02.016 (2008).

9 Raulet, D. H., Gasser, S., Gowen, B. G., Deng, W. & Jung, H. Regulation of ligands for the NKG2D activating receptor. *Annu Rev Immunol* **31**, 413-441, doi:10.1146/annurev-immunol-032712-095951 (2013).

10 Hilpert, J. *et al.* Comprehensive analysis of NKG2D ligand expression and release in leukemia: implications for NKG2D-mediated NK cell responses. *J Immunol* **189**, 1360-1371, doi:10.4049/jimmunol.1200796 (2012).

11 Eppert, K. *et al.* Stem cell gene expression programs influence clinical outcome in human leukemia. *Nat Med* **17**, 1086-1093, doi:10.1038/nm.2415 (2011).

12 Ng, S. W. *et al.* A 17-gene stemness score for rapid determination of risk in acute leukaemia. *Nature* **540**, 433-437, doi:10.1038/nature20598 (2016).

13 Shultz, L. D. *et al.* Human lymphoid and myeloid cell development in NOD/LtSz-scid IL2R gamma null mice engrafted with mobilized human hemopoietic stem cells. *J Immunol* **174**, 6477-6489, doi:174/10/6477 [pii] (2005).

14 McDermott, S. P., Eppert, K., Lechman, E. R., Doedens, M. & Dick, J. E. Comparison of human cord blood engraftment between immunocompromised mouse strains. *Blood* **116**, 193-200, doi:blood-2010-02-271841 [pii] 10.1182/blood-2010-02-271841 (2010).

15 Paczulla, A. M. *et al.* Long-term observation reveals high-frequency engraftment of human acute myeloid leukemia in immunodeficient mice. *Haematologica*, doi:10.3324/haematol.2016.153528 (2017).

16 Pabst, C. *et al.* GPR56 identifies primary human acute myeloid leukemia cells with high repopulating potential in vivo. *Blood*, doi:10.1182/blood-2015-11-683649 (2016).

17 Jordan, C. T. *et al.* The interleukin-3 receptor alpha chain is a unique marker for human acute myelogenous leukemia stem cells. *Leukemia* **14**, 1777-1784 (2000).

18 Jin, L., Hope, K. J., Zhai, Q., Smadja-Joffe, F. & Dick, J. E. Targeting of CD44 eradicates human acute myeloid leukemic stem cells. *Nat Med* **12**, 1167-1174, doi:10.1038/nm1483 (2006).

19 Majeti, R. *et al.* CD47 is an adverse prognostic factor and therapeutic antibody target on human acute myeloid leukemia stem cells. *Cell* **138**, 286-299, doi:10.1016/j.cell.2009.05.045 (2009).

20 van Rhenen, A. *et al.* The novel AML stem cell associated antigen CLL-1 aids in discrimination between normal and leukemic stem cells. *Blood* **110**, 2659-2666, doi:10.1182/blood-2007-03-083048 (2007).

21 Jan, M. *et al.* Clonal evolution of preleukemic hematopoietic stem cells precedes human acute myeloid leukemia. *Sci Transl Med* **4**, 149ra118, doi:10.1126/scitranslmed.3004315 (2012).

22 Jan, M. *et al.* Prospective separation of normal and leukemic stem cells based on differential expression of TIM3, a human acute myeloid leukemia stem cell marker. *Proc Natl Acad Sci U S A* **108**, 5009-5014, doi:10.1073/pnas.1100551108 (2011).

23 Hosen, N. *et al.* CD96 is a leukemic stem cell-specific marker in human acute myeloid leukemia. *Proc Natl Acad Sci U S A* **104**, 11008-11013, doi:10.1073/pnas.0704271104 (2007).

24 Chung, S. S. *et al.* CD99 is a therapeutic target on disease stem cells in myeloid malignancies. *Sci Transl Med* **9**, doi:10.1126/scitranslmed.aaj2025 (2017).

25 Saito, Y. *et al.* Identification of therapeutic targets for quiescent, chemotherapy-resistant human leukemia stem cells. *Sci Transl Med* **2**, 17ra19, doi:10.1126/scitranslmed.3000349 (2010).

26 Taussig, D. C. *et al.* Leukemia-initiating cells from some acute myeloid leukemia patients with mutated nucleophosmin reside in the CD34(-) fraction. *Blood* **115**, 1976-1984, doi:blood-2009-02-206565 [pii]

10.1182/blood-2009-02-206565 (2010).

27 Quek, L. *et al.* Genetically distinct leukemic stem cells in human CD34-acute myeloid leukemia are arrested at a hemopoietic precursor-like stage. *J Exp Med* **213**, 1513-1535, doi:10.1084/jem.20151775 (2016).

28 Pabst, C. *et al.* GPR56 identifies primary human acute myeloid leukemia cells with high repopulating potential in vivo. *Blood* **127**, 2018-2027, doi:10.1182/blood-2015-11-683649 (2016).

29 Daria, D. *et al.* GPR56 contributes to the development of acute myeloid leukemia in mice. *Leukemia* **30**, 1734-1741, doi:10.1038/leu.2016.76 (2016).

30 Saito, Y. *et al.* Maintenance of the hematopoietic stem cell pool in bone marrow niches by EVI1-regulated GPR56. *Leukemia* **27**, 1637-1649, doi:10.1038/leu.2013.75 (2013).

31 Gasser, S., Orsulic, S., Brown, E. J. & Raulet, D. H. The DNA damage pathway regulates innate immune system ligands of the NKG2D receptor. *Nature* **436**, 1186-1190, doi:10.1038/nature03884 (2005).

32 Biechonski, S., Yassin, M. & Milyavsky, M. DNA-damage response in hematopoietic stem cells: an evolutionary trade-off between blood regeneration and leukemia suppression. *Carcinogenesis* **38**, 367-377, doi:10.1093/carcin/bgx002 (2017).

33 Krishnakumar, R. & Kraus, W. L. The PARP side of the nucleus: molecular actions, physiological outcomes, and clinical targets. *Mol Cell* **39**, 8-24, doi:10.1016/j.molcel.2010.06.017 (2010).

34 Chiou, S. H. *et al.* Poly(ADP-ribose) polymerase 1 regulates nuclear reprogramming and promotes iPSC generation without c-Myc. *J Exp Med* **210**, 85-98, doi:10.1084/jem.20121044 (2013).

35 Esposito, M. T. *et al.* Synthetic lethal targeting of oncogenic transcription factors in acute leukemia by PARP inhibitors. *Nat Med* **21**, 1481-1490, doi:10.1038/nm.3993 (2015).

36 Falzacappa, M. V. *et al.* The Combination of the PARP Inhibitor Rucaparib and 5FU Is an Effective Strategy for Treating Acute Leukemias. *Mol Cancer Ther* **14**, 889-898, doi:10.1158/1535-7163.MCT-14-0276 (2015).

37 Orta, M. L. *et al.* The PARP inhibitor Olaparib disrupts base excision repair of 5-aza-2'-deoxycytidine lesions. *Nucleic Acids Res* **42**, 9108-9120, doi:10.1093/nar/gku638 (2014).

38 Robert, C. *et al.* Histone deacetylase inhibitors decrease NHEJ both by acetylation of repair factors and trapping of PARP1 at DNA double-strand breaks in chromatin. *Leuk Res* **45**, 14-23, doi:10.1016/j.leukres.2016.03.007 (2016).

39 Muvarak, N. E. *et al.* Enhancing the Cytotoxic Effects of PARP Inhibitors with DNA Demethylating Agents - A Potential Therapy for Cancer. *Cancer Cell* **30**, 637-650, doi:10.1016/j.ccell.2016.09.002 (2016).

40 Gaymes, T. J. *et al.* Inhibitors of poly ADP-ribose polymerase (PARP) induce apoptosis of myeloid leukemic cells: potential for therapy of myeloid

leukemia and myelodysplastic syndromes. *Haematologica* **94**, 638-646, doi:10.3324/haematol.2008.001933 (2009).

41 Horton, T. M. *et al.* Poly(ADP-ribose) polymerase inhibitor ABT-888 potentiates the cytotoxic activity of temozolomide in leukemia cells: influence of mismatch repair status and O6-methylguanine-DNA methyltransferase activity. *Mol Cancer Ther* **8**, 2232-2242, doi:10.1158/1535-7163.MCT-09-0142 (2009).

42 Gojo, I. *et al.* A Phase 1 Study of the PARP Inhibitor Veliparib in Combination with Temozolomide in Acute Myeloid Leukemia. *Clin Cancer Res* **23**, 697-706, doi:10.1158/1078-0432.CCR-16-0984 (2017).

43 Cimmino, L. *et al.* Restoration of TET2 Function Blocks Aberrant Self-Renewal and Leukemia Progression. *Cell* **170**, 1079-1095.e1020, doi:10.1016/j.cell.2017.07.032 (2017).

44 Bryant, H. E. *et al.* Specific killing of BRCA2-deficient tumours with inhibitors of poly(ADP-ribose) polymerase. *Nature* **434**, 913-917, doi:10.1038/nature03443 (2005).

45 Baragaño Raneros, A. *et al.* Methylation of NKG2D ligands contributes to immune system evasion in acute myeloid leukemia. *Genes Immun* **16**, 71-82, doi:10.1038/gene.2014.58 (2015).

46 Salih, H. R., Rammensee, H. G. & Steinle, A. Cutting edge: down-regulation of MICA on human tumors by proteolytic shedding. *J Immunol* **169**, 4098-4102 (2002).

47 Huang, J. *et al.* The PARP1 inhibitor BMN 673 exhibits immunoregulatory effects in a Brca1(-/-) murine model of ovarian cancer. *Biochem Biophys Res Commun* **463**, 551-556, doi:10.1016/j.bbrc.2015.05.083 (2015).

48 Döhner, H. *et al.* Diagnosis and management of AML in adults: 2017 ELN recommendations from an international expert panel. *Blood* **129**, 424-447, doi:10.1182/blood-2016-08-733196 (2017).

49 Ley, T. J. *et al.* Genomic and epigenomic landscapes of adult de novo acute myeloid leukemia. *N Engl J Med* **368**, 2059-2074, doi:10.1056/NEJMoa1301689 (2013).

50 Ullrich, E., Koch, J., Cerwenka, A. & Steinle, A. New prospects on the NKG2D/NKG2DL system for oncology. *Oncoimmunology* **2**, e26097, doi:10.4161/onci.26097 (2013).

51 Mundy-Bosse, B. L. *et al.* MicroRNA-29b mediates altered innate immune development in acute leukemia. *J Clin Invest* **126**, 4404-4416, doi:10.1172/JCI85413 (2016).

52 Dulphy, N. *et al.* Underground Adaptation to a Hostile Environment: Acute Myeloid Leukemia vs. Natural Killer Cells. *Front Immunol* **7**, 94, doi:10.3389/fimmu.2016.00094 (2016).

53 Sun, C., Dotti, G. & Savoldo, B. Utilizing cell-based therapeutics to overcome immune evasion in hematologic malignancies. *Blood* **127**, 3350-3359, doi:10.1182/blood-2015-12-629089 (2016).

54 Stern-Ginossar, N. *et al.* Human microRNAs regulate stress-induced immune responses mediated by the receptor NKG2D. *Nat Immunol* **9**, 1065-1073, doi:10.1038/ni.1642 (2008).

55 Reim, F. *et al.* Immunoselection of breast and ovarian cancer cells with trastuzumab and natural killer cells: selective escape of CD44high/CD24low/HER2low breast cancer stem cells. *Cancer Res* **69**, 8058-8066, doi:10.1158/0008-5472.CAN-09-0834 (2009).

56 Wang, B. *et al.* Metastatic consequences of immune escape from NK cell cytotoxicity by human breast cancer stem cells. *Cancer Res* **74**, 5746-5757, doi:10.1158/0008-5472.CAN-13-2563 (2014).

57 Malladi, S. *et al.* Metastatic Latency and Immune Evasion through Autocrine Inhibition of WNT. *Cell* **165**, 45-60, doi:10.1016/j.cell.2016.02.025 (2016).

58 Zhang, X. *et al.* IDH mutant gliomas escape natural killer cell immune surveillance by downregulation of NKG2D ligand expression. *Neuro Oncol* **18**, 1402-1412, doi:10.1093/neuonc/now061 (2016).

59 Nowbakht, P. *et al.* Ligands for natural killer cell-activating receptors are expressed upon the maturation of normal myelomonocytic cells but at low levels in acute myeloid leukemias. *Blood* **105**, 3615-3622, doi:10.1182/blood-2004-07-2585 (2005).

60 Trembath, A. P. & Markiewicz, M. A. More than Decoration: Roles for Natural Killer Group 2 Member D Ligand Expression by Immune Cells. *Front Immunol* **9**, 231, doi:10.3389/fimmu.2018.00231 (2018).

61 Cerboni, C. *et al.* The DNA Damage Response: A Common Pathway in the Regulation of NKG2D and DNAM-1 Ligand Expression in Normal, Infected, and Cancer Cells. *Front Immunol* **4**, 508, doi:10.3389/fimmu.2013.00508 (2014).

62 Eagle, R. A., Jafferji, I. & Barrow, A. D. Beyond Stressed Self: Evidence for NKG2D Ligand Expression on Healthy Cells. *Curr Immunol Rev* **5**, 22-34, doi:10.2174/157339509787314369 (2009).

63 Bao, Z. *et al.* Effectiveness and safety of poly (ADP-ribose) polymerase inhibitors in cancer therapy: A systematic review and meta-analysis. *Oncotarget* **7**, 7629-7639, doi:10.18632/oncotarget.5367 (2016).

64 Fong, P. C. *et al.* Inhibition of poly(ADP-ribose) polymerase in tumors from BRCA mutation carriers. *N Engl J Med* **361**, 123-134, doi:10.1056/NEJMoa0900212 (2009).

65 Audeh, M. W. *et al.* Oral poly(ADP-ribose) polymerase inhibitor olaparib in patients with BRCA1 or BRCA2 mutations and recurrent ovarian cancer: a proof-of-concept trial. *Lancet* **376**, 245-251, doi:10.1016/S0140-6736(10)60893-8 (2010).

66 Kruse, V. *et al.* PARP inhibitors in oncology: a new synthetic lethal approach to cancer therapy. *Acta Clin Belg* **66**, 2-9, doi:10.2143/ACB.66.1.2062507 (2011).

Figures

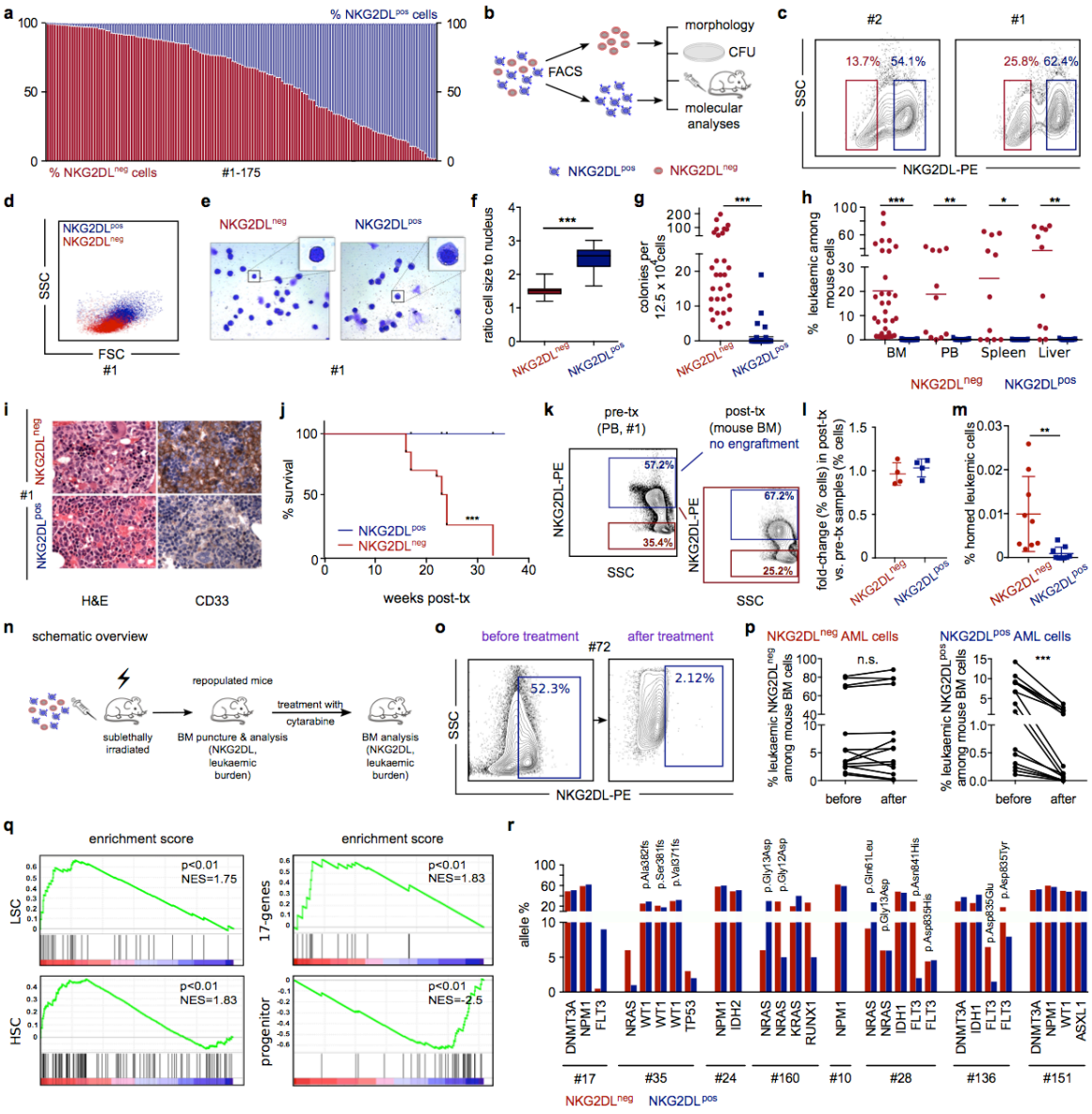
a
% NKG2DL^pos cells
% NKG2DL^neg cells
#1-175
b
FACS
morphology
CFU
molecular analyses
NKG2DL^pos
NKG2DL^neg
c
#2
#1
13.7%
54.1%
25.8%
62.4%
SSC
NKG2DL-PE
d
NKG2DL^pos
NKG2DL^neg
SSC
FSC
#1
e
NKG2DL^neg
NKG2DL^pos
#1
f
ratio cell size to nucleus
g
colonies per 12.5 x 10^4 cells
h
% leukaemic among mouse cells
BM
PB
Spleen
Liver
NKG2DL^neg
NKG2DL^pos
i
#1
H&E
CD33
j
% survival
weeks post-tx
k
pre-tx (PB, #1)
post-tx (mouse BM)
no engraftment
57.2%
35.4%
67.2%
25.2%
SSC
NKG2DL-PE
l
fold-change (% cells) in post-tx vs. pre-tx samples (% cells)
m
% homed leukemic cells
n
schematic overview
repopulated mice
sublethally irradiated
BM puncture & analysis (NKG2DL, leukaemic burden)
treatment with cytarabine
BM analysis (NKG2DL, leukaemic burden)
o
before treatment
after treatment
#72
52.3%
2.12%
SSC
NKG2DL-PE
p
NKG2DL^neg AML cells
NKG2DL^pos AML cells
n.s.
% leukaemic NKG2DL^neg among mouse BM cells
% leukaemic NKG2DL^pos among mouse BM cells
before
after
q
enrichment score
LSC
p<0.01
NES=1.75
17-genes
p<0.01
NES=1.83
HSC
p<0.01
NES=1.83
progenitor
p<0.01
NES=-2.5
r
allele %
DNMT3A
NPM1
FLT3
NRAS
WT1
TP53
IDH2
KRAS
RUNX1
IDH1
ASXL1
#17
#35
#24
#160
#10
#28
#136
#151
NKG2DL^neg
NKG2DL^pos

Figure 1: Absence of immunostimulatory NKG2DL enriches for chemotherapy resistant LSCs. (a) Flow cytometry analysis showing percentages of NKG2DL^{neg} (red) and NKG2DL^{pos} (blue) AML cells within individual patients. **(b-m)** NKG2DL^{neg} and NKG2DL^{pos} AML subpopulations isolated from the same patients were analyzed side-by-side at equal numbers. Schematic overview **(b)**, representative examples of gating strategies **(c)**, forward/sideward scatter plots **(d)**, and comparison of sorted cells by May-Grünwald-Giemsa staining (**e:** exemplary pictures; **f:** quantification of cell to nucleus size ratio, 50 cells quantified for each subpopulation and AML sample, #1, 3, 4, 5, 57), *in vitro* colony assays (**g:** #1-32, means of technical triplicates; note that in 81% of cases colonies exclusively emerged from NKG2DL^{neg} cells) and transplantation assays into NSG mice (**h:** summarized results on long-term infiltration with human leukaemic cells in mouse PB, BM and organs as detected by multicolor flow cytometry for human leukemic antigens, each dot represents one mouse, #1, 6-12, 33-34; **i:** representative BM histopathology pictures, left: H&E, right: anti-CD33, 630x magnification; **j:** Kaplan-Meier survival analysis; 4-5 mice per cellular subpopulation and patient; #1,6-8,12; **k:** representative and **l:** summarized results comparing NKG2DL^{neg} and NKG2DL^{pos} cell percentages in engrafted mouse-derived AML cells, post-tx, versus corresponding patient-derived pre-transplant (pre-tx) AML cells, #1, #6-8, n=3-4 mice per patient and subpopulation; **m:** homing asssays showing summarized percentages of CFSE-labeled cells homed to the BM, each dot represents one mouse, n=3 mice per subpopulation and patient, #35-37). **(n-p)** Effect of *in vivo* cytarabine treatment (1 mg/day s.c. for 2-4 days) on mouse BM leukaemic burden and percentages of NKG2DL^{neg} and NKG2DL^{pos} within infiltrating AML cells, (**n:** schematic overview, BM before treatment collected by BM puncture; **o**: exemplary flow cytometry plots; **p**: summarized results for NKG2DL^{neg} (left) and NKG2DL^{pos} (right) AML subpopulations (#9, #42, #72, #76, #99, #118, #125 and #174; dots connected by one line depict results collected before and after treatment in one animal). **(q-r)** LSC, HSC, common lineage-committed progenitor[1] and 17 genes stemness score[2] signatures and leukaemia-specific mutations (**q:** gene expression array and GSEA analyses; #1,6-8, #12). (* $p < 0.05$, ** $p < 0.01$, *** $p < 0.001$)

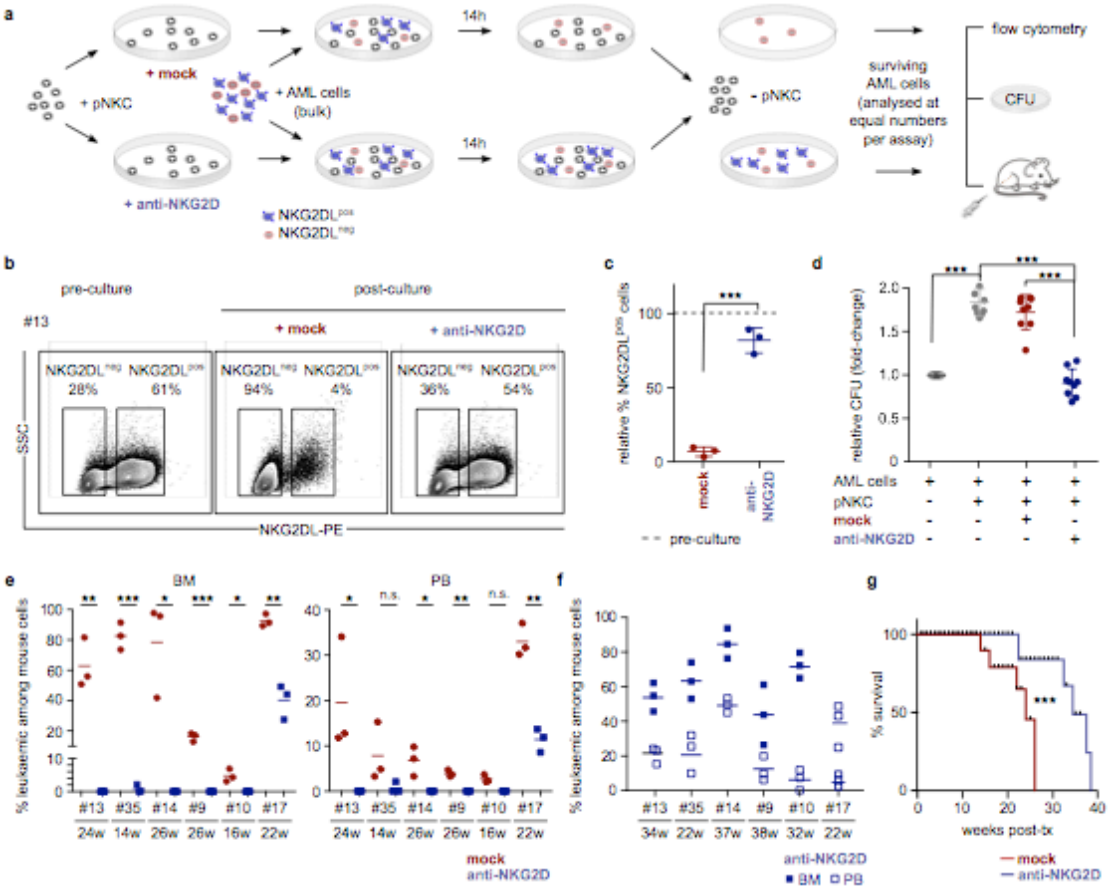

Figure 2: NK cells preferentially lyse non-LSCs. AML cells co-cultured +/- pNKCs and isotype control (mock+pNKCs, red) or blocking anti-NKG2D F(ab')$_2$ 6H7 (anti-NKG2D+pNKCs, blue) were analyzed by flow cytometry and in functional assays. **(a)** Schematic overview, **(b-c)** flow cytometry analysis (**b:** representative results, **c:** quantification indicating the ratio of % NKG2DL^{pos} cells in different treatment groups relative to corresponding cells analyzed prior to culture (#13, 36, 43; p<0.001; Students t-test). **(d)** Quantification of colony numbers (#9-10, 13-17, 35-36, means of technical triplicates) and **(e-g)** *in vivo* engraftment in NSG mice of AML cells separated from the different co-culture conditions (#9, #10, #13, #14, #17, #35; **e-g:** n=3 mice per AML sample and condition, each dot or square represents one mouse). Mice transplanted with AML cells derived from mock+pNKCs (red) or anti-NKG2D+pNKCs (blue) co-cultures were routinely screened[13] by flow cytometry in PB and BM (by BM puncture); if engraftment was detected, all mice transplanted with cells of the same sample were analysed for engraftment in BM (**e**, left) and PB (**e**, right)[13]; mice lacking engraftment at this time-point (all from anti-NKG2D+pNKCs conditions) were further followed and shown to engraft later (**f,** full squares: murine BM, empty squares: murine PB). Note that all AML showed engraftment, albeit at variable time-points. **g:** Kaplan-Meier survival analysis. (* $p < 0.05$, ** $p < 0.01$, *** $p < 0.001$)

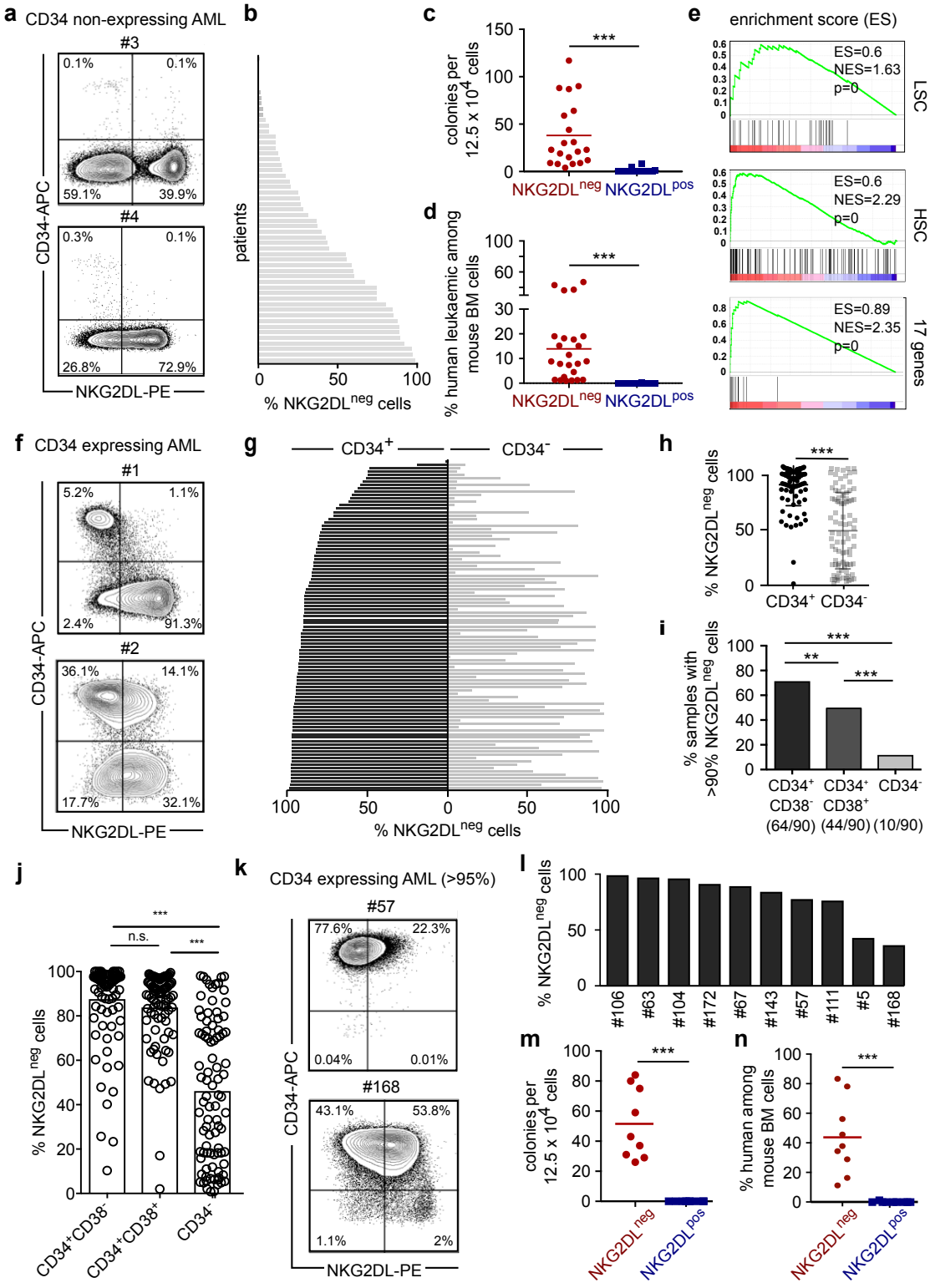
a
CD34 non-expressing AML
#3
0.1%
0.1%
59.1%
39.9%
#4
0.3%
0.1%
26.8%
72.9%
CD34-APC
NKG2DL-PE
b
patients
0
50
100
% NKG2DL^neg cells
c
colonies per 12.5 x 10^4 cells
150
100
50
0
***
NKG2DL^neg
NKG2DL^pos
d
% human leukaemic among mouse BM cells
100
60
30
20
10
0
***
NKG2DL^neg
NKG2DL^pos
e
enrichment score (ES)
ES=0.6
NES=1.63
p=0
LSC
ES=0.6
NES=2.29
p=0
HSC
ES=0.89
NES=2.35
p=0
17 genes
f
CD34 expressing AML
#1
5.2%
1.1%
2.4%
91.3%
#2
36.1%
14.1%
17.7%
32.1%
CD34-APC
NKG2DL-PE
g
CD34+
CD34-
100
50
0
50
100
% NKG2DL^neg cells
h
% NKG2DL^neg cells
100
50
0
***
CD34+
CD34-
i
% samples with >90% NKG2DL^neg cells
100
80
60
40
20
0
***
**
***
CD34+ CD38- (64/90)
CD34+ CD38+ (44/90)
CD34- (10/90)
j
% NKG2DL^neg cells
100
80
60
40
20
0
***
n.s.
***
CD34+CD38-
CD34+CD38+
CD34-
k
CD34 expressing AML (>95%)
#57
77.6%
22.3%
0.04%
0.01%
#168
43.1%
53.8%
1.1%
2%
CD34-APC
NKG2DL-PE
l
% NKG2DL^neg cells
100
50
0
#106
#63
#104
#172
#67
#143
#57
#111
#5
#168
m
colonies per 12.5 x 10^4 cells
100
80
60
40
20
0
***
NKG2DL^neg
NKG2DL^pos
n
% human among mouse BM cells
100
80
60
40
20
0
***
NKG2DL^neg
NKG2DL^pos

Figure 3: Absence of NKG2DL identifies LSCs independently of CD34 expression. (a-e) CD34 non-expressing AMLs: flow cytometry analysis (**a:** exemplary results; **b:** individual results from n=55 patients, see also Supplementary Table 1) and **(c-e)** comparison of NKG2DL^{neg} and NKG2DL^{pos} AML cells sorted from the same patients with respect to colony formation (**c:** #1, 6, 9-11, 33-34, mean of technical triplicates performed for each patient and subpopulation), *in vivo* engraftment in NSG mice (**d:** percentages of human leukaemic among murine BM cells; each dot represents one mouse; n=3-5 mice per subpopulation and AML case, #9-11, 33-34), and LSC, HSC and 17-gene signatures (**e:** biological triplicates for each subpopulation and patient; #9-11, 33-34). **(f-j)** CD34 expressing AMLs: flow cytometry analysis (**f:** exemplary results, **g:** individual results from n=98 patients, see also Supplementary Figure 4 and Supplementary Table 1, **h:** quantification of % NKG2DL^{neg} cells in CD34^{+} and CD34^{-} subpopulations, **i:** quantification of AML samples containing >90% NKG2DL^{neg} cells within CD34^{+}CD38^{-}, CD34^{+}CD38^{+} and CD34^{-} subpopulations and **j:** quantification of NKG2DL^{neg} cells within these subpopulations). **(k-n)** AML with ubiquitous CD34 expression: flow cytometry analysis (**k:** exemplary results, **l:** individual patient results) and comparison of colony formation (**m,** #57, 111, 168, all in triplicates) and *in vivo* engraftment in NSG mice (**n;** each dot represents one mouse, n=3 mice per subpopulation and patient, #5, 111, 168) from CD34^{+}NKG2DL^{neg} and CD34^{+}NKG2DL^{pos} AML cells sorted from the same patients. (* $p < 0.05$, ** $p < 0.01$, *** $p < 0.001$)

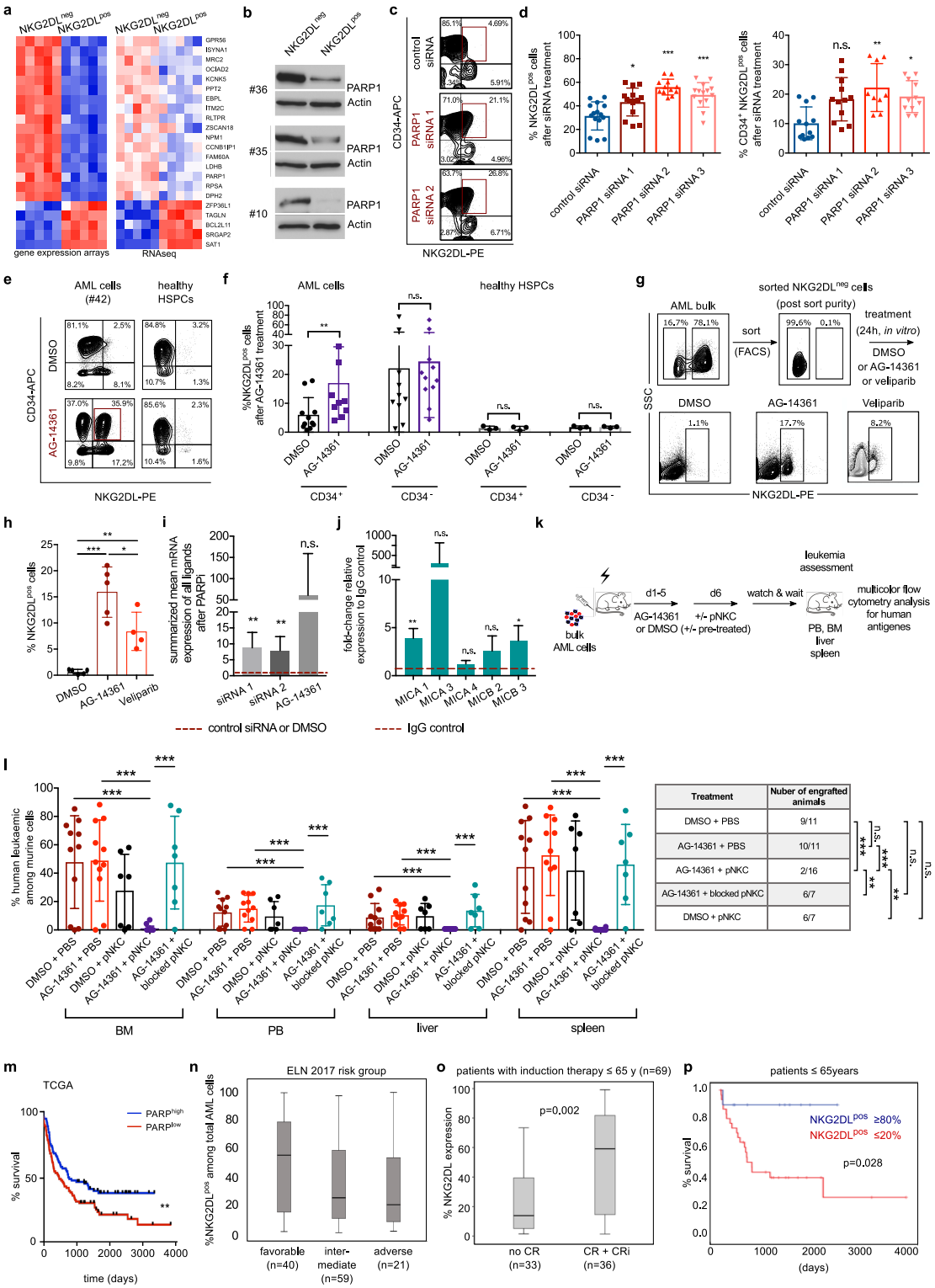
a
NKG2DL neg
NKG2DL pos
GPR56
ISYNA1
MRC2
OCIAD2
KCNK5
PPT2
EBPL
ITM2C
RLTPR
ZSCAN18
NPM1
CCNB1IP1
FAM60A
LDHB
PARP1
RPSA
DPH2
ZFP36L1
TAGLN
BCL2L11
SRGAP2
SAT1
gene expression arrays
RNAseq
b
#36
#35
#10
PARP1
Actin
c
control siRNA
PARP1 siRNA 1
PARP1 siRNA 2
CD34-APC
NKG2DL-PE
d
% NKG2DL pos cells after siRNA treatment
% CD34+ NKG2DL pos cells after siRNA treatment
n.s.
e
AML cells (#42)
healthy HSPCs
DMSO
AG-14361
f
AML cells
healthy HSPCs
%NKG2DL pos cells after AG-14361 treatment
CD34+
CD34-
g
sorted NKG2DL neg cells (post sort purity)
AML bulk
sort (FACS)
treatment (24h, in vitro)
DMSO or AG-14361 or veliparib
SSC
Veliparib
h
% NKG2DL pos cells
i
summarized mean mRNA expression of all ligands after PARPi
siRNA 1
siRNA 2
AG-14361
j
fold-change relative expression to IgG control
MICA 1
MICA 3
MICA 4
MICB 2
MICB 3
control siRNA or DMSO
IgG control
k
bulk AML cells
d1-5
AG-14361 or DMSO (+/- pre-treated)
d6
+/- pNKC
watch & wait
leukemia assessment
PB, BM liver spleen
multicolor flow cytometry analysis for human antigenes
l
% human leukaemic among murine cells
DMSO + PBS
AG-14361 + PBS
DMSO + pNKC
AG-14361 + pNKC
AG-14361 + blocked pNKC
BM
PB
liver
spleen
Treatment
Nuber of engrafted animals
DMSO + PBS
9/11
AG-14361 + PBS
10/11
AG-14361 + pNKC
2/16
AG-14361 + blocked pNKC
6/7
DMSO + pNKC
6/7
m
TCGA
PARP high
PARP low
% survival
time (days)
n
ELN 2017 risk group
%NKG2DL pos among total AML cells
favorable (n=40)
inter-mediate (n=59)
adverse (n=21)
o
patients with induction therapy ≤ 65 y (n=69)
p=0.002
% NKG2DL expression
no CR (n=33)
CR + CRi (n=36)
p
patients ≤ 65years
NKG2DL pos ≥80%
NKG2DL pos ≤20%
p=0.028
% survival
(days)

Figure 4: Increased PARP1 expression in LSCs contributes to their selective escape from NK cell immune surveillance. (a) Overlap of differentially regulated genes in NKG2DL^{neg} versus NKG2DL^{pos} cells isolated from the same AMLs and analysed by gene expression arrays (#1,6-8, 12; right panel) and RNA sequencing (#9-11, 33-34; left panel). **(b)** Exemplary immunoblots showing PARP1 protein expression (loading control: actin) in sorted NKG2DL^{neg} and corresponding NKG2DL^{pos} AML subpopulations (cropped images are shown, for additional patients and full images see Extended Data Fig. 7 and Source Data File 1). **(c-j)** *In vitro* PARP1 inhibition in bulk AML cells. Shown are flow cytometry analyses after treatment with PARP1 versus control siRNAs (**c:** exemplary results, #42; **d:** summarized results, #36-37, 42, 151), and PARP1 inhibitors (AG-14361, 20 μM; veliparib, 10 μM) versus DMSO (0.2%) as carrier control (**e**: exemplary results; **f**: summarized results, each dot, square or triangle represents the average of technical triplicates from one subpopulation in one AML, left panel: #2, 16-18, 27, 29-30, 35-36, 38-39, 40-42, 47, 82, 100, 148, or healthy cord blood, right panel: n=3 donors). **(g-h)** *In vitro* PARP1 inhibition in sorted NKG2DL^{neg} AML cells using AG-14361 (20 μM) or Veliparib (1 μM) versus DMSO carrier control (0.2%) (**g**: schematic procedure with representative results; **h**: quantification of NKG2DL^{pos} cells post-treatment; each dot represents the average of technical replicates obtained from one AML case; #16, 35-37, 151). **(i)** Bulk AML cells were treated with PARP1 versus control siRNAs (#4, 151), or with AG-14361 (20 μM) versus DMSO control (#36, 37, 151). Shown are summarized relative mRNA data of single NKG2DL from PARP1 inhibition versus control conditions (see Supplementary Figure 7 for results on single NKG2DL). **(j)** ChIP analysis illustrating direct recruitment of PARP1 to the MICA and MICB promoter (#35-37, biological triplicates). **(k-l)** Leukemia development in NSG mice transplanted with AML cells and treated with AG-14361 or DMSO +/- pNKC (**k**: schematic illustration of experimental setup; **l**: summarized flow cytometry data in PB, BM and organs, each dot represents one mouse; n=7-16 mice per condition, #42) **(m-o)** Correlation of NKG2DL surface expression and clinical AML characteristics (all patients with AML at first diagnosis, APL excluded, n=175; **n:** genetic and molecular characteristics; **o:** achievement of complete remission (CR) or incomplete CR (CRi) after induction chemotherapy, **p**: and overall survival). **(p)** Survival analysis of AML patients with enhanced (above median) versus low (below median) PARP1 (TCGA, n=179 patients[23]). (* $p < 0.05$, ** $p < 0.01$, *** $p < 0.001$)

For all Figure legends: if not mentioned otherwise, a Mann-Whitney U Test was performed for statistical analysis.

References Figure Legends:

1. Eppert, K., *et al.* Stem cell gene expression programs influence clinical outcome in human leukemia. *Nat Med* **17**, 1086-1093 (2011).

2. Ng, S.W., *et al.* A 17-gene stemness score for rapid determination of risk in acute leukaemia. *Nature* **540**, 433-437 (2016).

Supplementary Material

Primary AML cells and blood samples of healthy donors

Peripheral blood mononuclear cells (PBMC) cells of patients with AML or healthy donors were isolated by density gradient centrifugation after informed consent in accordance with the declaration of Helsinki. Cells were viably frozen (in RPMI1640, Sigma-Aldrich, St. Louis, MO, USA, supplemented with 20% FCS, Sigma-Aldrich and 10% dimethyl sulfoxide solution, AppliChem, Darmstadt, Germany) and freshly thawed for each experiment. For AML samples containing <95% leukemic cells, leukemic cells were enriched by MACS or FACS sorting for leukemic antigens (see Supplementary Table 1) prior to use. Post-sort purity was routinely above 95%. Patient characteristics are summarized in Supplementary Table 1. Cord blood $CD34^+$ cells were isolated from healthy full-term deliveries by ficoll gradient, further purified using the indirect CD34 microbead kit from MACS (Miltenyi, Bergisch-Gladbach, Germany) and frozen in fetal calf serum (FCS) containing 10% dimethyl sulfoxide solution. The study was conducted according to the guidelines of the Eberhard-Karls-University Tuebingen, the Ethikkomission Nordwest- und Zentralschweiz and the DKFZ and University of Heidelberg Ethics committees. Informed consent was obtained from all patients included in the study.

Flow cytometry and sorting into $NKG2DL^{neg}$ and $NKG2DL^{pos}$ cells

For flow cytometry analyses, fluorescence conjugates targeting human CD33, CD34, CD133, CD117, CD45, CD44, CD123, CD99, CD96, CD25 and TIM3 (BD Biosciences, Franklin Lakes, NJ, USA), CD14, CD13 (eBiosciences, San Diego, CA, USA), CD3 and CD19 (Biolegend, San Diego, CA, USA) were used, and analysis was performed on either a FACS CantoII or LSR II Fortessa (both BD Biosciences) or Cytoflex (Beckman Coulter, Brea, CA, USA). SytoxBlue or 7-AAD was used for live and dead cell discrimination.

For simultaneous staining of all NKG2DL, a recombinant NKG2D-Fc chimera (fusion protein) and the corresponding isotype control were purchased from

R&D (Minneapolis, MN, USA) and biotinylated with the One-step biotinylation kit (MACS Miltenyi) according to manufactures instructions. Prior to staining, cells were blocked with human IgG (Sigma-Aldrich) and washed. Then biotinylated fusion protein or control (10µg/ml each) were added followed by streptavidin-PE (LifeTechnologies, Carlsbad, CA, USA) and selection antibodies. In some cases, AML cells were stained with non-biotinylated fusion protein as described above except that cells were not blocked and PE-anti-human IgG1 (SouthernBiotech, Birmingham, AL, USA) was used as secondary reagent. 7-AAD was used to exclude dead cells, and sorting was performed using a FACS Aria III or FACSFusion (both BD Biosciences). Post-sort purity was routinely >95%.

For staining of individual NKG2DL, previously described antibodies against human MICA, MICB, ULBP1 and ULBP2/5/6 or isotype control (all at 10µg/ml) followed by goat anti-mouse–PE $F(ab')_2$ fragments (Dako) were used as described above.

For all analyses log scale ranging from 10^1 to 10^7 was used.

May-Grünwald-Giemsa staining

For morphological analyses, sorted $NKG2DL^{neg}$ and $NKG2DL^{pos}$ cells were spinned on poly-L-lysine coated slides (Sigma-Aldrich, St. Loius, MO, USA) using a Cytospin 4 (ThermoFisher Scientific, Waltham, MA, USA). Afterwards, slides were stained in May-Grünwald solution, washed, stained in Giemsa solution, again washed and air-dried overnight. Pictures were taken at 60x magnification on a Leica digital MC170 HD camera attached to a Leica DM 2000 LED (Leica Microsystems AG, Switzerland).

Colony forming unit (CFU) assays

For CFU assays, equal numbers of $NKG2DL^{neg}$ or $NKG2DL^{pos}$ cells sorted by FACS were plated in methylcellulose (Methocult H4434, StemCell Technologies, Vancouver, Canada) in triplicates, incubated at 37°C in 5% CO_2 and scored for CFUs at day 14. Depending on the availability of patient material,

12.5x10^3 or 25x10^3 cells were plated per well in this assay (same numbers for all conditions per individual patient).

Mice and xenotransplantation assays

NOD.Cg-*Prkdc*^{scid} *IL2rg*^{tmWjl}/Sz (also termed NOD/SCID/IL2Rγ^{null}, NSG) mice purchased from Jackson Laboratory (Bar Harbor, ME, USA) were maintained under pathogen-free conditions according to the Swiss and German federal and state regulations. All animal experiments were approved by the Regierungspräsidium Karlsruhe (Tierversuchsantrag numbers G108/12 and G243/16), Tübingen (M12/12) and the Veterinäramt Basel-Stadt (24981 and 28218).

Freshly thawed primary AML cells were transplanted (between 4x10^5 and 1x10^6 cells per mouse, depending on availability but in any case at equal numbers for all fractions derived from an individual patient) into 6-10 weeks old gender-matched animals with or without prior sublethal irradiation via the tail vein or intrafemorally[1] after resuspension in 200 or 25 µl PBS, respectively. AML cells were selected based on CD33$^+$ or other pan-leukemic antigen expression, depending on the AML sample. Alternatively, CD3 depletion was performed before cells were sorted into NKG2DL^{neg} and NKG2DL^{pos} cells and used for further experiments. Patients analyzed in individual experiments are indicated in the figure or figure legend, and patient' characteristics are summarized in Supplementary Table 1. Engraftment was assessed in PB and BM at signs of distress (e.g. decreased food and water consumption, rapid breathing, altered movement) or routinely every 4 to 5 weeks in one mouse per group for each AML case following a protocol recently published by our group.[2] Engraftment was defined as ≥1% leukemic cells in murine PB or BM as assessed by multi-color flow cytometry using antibodies against human leukemic antigens according to the individual AML specific phenotype. Lineage markers (CD3, CD19) were used to exclude engraftment with healthy hematopoietic cells. For survival analyses, mice of the experimental group were euthanized at sickness (weight loss, ruffled coat, weakness, reduced motility, other severe pathology, according to regulations contained in our animal protocol and the German and Swiss animal handling guidelines) and/or detection of heavy infiltration (>50%) with human AML among murine bone marrow (BM) cells as revealed by routine testing conducted every 4-5 weeks in at least one mouse per group.[3,4] Upon detection of heavy leukemic infiltration, all mice of the corresponding group were euthanized; in case leukemia

was not similarly detected the respective mice were scored as lost for follow-up in the Kaplan-Meier analysis. Upon termination of experiments, all mice underwent final assessment consisting of multi-color flow cytometry of PB, BM, liver and spleen performed as described above. Leukemic engraftment was further verified by whole body histopathology (see below). For secondary transplantations, BM cells freshly isolated from mice (taken from both femora and tibiae) were sorted again into NKG2DL^{neg} and NKG2DL^{pos} fractions as described above, and used for re-transplantation at equal numbers as in corresponding primary transplantations.

BALB/c mice were purchased from Charles River (Wilmington, MA, USA) and maintained under pathogen-free conditions according to the Swiss federal and state regulations.

Histopathological analysis

For histopathological analyses, murine organs were fixed in 4% phosphate buffered formalin and then embedded in paraffin. Immunohistochemical analysis was performed as previously described, using H&E staining and antibodies against human CD33 (Ventana, Tucson, Arizona, USA, Mouse monoclonal, Clone: QBEnd 10, RTU) and human CD34 (Ventana, Mouse monoclonal, Clone: QBEnd 10, RTU).[5]

Homing assay

AML cells were separated into NKG2DL^{neg} and NKG2DL^{pos} fractions as described above, labeled with CFSE (CellTrace CFSE Cell Proliferation Kit, ThermoFisher Scientific, Waltham, MA, USA) and injected at $1x10^6$ cells per mouse via the tail vein in n=3 NSG mice per group and per patient. After 12 hours, mice were euthanized and BM analyzed by flow cytometry recognizing CFSE as well as human leukemic antigens (CD33, CD34) using a LSR II Fortessa (BD Biosciences).

Microarray and quantitative real-time reverse transcription PCR (qRT-PCR) analyses

Microarray gene expression analyses were performed on RNA extracted using the RNeasy Mini Kit (Qiagen) from NKG2DL^{neg} and NKG2DL^{pos} sorted patient blasts. Triplicate independent biological experiments were performed for each individual sample. Concentration and purity of RNA samples were determined with a NanoDrop photometer (peqlab), and integrity confirmed on a 2100 Bioanalyzer (Agilent Technologies, Santa Clara, CA). Only RNA samples with RIN values ≥ 7.5 were considered. Per condition, 100 ng of RNA were used to prepare cyanine-3-labeled cRNA for hybridizations, which were performed according to standard protocols using Agilent SurePrint G3 Human Gene Expression 8x60K v2 Microarrays. After extensive washing, fluorescence intensities were detected with the Scan Control A.8.4.1 software (Agilent) on an Agilent DNA Microarray Scanner and extracted from images using Feature Extraction 10.7.31 software (Agilent). Quantile normalization was applied to the data set and correlation analysis was performed. After normalization, the microarray probes were filtered according to the flag information provided by Feature Extraction 10.7.3.1 software. Fold changes were calculated, and differentially expressed RNAs were identified accordingly. The log2-normalized data were linearized and used as input for Gene set enrichment analysis (GSEA, Broadinstitute.org). One gene matrix transposed file was generated containing the transcripts from up- and down-regulated genes in the comparison of NKG2DL^{neg} and NKG2DL^{pos} blasts (CD34expressing and non-expressing AMLs separately), and the transcripts of the LSC signature, the HSC signature and the progenitor signature published previously[6]. GSEA computes if the gene set is enriched in the generated gene expression data.

For qRT-PCR, the QuantiTect Whole Transcriptome Kit (Qiagen) was used for pre-amplification and reverse transcription of limited amounts of RNA to obtain high yields of cDNA. Gene transcripts were detected using an Applied Biosystems® Real-Time PCR 7500 Fast System instrument and Fast Start Universal SYBR Green Master with Rox (Roche) and gene-specific primers. A PBGD control for equal loading was used throughout the experiments to later normalize the real-time PCR data. Fold change values of gene expression by averages from triplicate measurements were calculated using the $\Delta\Delta C_T$ method as described by Livak and Schmittgen[7]. For gene expression analyses, RNA was isolated using either the Promega ReliaPrep™ RNA Miniprep Systems (Promega, Madison, WI, USA) or the RNeasy Plus Micro Kit

(Qiagen) and transcribed into cDNA using the High-Capacity cDNA Archive Kit (Applied Biosystems, Foster City, CA, USA) or the FastStart Universal SYBR Green Master (ROX) (Roche). qRT-PCR was performed as detailed above. All primers are listed in the Supplementary Table 8.

RNA-sequencing and Gene set enrichment analysis (GSEA)

Total RNA isolation from 50,000 sorted cells was performed using an Arcturus PicoPure RNA isolation kit (Life Technologies, Invitrogen) according to the manufacturer's instructions. cDNA libraries were generated with 10 ng of total RNA using the SMARTer Ultra Low RNA kit for Illumina sequencing (Clontech Laboratories) according to the manufacturer's indications. Sequencing was performed with a HiSeq2000 device (Illumina) and three samples per lane. Sequences were aligned to hg19 reference genome using the STAR alignment software[8] with Gencode v19 as the transcriptome annotation. DESeq2[9] was used to generate a list of differentially expressed protein-coding genes between $NKG2DL^{neg}$ and $NKG2DL^{pos}$ samples. This pre-ranked list was used for Gene Set Enrichment Analysis (GSEA) using the GSEA desktop application and gene sets databases downloaded from the Broad Institute using default settings with 2000 permutations. Calculations were performed with R version 3.3.1 in R-Studio (version 0.99.903).

Targeted Next Generation Sequencing (NGS) for analysis of leukaemia-specific mutations

NGS analysis was performed on sorted $NKG2DL^{pos}$ versus $NKG2DL^{neg}$ subpopulations from n=8 AML samples. DNA for NGS was isolated using ZR-Duet DNA/RNA MiniPrep kit (ZymoResearch, Irvine, CA, USA) according to the manufacturer's protocol and NGS analysis performed as previously described[2]. Patient NGS libraries were prepared using the AML community panel from Thermo Fisher containing 19 genes frequently mutated in AML (see ampliseq.com). Patient libraries were sequenced using the Ion PGM platform and analyzed using the Ion Reporter AML pipeline (version 5.0). The average coverage per sample was ~1.400-fold. Sensitivity for calling a mutation was set at 3%. If a mutation was observed in a "post-transplantation"

sample but not reported to be present in the initial patient sample, the mapped reads were manually analyzed to assess whether the mutation was present but with a lower allelic burden than 3%. The sensitivity of such retrospective analysis is dependent on the coverage of the specific region (normally around 0.25%).

In vitro co-cultures of AML and NK cells

Polyclonal NK cells (pNKC) were generated by incubation of PBMC with K562-41BBL-IL15 feeder cells obtained from St. Jude's Children's Research Hospital as described previously[10]. Cultures of primary AML cells with or without pNKC (E:T ratio 10:1) were conducted for 16h in the presence or absence of $F(ab')_2$ fragments of a blocking anti-NKG2D mAb (clone 6H7 kindly provided by Amgen Inc.)[11] or isotype control (SouthernBiotech, Clone 15H6, 5µg/ml each). Afterwards, AML cells were retrieved by removing dead cells using a ficoll gradient followed by MACS (Miltenyi) selection for leukemic antigens expressed in the initial patient sample (see Supplementary Table 1) and further analyzed at equal numbers in CFU and *in vivo* xenotransplantation assays in NSG mice. Mice were screened by flow cytometry in PB and BM (by BM puncture) performed routinely in one mouse per experimental group; if engraftment was detected, all mice transplanted with cells of the same AML case (from all different experimental groups) were analysed.

Immunoblot

$1x10^6$ AML cells sorted as described above by NKG2D-Fc FACS in $NKG2DL^{pos}$ and $NKG2DL^{neg}$ fractions or by MACS (Miltenyi) in $CD34^+$ and $CD34^-$ cells were re-suspended in Lysis Buffer (#9803, Cell Signaling, Danvers, MA, USA) supplemented with Protease/Phosphatase Inhibitor Cocktail (#78442 ThermoFisher Scientific) and disrupted by vortexing. Samples were cleared by centrifugation, soluble protein denatured in Laemmli buffer, 10 µg total protein separated in bis-acrylamide gels (#161-0148, BioRad, Hercules, CA, USA) by Disc-SDS-PAGE, and transferred onto PVDF membrane (#10600021, Amersham, GE Healthcare Life Sciences, Chalfont St. Giles, UK) in a semi-dry blotting apparatus (Trans-Blot Turbo, BioRad). Membranes were blocked with

10% nonfat dry milk (#9999S, Cell Signaling, diluted in TBS 0.1% Tween-20, p1379, Sigma). Proteins were stained with anti-human PARP1 (#9542S) and anti β–actin (#3700S) antibodies, and detected by ECL reaction using HRP-linked secondary reagents (#7074S, anti-rabbit IgG and #7076S, anti-mouse IgG, all from Cell Signaling Technology, see manufacturer's instructions).

In vitro treatments with AG-14361, veliparib, azacytidine, ATRA, valproic acid or doxorubicine

Bulk AML cells were cultured in RPMI1640 supplemented with 10% FCS and cord blood $CD34^+$ cells respectively in X-Vivo 20 (Lonza, Basel, Switzerland) supplemented with 100 ng/ml SCF, 100 ng/ml TPO, 100 ng/ml Flt3-L and 60 ng/ml IL-3 (all Peprotech, Rocky Hill, NJ, USA). Treatments with 20 μM AG-14361 (Selleckchem, Munich, Germany) or DMSO as vehicle control were performed for 24h for AML cells and respectively 48h for cord blood cells. Alternatively, bulk AML cells were cultured in the presence or absence of azacytidine (5μM, Sigma-Aldrich), all-trans retinoic acid (ATRA, 1 μM, Sigma-Aldrich), valproic acid (VPA, 2 μM, Sigma-Aldrich) or vehicle control for 24 hours.

For treatments of sorted $NKG2DL^{neg}$ AML cells, the latter were sorted from bulk AML cells as described into $NKG2DL^{neg}$ cells as described and then cultured in the presence of either AG-14361 (20 μM), veliparib (10 μM, Selleckchem, Munich, Germany) or DMSO vehicle control for 24h and then analyzed for NKG2DL expression as described.

For *in vitro* analysis of chemotherapy resistance, AML cells sorted into $NKG2DL^{neg}$ and $NKG2DL^{pos}$ subpopulations were separately cultured in the presence of Doxorubicine (10 ng/ml, Adriblastin, Pfizer, New York City, NY, USA) or PBS control for 24h or 48h and then analysed using AnnexinV/7-AAD staining (BD Biosciences, Franklin Lakes, NJ, USA, according to manufacturer's protocol) using a Beckman Coulter Cytoflex (Beckman Coulter, Brea, CA, USA).

In vivo treatments with AG-14361 or cytarabine

For *in vivo* treatments with AG-14361, BALB/c mice or NSG mice engrafted with human AML cells (>40% of leukemic cells among murine BM or PB cells as assessed by BM puncture or PB analysis) were divided into two groups, one receiving 10 mg/kg AG-14361, the other DMSO control for 5 consecutive days by intraperitoneal injections as previously described[12]; all mice were sacrificed for final analysis at day 6.

For *in vivo* analysis of chemotherapy resistance, NSG mice were engrafted as described above with bulk AML cells and leukemic engraftment screened by BM puncture. Upon detection of engraftment, BM was stained for leukemic infiltration and NKG2DL distribution on human leukemic cells. Mice were then treated with 1 mg/day cytarabine (Cytostar, Pfizer) for 2 to 4 consecutive days via subcutaneous injections and analyzed 48h later for human leukemic among murine BM cells and NKG2DL expression using a Beckman Coulter Cytoflex.

siRNA treatment

AML cells cultured *in vitro* as described above were transfected with Silencer Select small interfering RNAs (siRNAs) for PARP1 or respectively control siRNAs (both purchased from LifeTechnologies, Carlsbad, CA, USA) using Lipofectamine RNAiMAX reagent (LifeTechnologies). 24 hours later the transfected cells were harvested and analyzed by qRT-PCR analysis for knockdown efficiency and by flow cytometry for NKG2DL expression. Treatments were performed with three different PARP1 siRNAs (used separately or as scrambled mix) or with a scrambled mix of two non-coding siRNAs as control.

Analysis of healthy hematopoietic stem and progenitor cells and blood counts

DMSO and AG-14361 treated BALB/c mice were sacrificed and whole BM (from both femora and tibiae) as well as PB were isolated and stained as described[13]. For HSC staining, the following antibodies were used: anti-mouse lineage cocktail, anti-mouse Ly6A/E (Sca-1), anti-mouse CD117 (c-kit), anti-

mouse CD48 and anti-mouse CD150 (all Biolegend). For progenitor staining, anti-mouse lineage cocktail, anti-mouse CD117, anti-mouse CD34 and anti-mouse CD16/32 antibodies were used (all Biolegend, except CD34 eBiosciences). HSCs were identified as previously described[13]. Murine NKG2DL expression was determined using FITC-labeled tetramers of mouse NKG2D ectodomains. Biotinylated murine NKG2D monomers were generated as described before[14]. Tetramerization was performed with streptavidin-FITC (Life Technologies) in a 4:1 molar ratio as described before for human NKG2D tetramers[15]. Control tetramers were generated from biotinylated HLA-A*0201 monomers containing influenza A virus peptide (58–66) GILGFVFTL (kindly provided by S. Stevanović, University of Tübingen, Germany). All samples were analyzed using a LSR II Fortessa (BD Biosciences). Complete blood counts (CBCs) were determined on an Advia120 Hematology Analyzer using Multispecies version 5.9.0-MS software (Bayer).

Analysis of external datasets

RSEM normalised RNA-sequencing expression data of 179 primary AML samples from The Cancer Genome Atlas (TCGA)[16] were downloaded from the Broad Institute. Clinical data and mutational status were downloaded from the TCGA website. Samples were stratified according to PARP1 expression (RPKM, high=above the median, low=below the median). Survival analysis was performed by using the Mantel-Cox log-rank test in GraphPad Prism 7 software.

Raw counts of the GSE74246[17] dataset was downloaded from the GEO portal. DESeq2[9] was used to generate a list of differentially expressed genes between LSC and Blast samples. This preranked list was used for Gene Set Enrichment Analysis (GSEA) using the GSEA desktop application and gene sets databases downloaded from the Broad Institute using default settings with 2000 permutations. Calculations were performed with R version 3.3.1 in R-Studio (version 0.99.903).

In vivo killing of human AML cells by pNKC

For the experiments depicted in Extended Data Figure 13, bulk AML cells were cultured *in vitro* in the presence of DMSO or 20 μM AG-14361 for 24h, labeled with CFSE and transplanted into NSG mice which were co-transplanted or not with pNKC (AML cells, $1.5x10^6$; NK cells, $15x10^6$). 12h after transplantation mice of all conditions were sacrificed and analyzed for human leukemic cells in BM, PB and organs by flow cytometry using a LSR II Fortessa (CFSE and antibody staining with CD33 and CD34, both BD Biosciences).

For the experiments depicted in Figure 4k-l, sublethally irradiated NSG mice were transplanted with $6x10^5$ bulk primary AML cells/mouse at day 0. Mice then received either DMSO (15% in PBS) or AG-14361 (10mg/kg) via intraperitoneal injections from day 1 to 5 post-transplantation. At day 6 post-transplantation, mice received either $12x10^6$ pNK cells (untreated or pre-treated *in vitro* with 5μg/ml anti-NKG2D 6H7 $F(ab')_2$ fragments or isotype control) or PBS as control via tail vein injection. Mice of all treatment groups were then followed for signs of sickness. Final analysis was performed in all mice at week 12 (experiment 1) or week 9 post-transplantation (experiments 2 and 3) when routine BM analysis detected first robust engraftment in mice of the control group. In all cases, analysis consisted of multicolour flow cytometry for human leukemic antigens as well as human CD3 and CD19 (to exclude engraftment with healthy hematopoietic cells) performed using a Beckman Coulter Cytoflex on PB, BM, spleen and liver of all mice included in the experiment.

Chromatin immunoprecipitation assay (ChIP)

ChIP was essentially performed as described by Wang et al. (2017) using PARP1 antibody (Cell signaling, #S9542) and the primers summarized in Supplementary Table 9.[18] Briefly, 1×10^7 primary AML blasts were fixed in 1% formaldehyde, sonicated, precleared, and incubated with 10 μg anti-PARP-1 or isotype control IgG antibodies overnight at 4°C. Complexes were washed, DNA-extracted, precipitated, and amplified by RT-PCR using primers sets homologous to regions of the human MICA or the MICB promoter. Non-immunoprecipitated chromatin was used as input control.

Shedding assays

Primary AML cells were sorted by MACS in $CD34^+$ (black) and $CD34^-$ (grey) populations and cultured for 72h before sMICA, sMICb, sULBP1 and sULBP2 were analysed in supernatants by ELISA as described previously (Hilpert et al., 2012).

Statistical analysis

Data represent mean ±SEM. *P*-values are derived via the application of the students t-test, Mann-Whitney U test or two-tailed Fisher's exact test.

Data availability statement

Data that support the findings of this study will be deposited in Gene Expression Omnibus prior to publication. All other relevant data are available from the corresponding author.

References Supplementary Material

1 Mazurier, F., Doedens, M., Gan, O. I. & Dick, J. E. Rapid myeloerythroid repopulation after intrafemoral transplantation of NOD-SCID mice reveals a new class of human stem cells. *Nat Med* **9**, 959-963, doi:10.1038/nm886 (2003).

2 Paczulla, A. M. *et al.* Long-term observation reveals high-frequency engraftment of human acute myeloid leukemia in immunodeficient mice. *Haematologica*, doi:10.3324/haematol.2016.153528 (2017).

3 Andersson, A. *et al.* Microarray-based classification of a consecutive series of 121 childhood acute leukemias: prediction of leukemic and genetic subtype as well as of minimal residual disease status. *Leukemia* **21**, 1198-1203, doi:2404688 [pii] 10.1038/sj.leu.2404688 (2007).

4 Sanchez, P. V. *et al.* A robust xenotransplantation model for acute myeloid leukemia. *Leukemia* **23**, 2109-2117, doi:10.1038/leu.2009.143 (2009).

5 Kunder, S. *et al.* A comprehensive antibody panel for immunohistochemical analysis of formalin-fixed, paraffin-embedded hematopoietic neoplasms of mice: analysis of mouse specific and human antibodies cross-reactive with murine tissue. *Toxicol Pathol* **35**, 366-375, doi:10.1080/01926230701230296 (2007).

6 Eppert, K. *et al.* Stem cell gene expression programs influence clinical outcome in human leukemia. *Nat Med* **17**, 1086-1093, doi:10.1038/nm.2415 (2011).

7 Livak, K. J. & Schmittgen, T. D. Analysis of relative gene expression data using real-time quantitative PCR and the 2(-Delta Delta C(T)) Method. *Methods* **25**, 402-408, doi:10.1006/meth.2001.1262 (2001).

8 Dobin, A. *et al.* STAR: ultrafast universal RNA-seq aligner. *Bioinformatics* **29**, 15-21, doi:10.1093/bioinformatics/bts635 (2013).

9 Love, M. I., Huber, W. & Anders, S. Moderated estimation of fold change and dispersion for RNA-seq data with DESeq2. *Genome Biol* **15**, 550, doi:10.1186/s13059-014-0550-8 (2014).

10 Koerner, S. P. *et al.* An Fc-optimized CD133 antibody for induction of NK cell reactivity against myeloid leukemia. *Leukemia*, doi:10.1038/leu.2016.194 (2016).

11 Steigerwald, J. *et al.* Human IgG1 antibodies antagonizing activating receptor NKG2D on natural killer cells. *MAbs* **1**, 115-127 (2009).

12 Calabrese, C. R. *et al.* Anticancer chemosensitization and radiosensitization by the novel poly(ADP-ribose) polymerase-1 inhibitor AG14361. *J Natl Cancer Inst* **96**, 56-67 (2004).

13 Hilpert, M. *et al.* p19 INK4d controls hematopoietic stem cells in a cell-autonomous manner during genotoxic stress and through the microenvironment during aging. *Stem Cell Reports* **3**, 1085-1102, doi:10.1016/j.stemcr.2014.10.005 (2014).

14 André, M. C. *et al.* Impaired tumor rejection by memory CD8 T cells in mice with NKG2D dysfunction. *Int J Cancer* **131**, 1601-1610, doi:10.1002/ijc.26191 (2012).

15 Welte, S. A. *et al.* Selective intracellular retention of virally induced NKG2D ligands by the human cytomegalovirus UL16 glycoprotein. *Eur J Immunol* **33**, 194-203, doi:10.1002/immu.200390022 (2003).

16 Ley, T. J. *et al.* Genomic and epigenomic landscapes of adult de novo acute myeloid leukemia. *N Engl J Med* **368**, 2059-2074, doi:10.1056/NEJMoa1301689 (2013).

17 Corces, M. R. *et al.* Lineage-specific and single-cell chromatin accessibility charts human hematopoiesis and leukemia evolution. *Nat Genet* **48**, 1193-1203, doi:10.1038/ng.3646 (2016).

18 Wang, H. *et al.* Prominent oncogenic roles of EVI1 in breast carcinoma. *Cancer Res*, doi:10.1158/0008-5472.CAN-16-0593 (2017).

Extended Data Figures

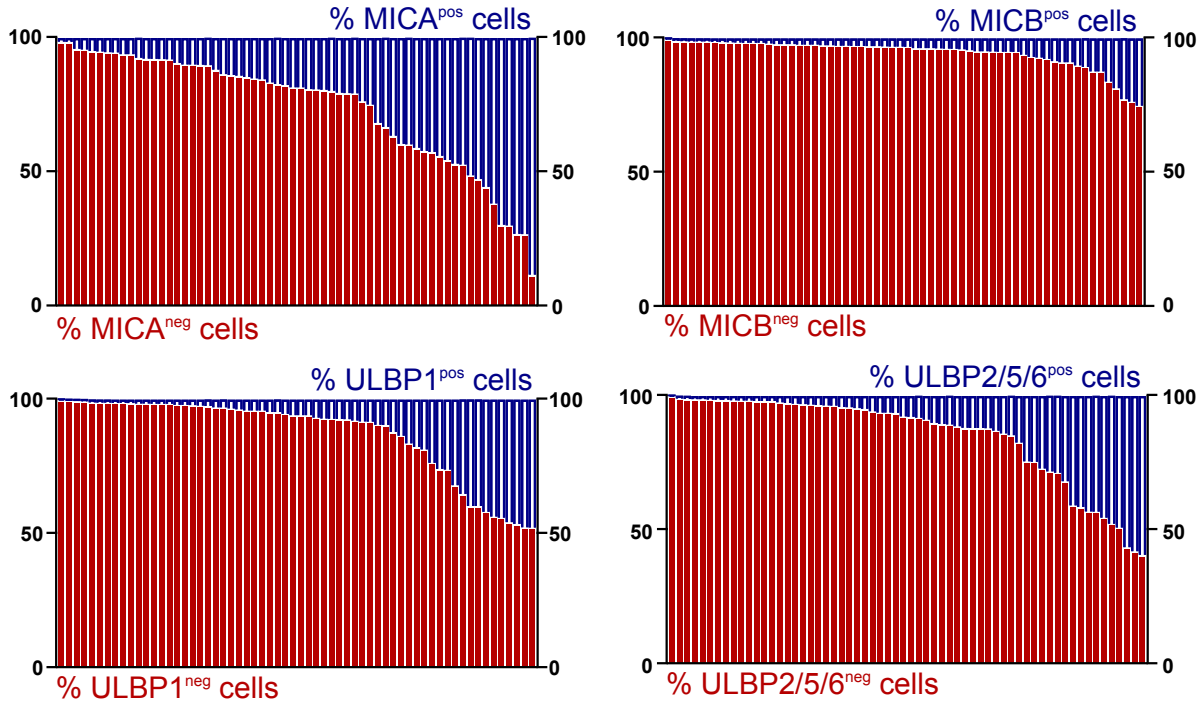

Extended Data Figure 1: Expression of single NKG2DL in primary AML samples. Flow cytometry analysis using antibodies against human MICA, hMICB, hULBP1 or ULBP2/5/6 in primary AML cells from n=62 patients. The heterogeneous expression within the same patients mirrors the results obtained upon combined analysis of all NKG2DL using NKG2D-Fc chimeric protein (shown in Figure 1a).

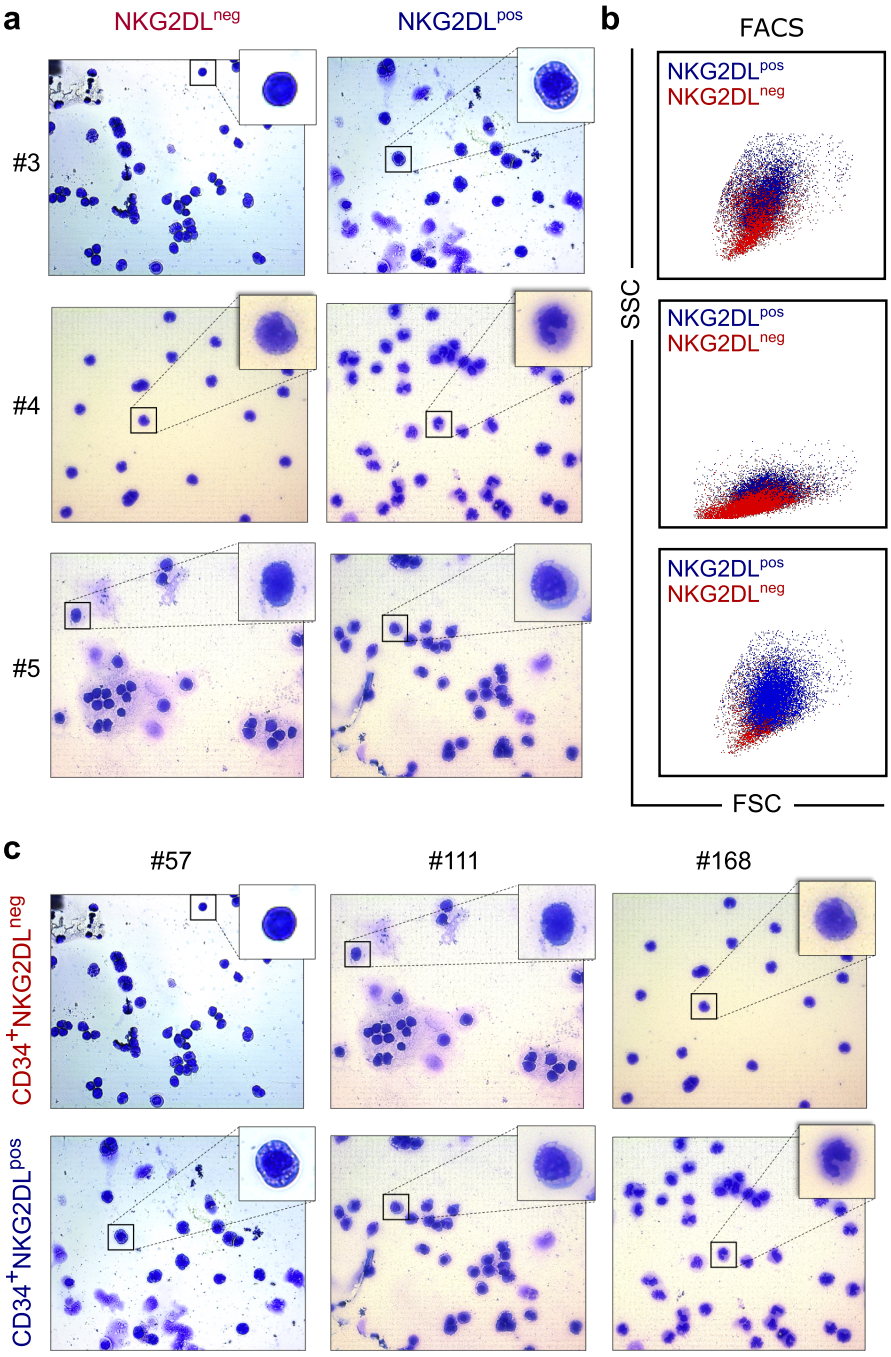

Extended Data Figure 2: May-Grünwald-Giemsa staining of NKG2DL^{neg} and corresponding NKG2DL^{pos} AML cells **(a-b)** and forward/sideward flow cytometry plots indicating NKG2DL^{neg} and NKG2DL^{pos} AML subpopulations **(c)**. Note that, irrespectively of CD34 expression, NKG2DL^{pos} AML cells show more mature morphology (with mostly larger cell size and enhanced granularity) when compared to corresponding NKG2DL^{neg} AML cells isolated from the same patient sample.

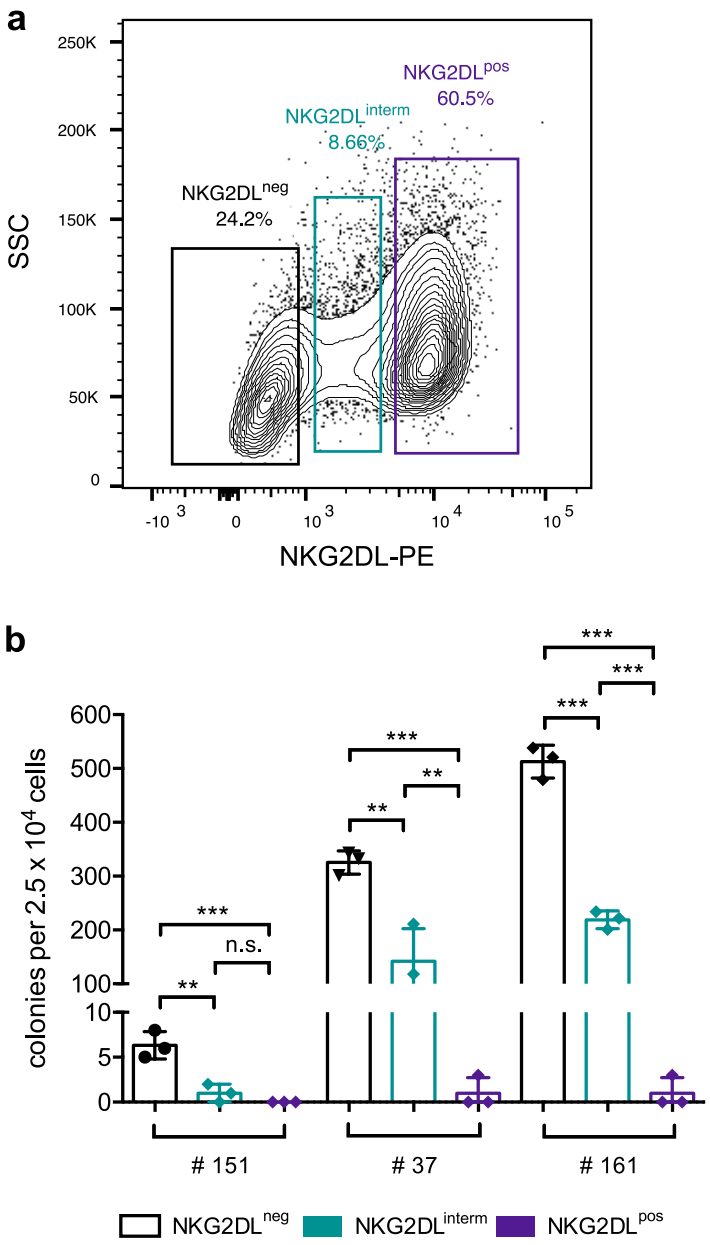

Extended Data Figure 3. Colony forming (CFU) assays of NKG2DL^{neg}, NKG2DL^{interm} and NKG2DL^{pos} AML cells isolated from the same patients. Shown are **(a)** representative flow cytometry plots indicating the sorting strategy (#37) and **(b)** summarized results from three AML cases as indicated (each dot or rhombus represents the result from technical triplicates performed with one subpopulation from one patient). Note that, in all analysed patients, the clonogenicity of NKG2DL^{interm} cells is higher than that of corresponding NKG2DL^{pos}, but lower than that of corresponding NKG2DL^{neg} AML cells. A one-way ANOVA was used for statistical analysis.

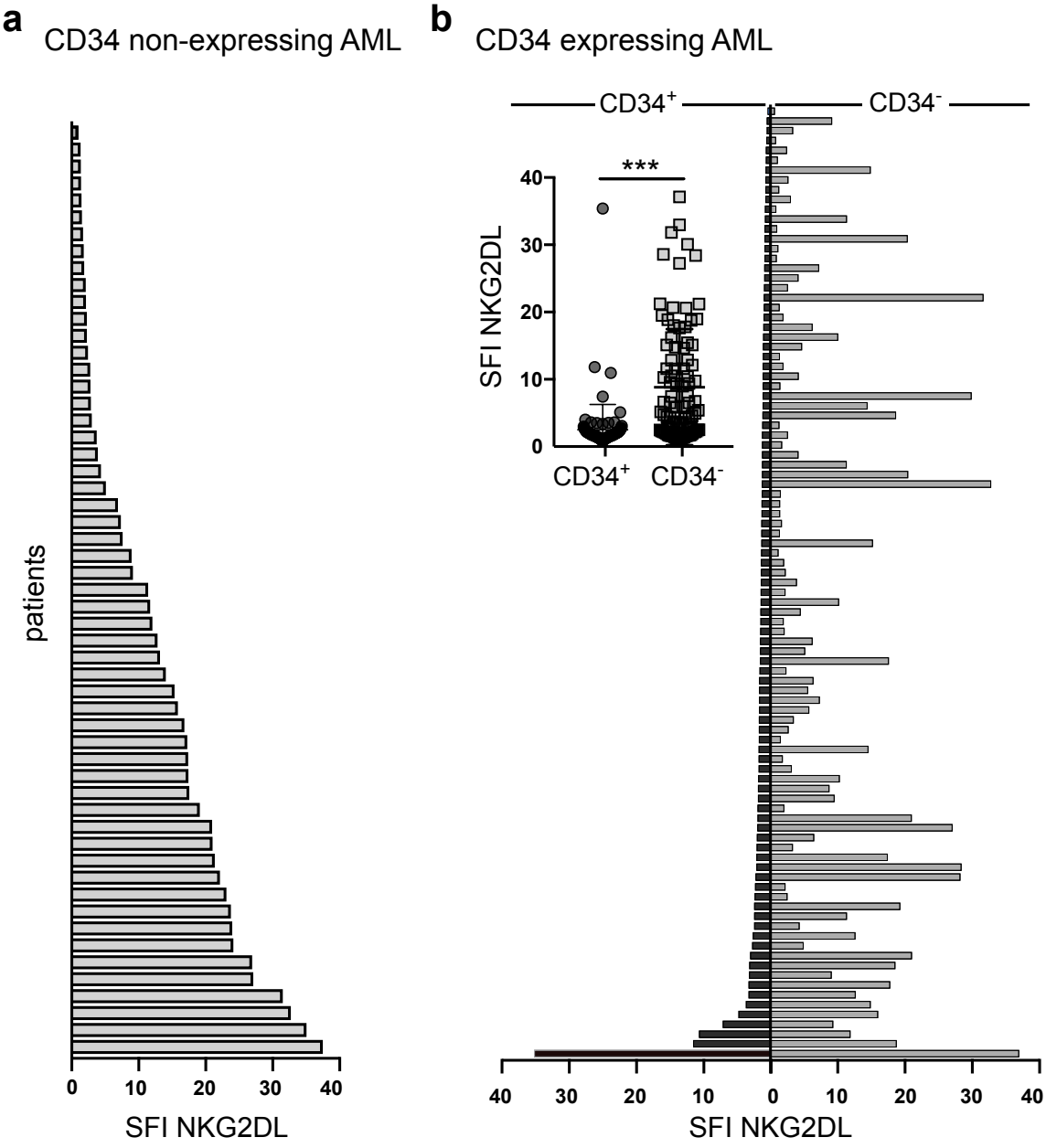

Extended Data Figure 4: Specific fluorescence intensity indices (SFI) quantitation of NKG2DL expression. n=55 CD34 non-expressing **(a)** and n=98 CD34 expressing **(b)** primary AML samples were quantified for NKG2DL expression using NKG2D-Fc chimeric protein staining. Shown are SFI of individual patients and subpopulations. A Mann-Whitney Test was used for statistical analysis.

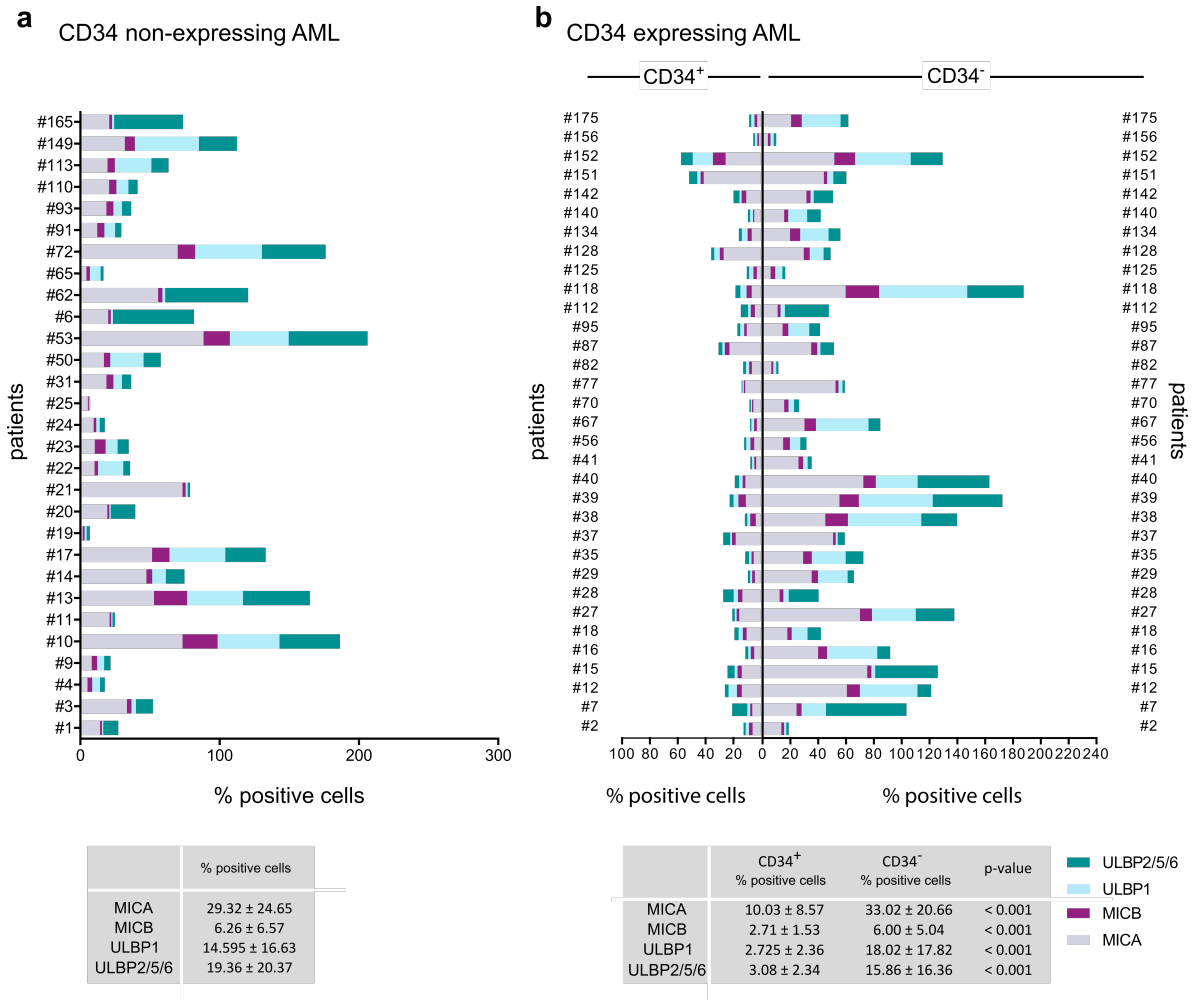

	% positive cells
MICA	29.32 ± 24.65
MICB	6.26 ± 6.57
ULBP1	14.595 ± 16.63
ULBP2/5/6	19.36 ± 20.37

	CD34+ % positive cells	CD34- % positive cells	p-value
MICA	10.03 ± 8.57	33.02 ± 20.66	< 0.001
MICB	2.71 ± 1.53	6.00 ± 5.04	< 0.001
ULBP1	2.725 ± 2.36	18.02 ± 17.82	< 0.001
ULBP2/5/6	3.08 ± 2.34	15.86 ± 16.36	< 0.001

Extended Data Figure 5: Single ligand staining. Primary AML samples (**a:** n=29 CD34 non-expressing AML; **b:** n=33 CD34 expressing AML) were stained with antibodies against human MICA, MICB, ULBP1 and ULBP2/5/6 and in **(b)** co-stained with anti-hCD34. Of note, in some cases the sum of % positive cells exceeds 100%, which reflects the fact that individual AML cells can express more than one NKG2DL. A Mann-Whitney Test was used for statistical analyses.

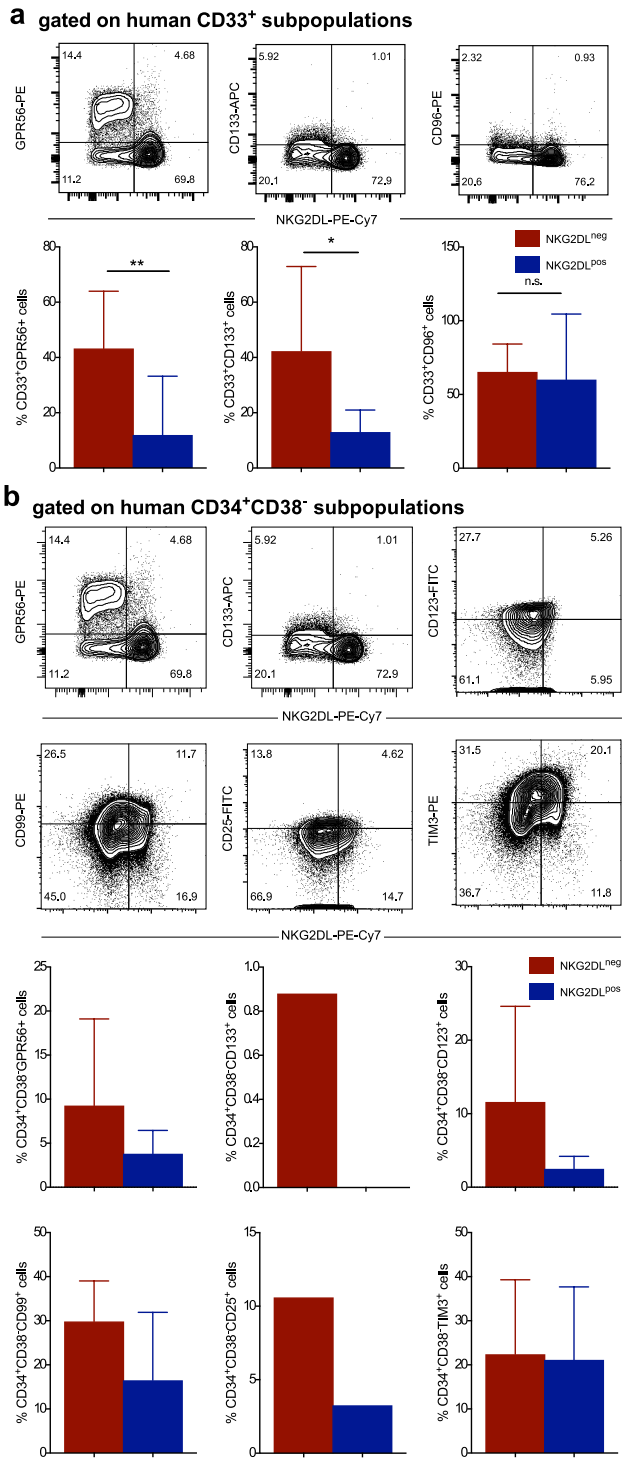

Extended Data Figure 6. Co-staining of NKG2DL with other LSC markers. (a) Flow cytometry analysis of NKG2DL and GPR56, CD133 or CD96 on leukaemic cells distinguished by pre-gating with anti-human CD33-BV421. Shown are exemplary results (upper panel) and summarized percentages of GPR56^{+}, CD133^{+} and CD96^{+} (lower panel) among NKG2DL^{neg} and NKG2DL^{pos} AML cells (#2, #9, #17, #18, #28, #31, #42, #151, #168; of note, 9/9 cases expressed GPR56, 8/9 CD133 and only 2/9 CD96). **(b)** Analysis of GPR56, CD133, CD123, CD99, CD25 or TIM3 among CD34^{+}CD38^{-}NKG2DL^{neg} and CD34^{+}CD38^{-}NKG2DL^{pos} subpopulations. Shown are exemplary results (upper panel) and summarized data from 3 AML cases (#35, 37, 128; lower panel); of note, another 7 AML (#29, 36, 38-39, 66, 95 , 101) were analysed but were not included in the analysis because all CD34^{+}CD38^{-} cells were found to lack NKG2DL expression. Statistical analyses were performed using a Mann-Whitney U-Test or a Student's t-test.

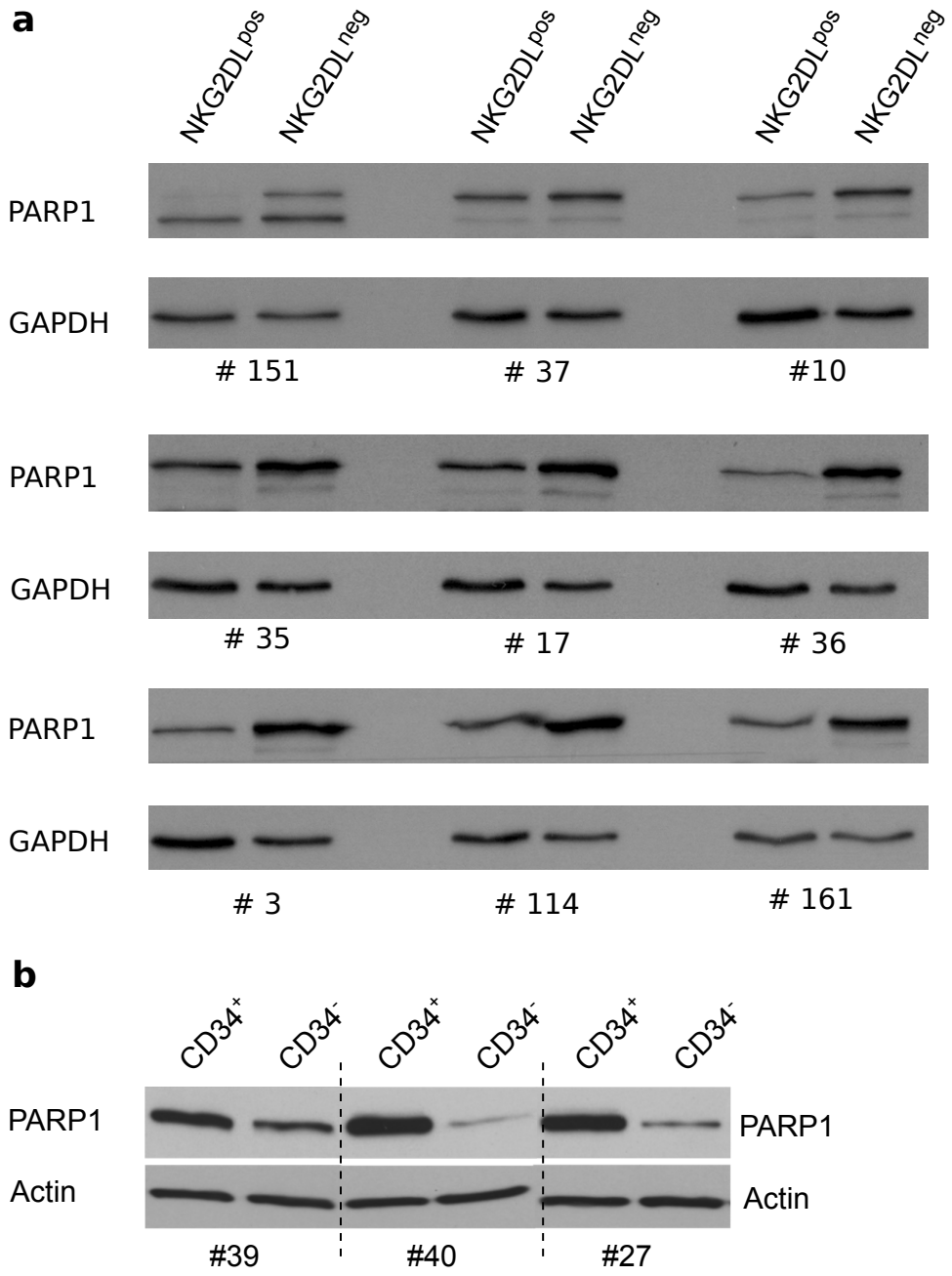

Extended Data Figure 7. PARP1 protein expression in NKG2DL^{neg} versus NKG2DL^{pos} and CD34^{+} versus CD34^{-} AML cells sorted from the same patient sample. Shown are immunoblot analyses on sorted cells; GAPDH and Actin were used as housekeeping controls. Quantifications are shown in Supplementary Table 6.

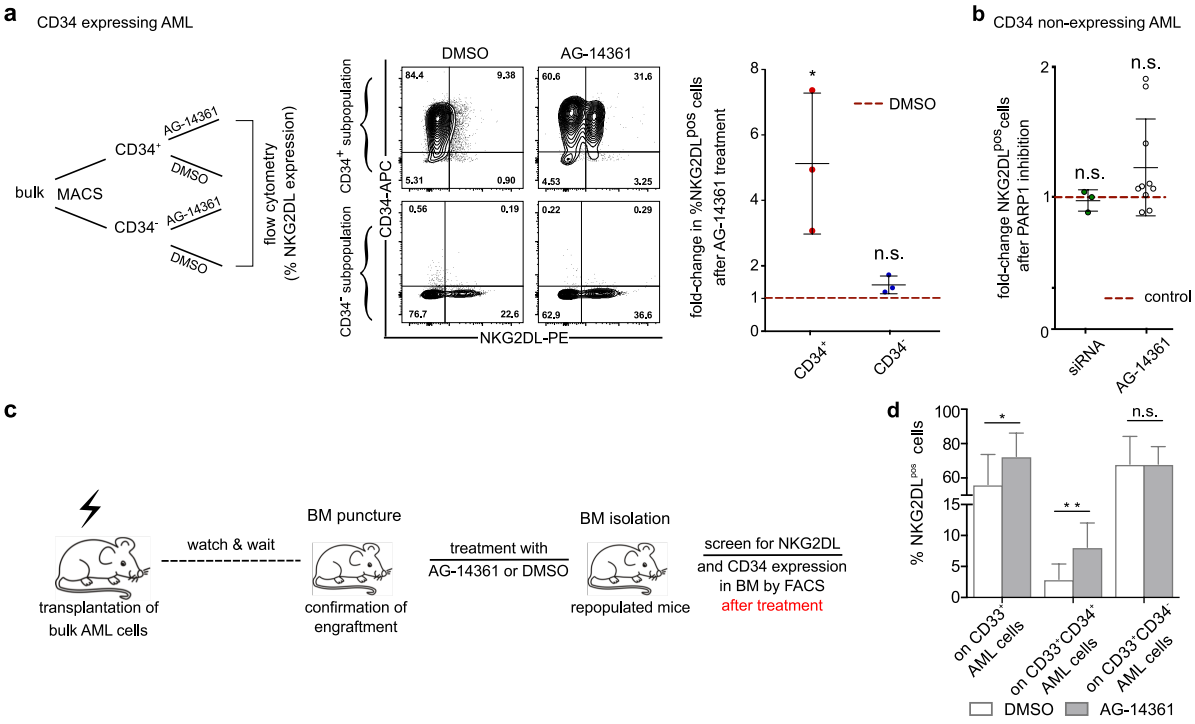

Extended Data Figure 8. Analysis of NKG2DL surface expression in CD34⁺ versus CD34⁻ AML cells after PARPi. *In vitro* treatment of **(a)** sorted CD34⁺ and corresponding CD34⁻ AML cells (**a:** schematic outline, left; representative results, middle; summarized fold changes of NKG2DL^{pos} cells in AG-14361, 20 µM, versus DMSO cultured cells; #2, 27, 35) and **(b)** CD34 non-expressing AML cells after PARP1 siRNA versus control siRNA (left; #9, #11, #19) and AG-14361 versus DMSO (right; #4, #9, #10, #11, #14, #19, #24, #75, #99, #110); shown are summarized fold changes in NKG2DL^{pos} AML cells in PARPi versus corresponding control conditions. **(c-d)** *In vivo* treatment with AG-14361 (**c:** schematic outline; **d:** summarized data on %NKG2DL^{pos} within CD33⁺, CD33⁺CD34⁺ and CD33⁺CD34⁻ AML subpopulations infiltrating murine BM after n=5 days of *in vivo* treatment with AG-14361 or DMSO as vehicle control (n=10 mice, #18, 27, 42).

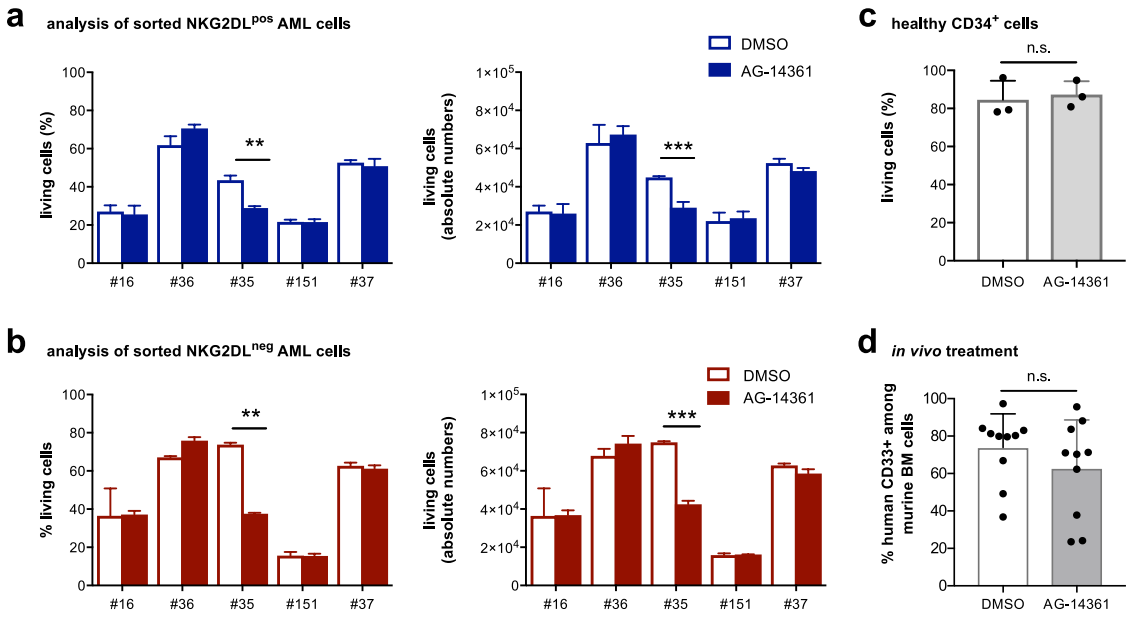

Extended Data Figure 9. Influence of AG-14361 on cell numbers and viability of AML cells and healthy cord blood derived CD34⁺ hematopoietic stem and progenitor cells (HSPCs). **(a)** Sorted NKG2DL^{pos} and **(b)** corresponding NKG2DL^{neg} AML cells (#16, #35, #36, #37, #151), as well as **(c)** healthy CD34⁺ cells from n=3 cord bloods (each analysed in technical triplicates of which mean values are shown) were treated with AG-14361 (20 µM) or control DMSO (0.2%) and afterwards analysed using DAPI for the percentage of living cells (left) and by cell counts for absolute cell numbers. In **(d)** we show the effect of *in vivo* treatment with AG-14361 (d1-5, 10-15 mg/kg/day) versus DMSO (d1-5, 20%) on leukemic infiltration (% human CD33⁺ AML among murine BM cells); note that no reduction in leukemic load is observed after 5 days of AG-14361 treatment.

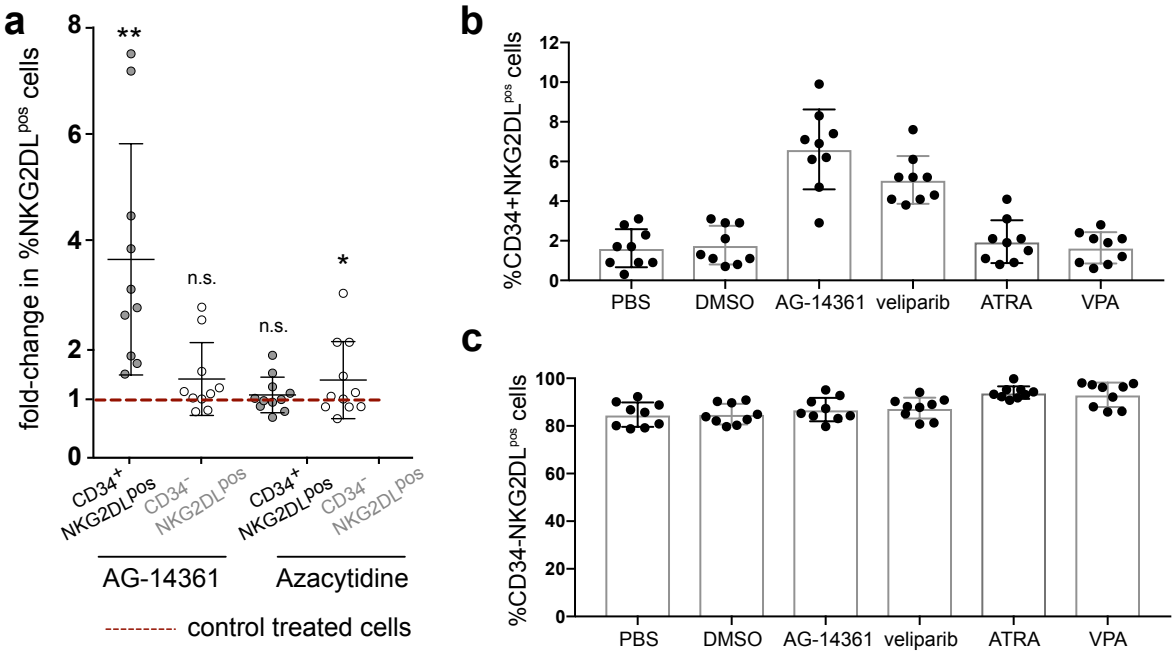

Extended Data Figure 10: Analysis of NKG2DL after treatment of bulk AML cells with AG-14361, 5-azacytidine Veliparib, ATRA and VPA. (a) Shown are quantified summarized fold-changes in $CD34^{+}NKG2DL^{pos}$ and $CD34^{-}NKG2DL^{pos}$ populations resulting after AG-14361 (20 μM) or 5-azacytidine (5 μM) (#2, #16-18, #27, #30, #35-36, #38, #41), and respectively of **(b)** $CD34^{+}NKG2DL^{pos}$ and **(c)** $CD34^{-}NKG2DL^{pos}$ cells emerging after all-trans retinoic acid (ATRA, 1 μM), valproic acid (VPA, 2 μM), veliparib (10 μM), AG-14361 (20 μM), DMSO (0.2%, vehicle control) or PBS (vehicle control) (#16, 36 and 38, all analysed in technical triplicates).

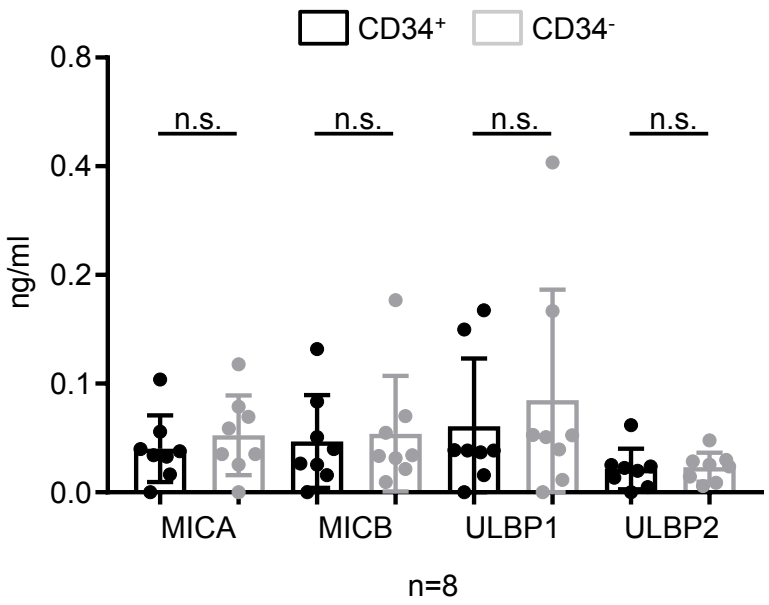

Extended Data Figure 11: Comparison of NKG2DL shedding in **CD34⁺ versus CD34⁻ AML subpopulations isolated from the same patients** (#16, 26, 29, 36, 40-41, 112, 118). Note that comparable levels of sNKG2DL were released from the two subpopulations. Mean results with SD are shown; a Mann-Whitney Test was performed for statistical analysis.

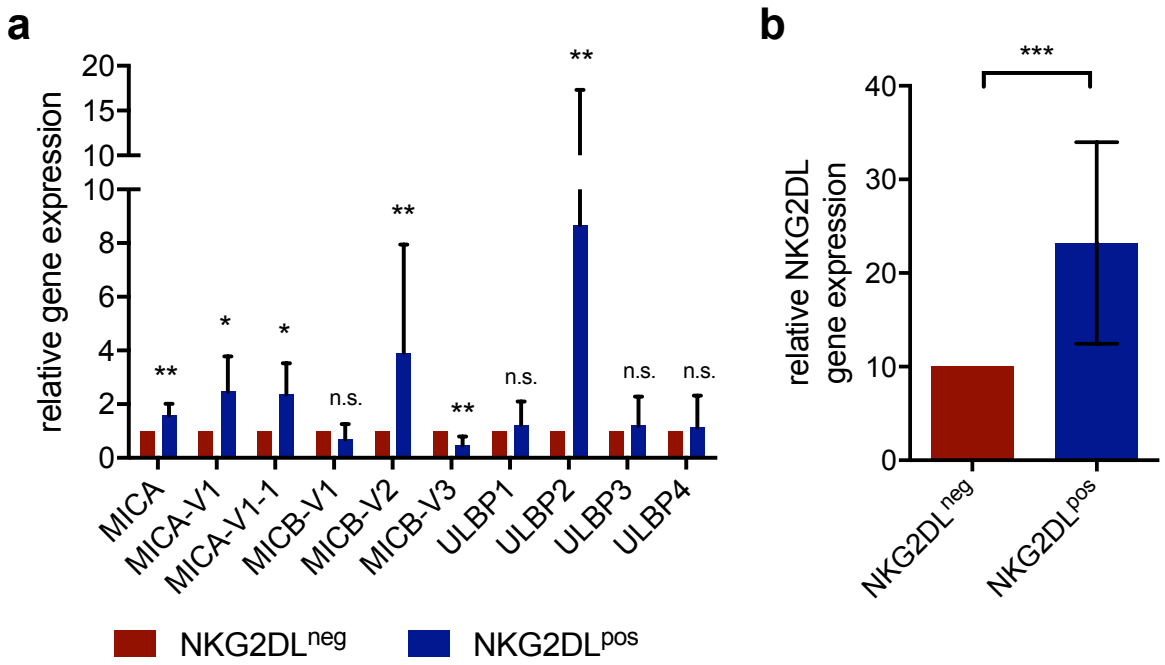

Extended Data Figure 12: Analysis of NKG2DL mRNA expression in NKG2DL^{neg} versus NKG2DL^{pos} AML cells sorted from n=10 AML cases (#3, 10, 17, 28, 35-37, 114, 151, 168). Shown are relative single **(a)** and summarized **(b)** mRNA values for NKG2DL (MICA and as variants thereof MICA-V1, MICA-V1-1, MICB and the variants thereof MICB-V1, MICB-V2, MICB-V3 and ULBP1-4). A Student's t-test was performed to test for statistical significance.

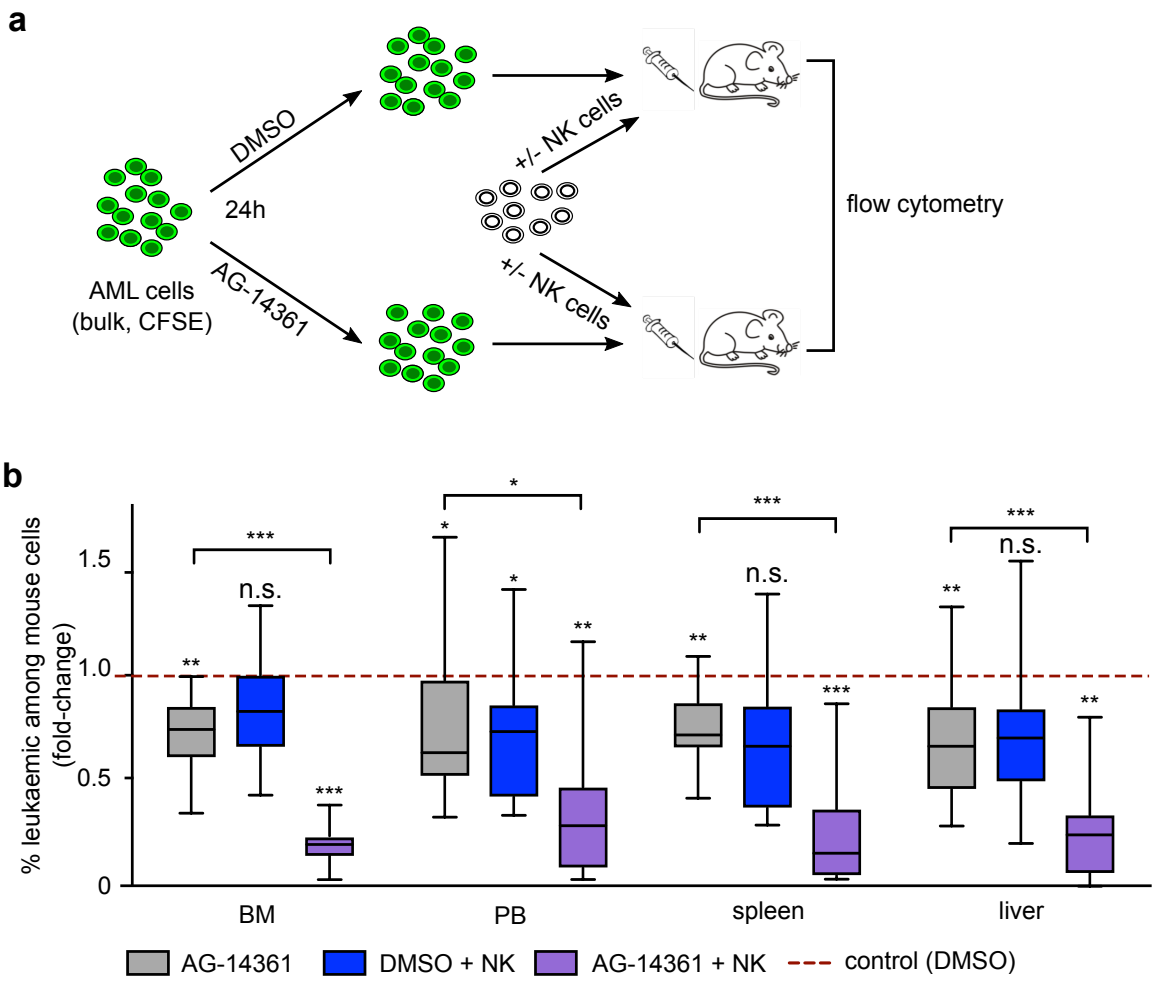

Extended Data Figure 13. NSG mouse xenotransplantation assays with human AML cells treated with AG-14361 prior to transplantation, and then co-transplanted with NK cells *in vivo*. AML cells (#27, #35, #41-43) pre-treated *in vitro* with AG-14361 (20uM) or DMSO (0.2%) were transplanted via tail vein injection into NSG mice ($1x10^6$ AML cells/mouse), which afterwards were co-transplanted or not with pNKC ($15x10^6$ pNKC/mouse) (n=3 mice per condition and patient). Mice were analyzed for the presence of leukaemic cells in bone marrow (BM), peripheral blood (PB), liver and spleen at 16h post-transplantation. Shown are **(a)** the experimental setup and **(b)** summarized results of n=5 independent biological experiments after normalization to "DMSO control without NK cells" control, which was set to 1. Statistical analysis was performed using Mann-Whitney-U Test.

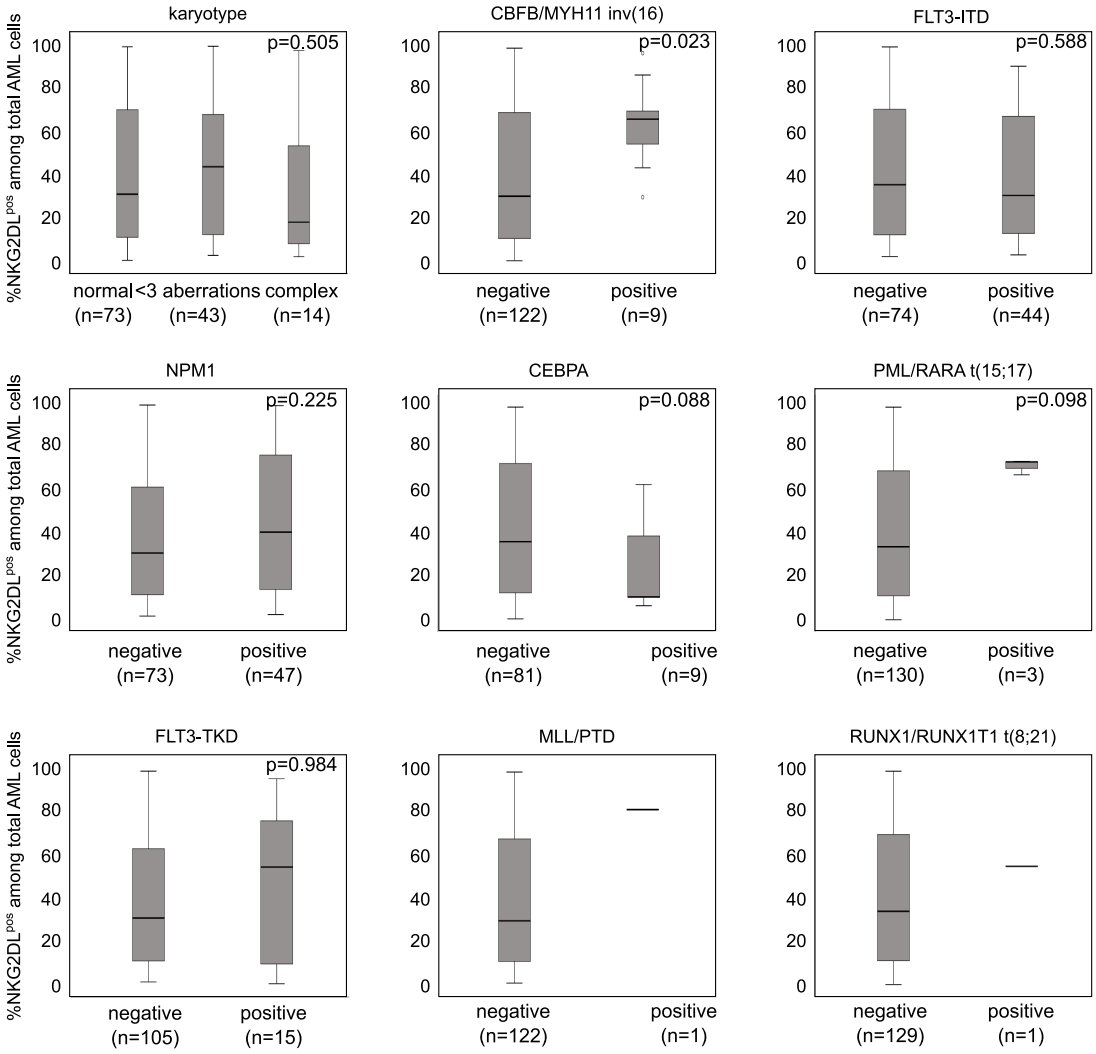

Extended Data Figure 14. Correlations between NKG2DL surface expression and molecular and genetic parameters. AML with inv(16), which belong to the favourable molecular ELN risk group, showed significantly higher NKG2DL expression when compared to cases without inv(16). All 175 patients analysed for NKG2DL expression with known genetic/molecular profile were included in the analyses (see respective numbers of positive/negative patients below each analysis; not depicted are patients with unknown result for the particular analysis). A Kruskal-Wallis Test (karyotype) or a Mann-Whitney-U-Test (all other) was used for statistical analysis.

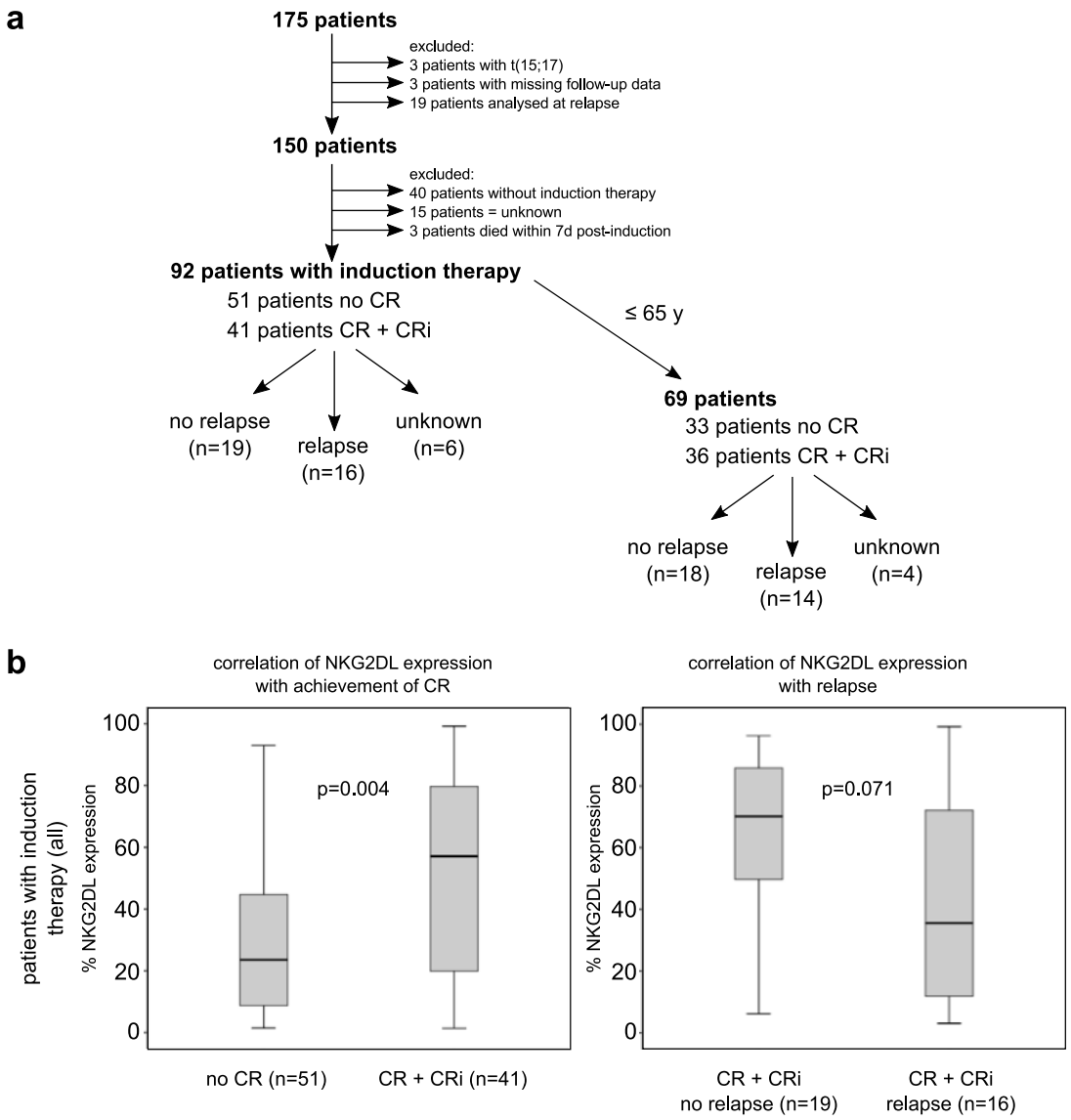

Extended Data Figure 15. Association between NKG2DL surface expression and achievement of complete remission (CR)/incomplete CR (CRi) and subsequent relapse. (a) Overview of included patients. **(b)** Left panel: Average percentage of NKG2DL^{pos} among total AML cells (at diagnosis) in patients that did not achieve CR/CRi after induction therapy (left) versus those that did (right). Right panel: Average percentage of NKG2DL^{pos} among total AML cells (at diagnosis) in patients that, after having achieved CR/CRi, subsequently maintained remission (left) versus those that showed relapse (right). Note that patients with initial high percentage of NKG2DLpos among total AML cells more often achieve, and by trend also sustain remission.

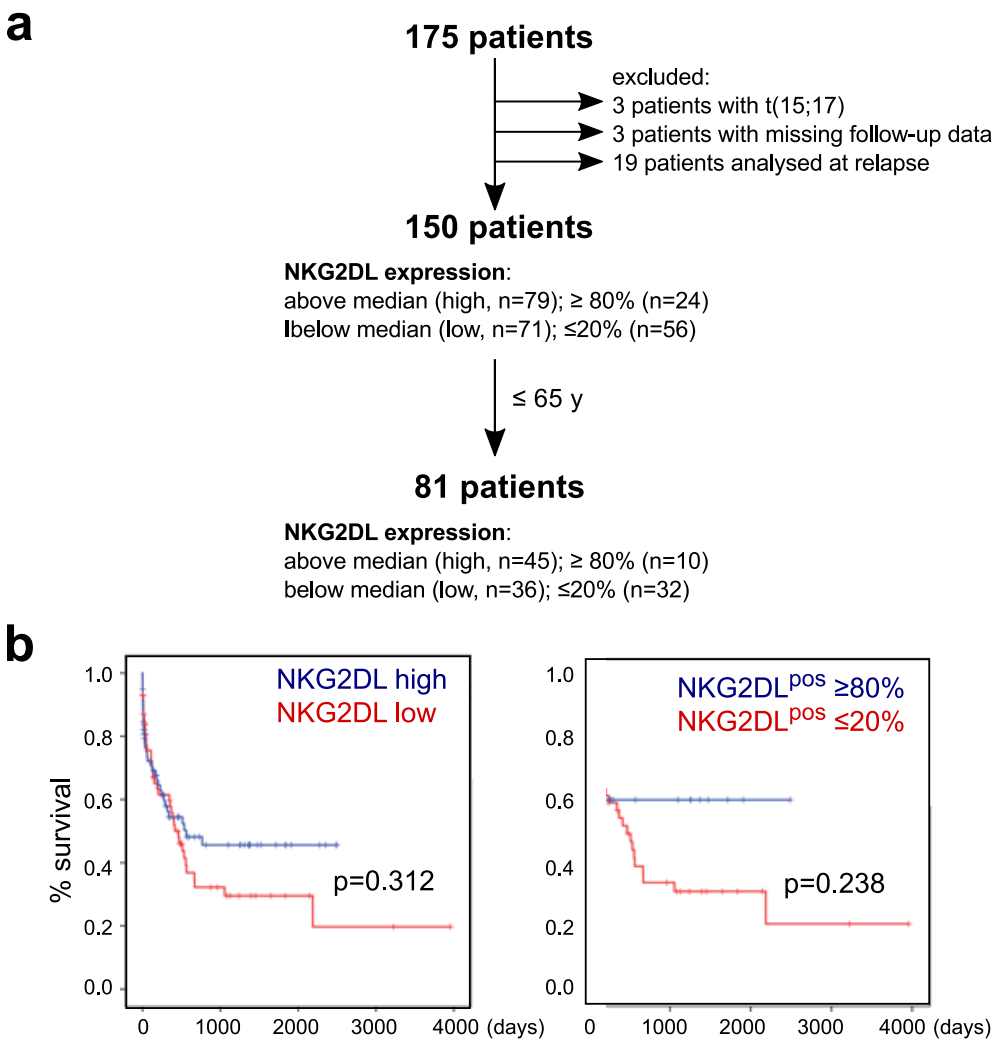

Extended Data Figure 16. Association of NKG2DL surface expression and overall survival in patients with AML (non-APL) (a) Overview of the analysed patients. **(b)** Correlation between percentages of NKG2DL^{pos} among total AML cells and overall survival. Compared were patients with high versus low NKG2DL expression (left panel), and patients with ≥80% NKG2DL^{pos} versus ≤20% NKG2DL^{pos} among total AML cells (right panel); note first show longer survival.

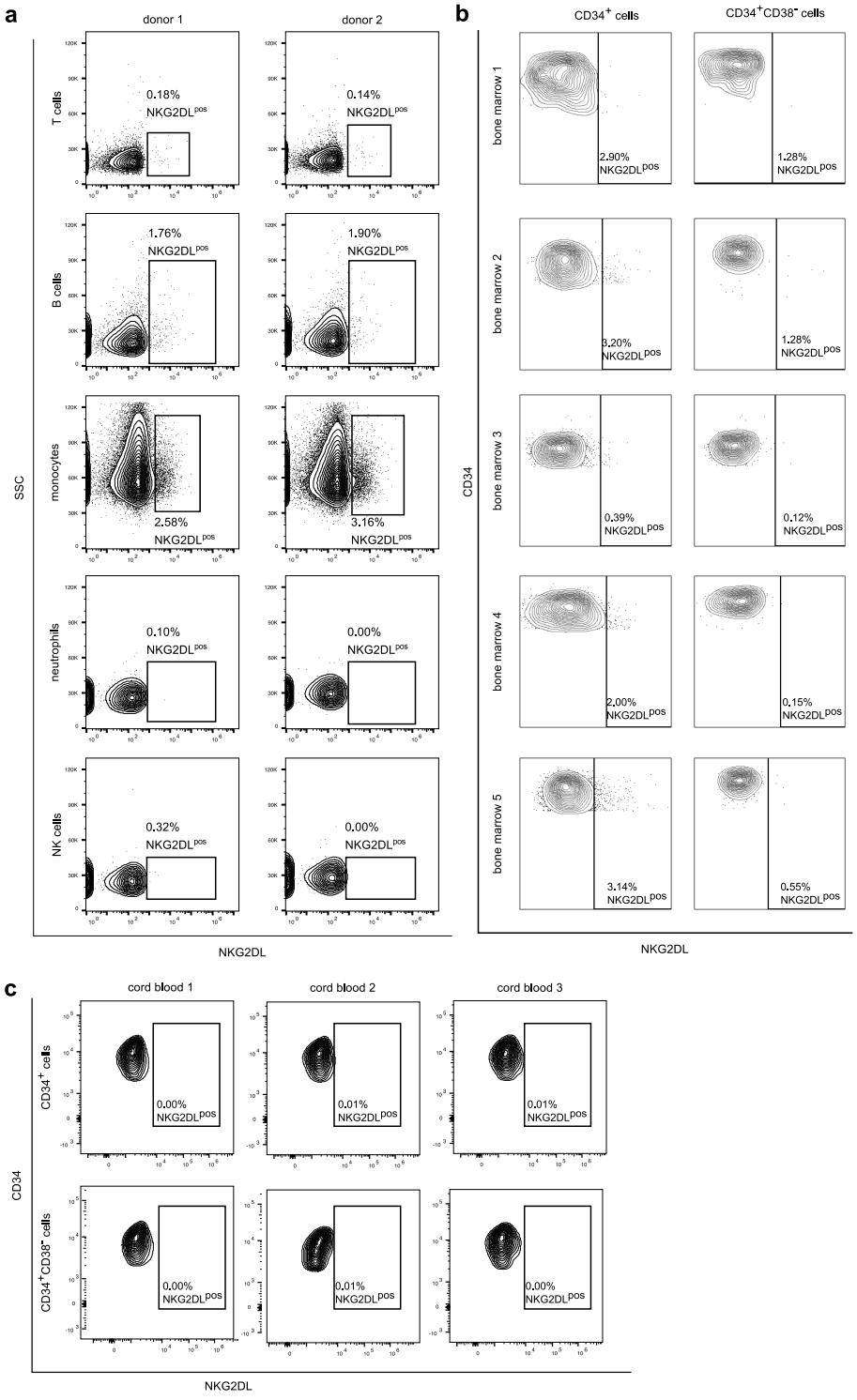

Extended Data Figure 17. Investigation of NKG2DL surface expression on healthy hematopoietic cells. Shown are flow cyometry data of **a)** mature blood cells derived from the PB of n=2 healthy donors, **(b)** BM $CD34^+$ and $CD34^+CD38^-$ cells derived from n=5 adult healthy donors and **(c)** $CD34^+$ and $CD34^+CD38^-$ cells derived from n=3 cord bloods.

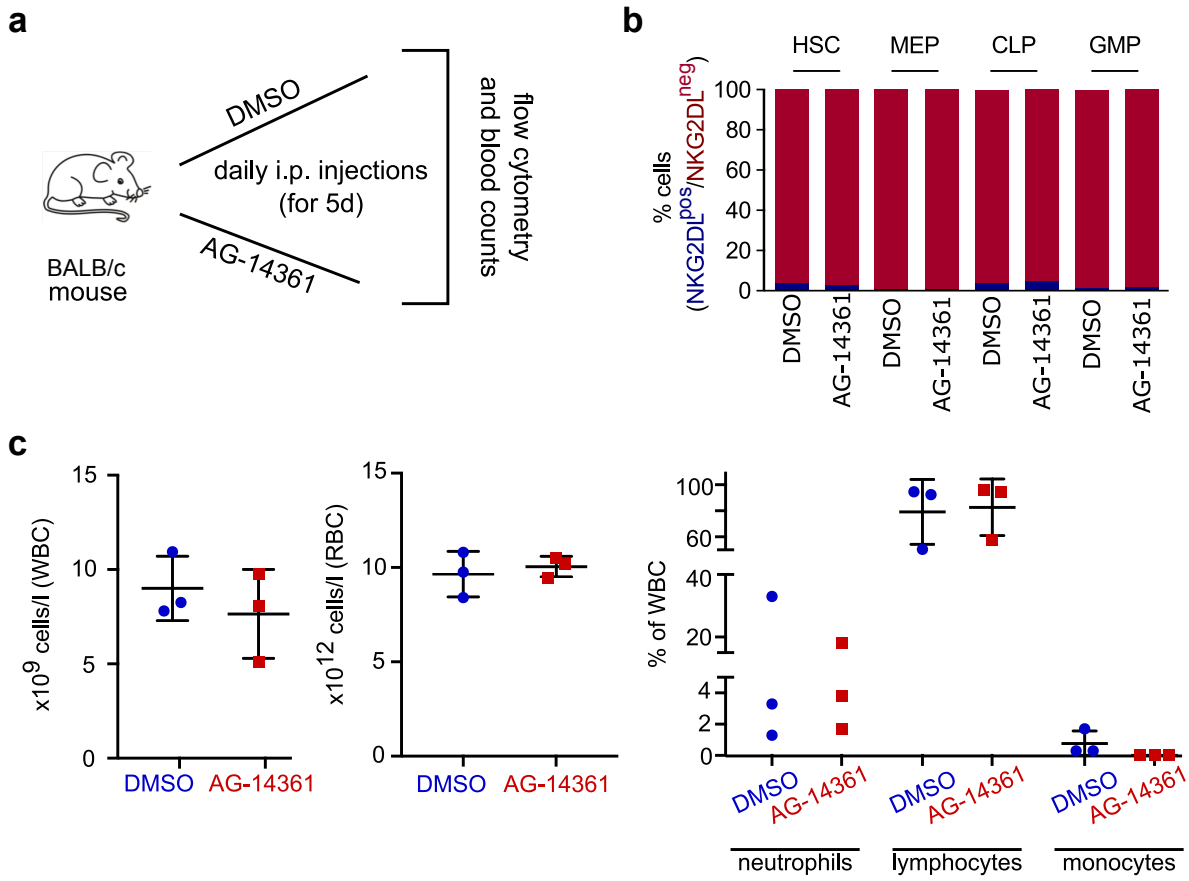

Extended Data Figure 18. Analysis of healthy hematopoietic cells after *in vivo* treatment with AG-14361 (a) Schematic overview of the experimental procedure. **(b)** % NKG2DL^{pos} vs. NKG2DL^{neg} cells among total murine hematopoietic cells of specific compartments after n=5 days of *in vivo* treatment with AG-14361 (20 µM) or DMSO vehicle control. **(c)** Absolute numbers of white (WBC, with distribution of neutrophils, lymphocytes and monocytes) and red blood cell counts (RBC) in healthy mice that received AG-14361 or DMSO (n=3 mice per group). Note that no differences were observed between the two treatment conditions.

Supplementary Data Figures

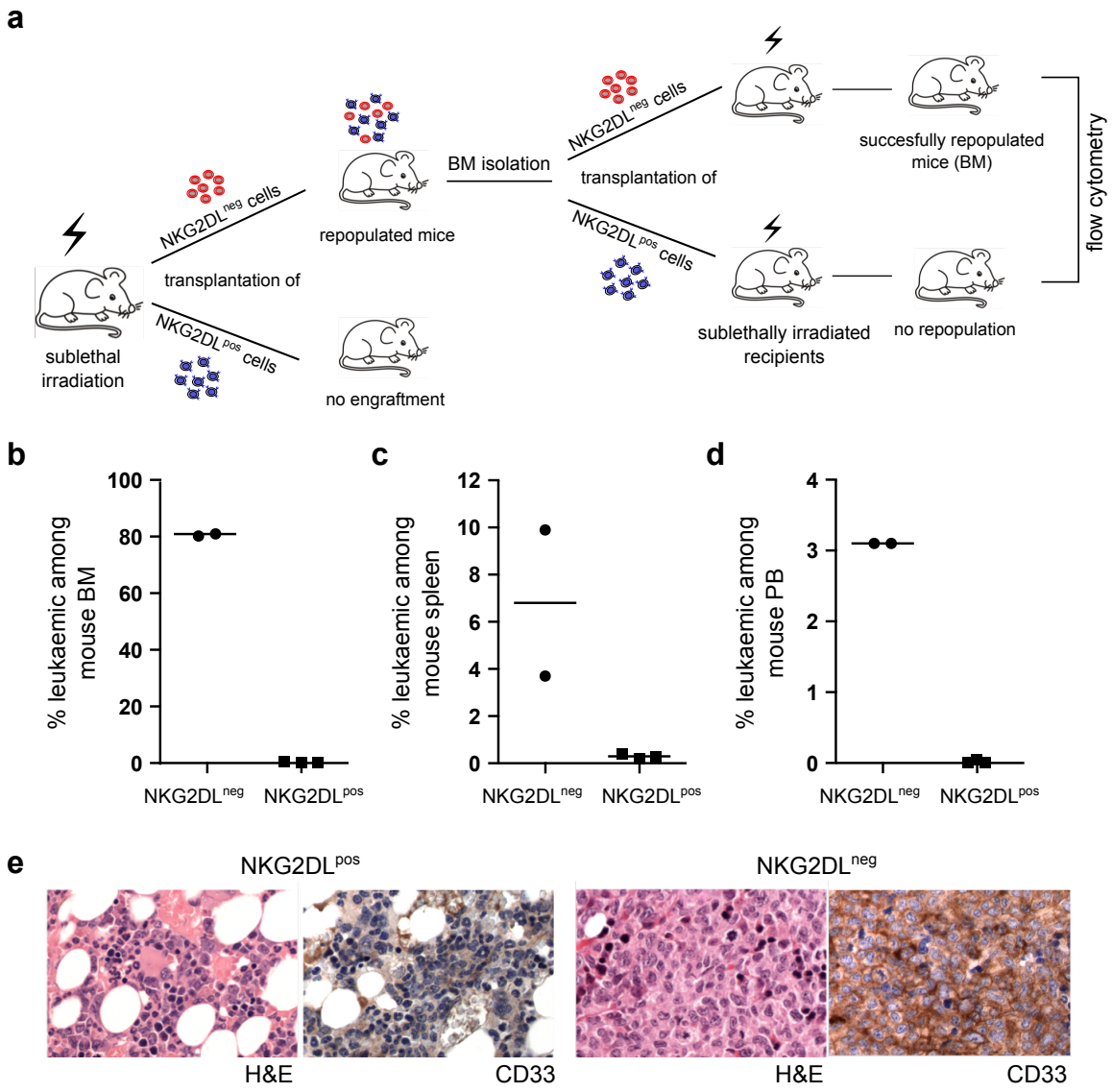

Supplementary Figure 1. Re-transplantation assays. (a) Schematic overview of the procedure. Briefly, engrafted human AML cells isolated from femora and tibiae of primarily transplanted mice were again sorted into NKG2DL^{pos} and NKG2DL^{neg} fractions and re-transplanted intravenously into pre-irradiated secondary recipients (n=2-3 mice per group). Engraftment in the latter was analyzed by **(b-d)** flow cytometric **(b**: BM, **c:** spleen; **d:** PB) and/or **(e)** histopathological analysis (H&E, anti-CD33, exemplary data, #1). Note that only NKG2DL^{neg} subpopulations engrafted and then gave rise to both NKG2DL^{neg} and NKG2DL^{pos} progeny.

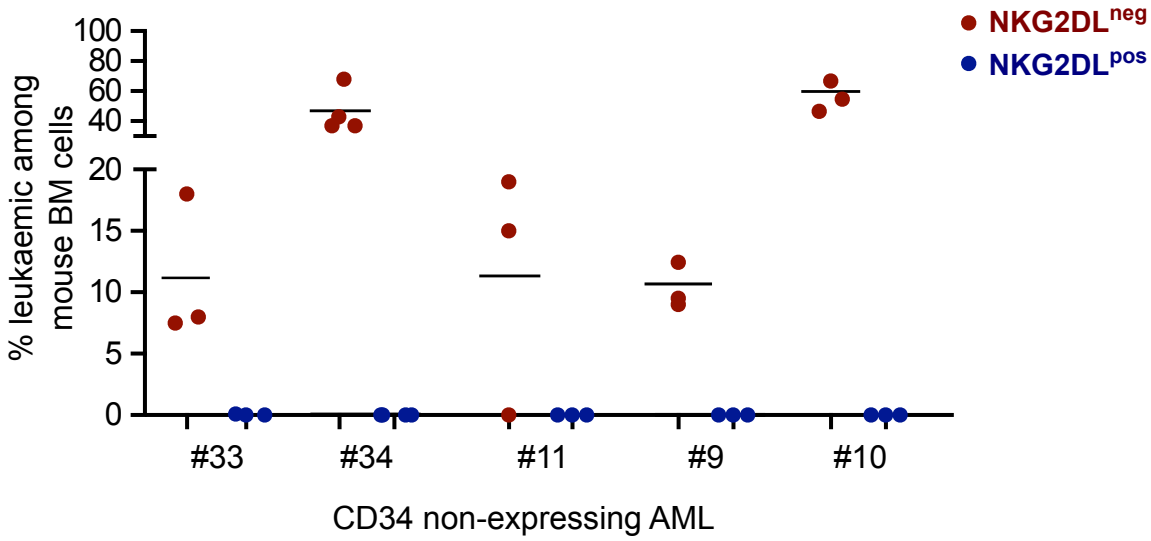

Supplementary Figure 2. Intrafemoral transplantation of NKG2DL^{neg} and NKG2DL^{pos} AML subpopulations isolated from the same AML samples. Sorted NKG2DL^{neg} and corresponding NKG2DL^{pos} cells (#33, #34, #11, #9, #10) were transplanted at equal numbers for each AML case intra-femorally in pre-irradiated NSG mice (n=3-4 mice per group) and engraftment assessed in murine BM 12 weeks after transplantation; shown are percentages of human leukaemic among murine BM cells in mice transplanted with NKG2DL^{neg} or NKG2DL^{pos} subpopulations for each AML case, each dot represents one mouse. Note that even upon transplantation directly into the BM, NKG2DL^{pos} cells failed to engraft, while corresponding NKG2DL^{neg} subpopulations successfully repopulated mice.

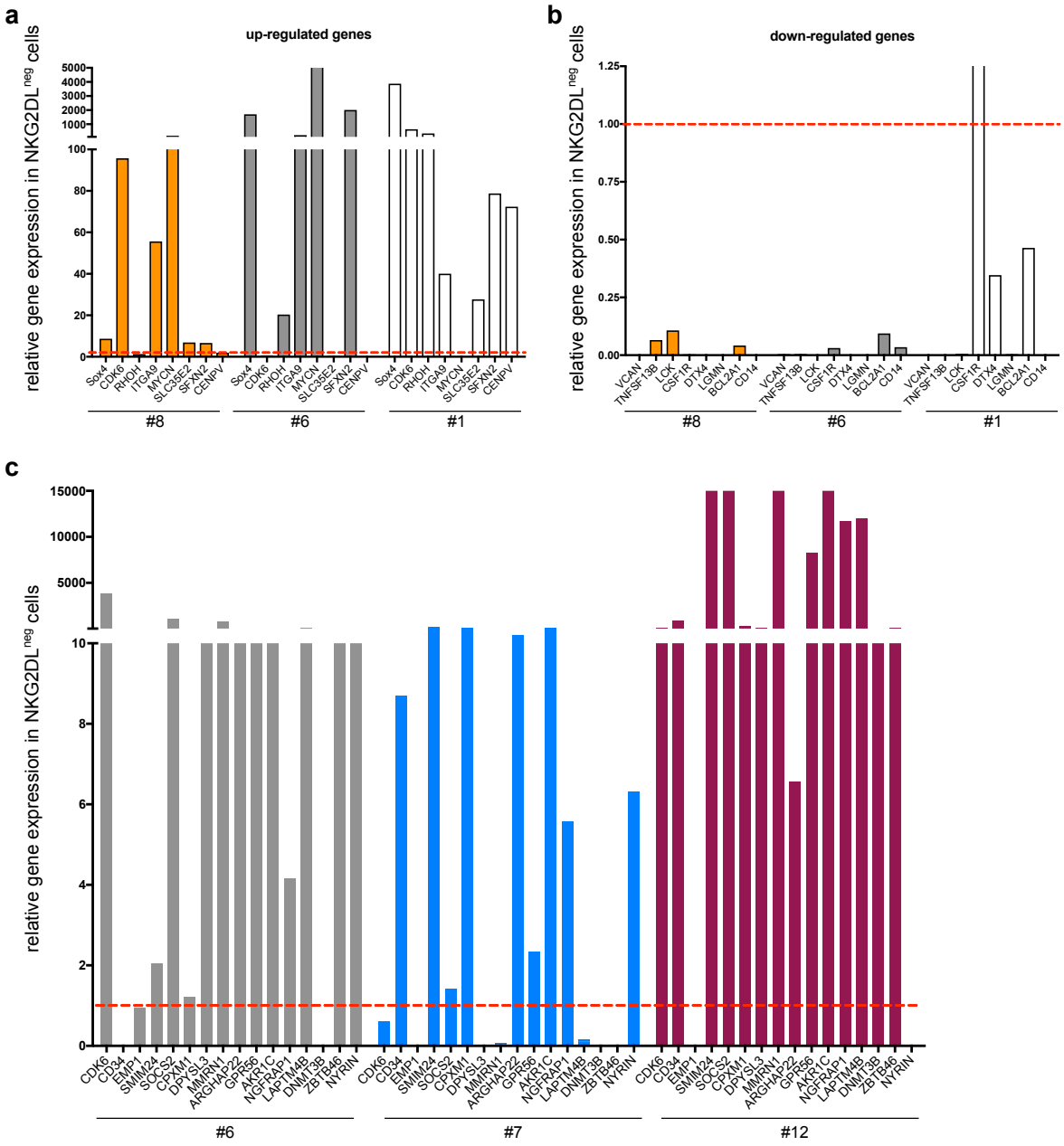

Supplementary Figure 3. Validation of differential gene expression by quantitative real-time PCR. (a-b) To validate differential expression in NKG2DL^{neg} versus NKG2DL^{pos} subpopulations, qRT-PCR analysis was performed on genes found up- **(a)** or down-regulated **(b)** in the microarray data set; shown are results of n=3 AML (#8, #6, #1), analysed each in technical triplicates; the dotted line represents gene expression in NKG2DL^{pos} subpoulations. **(c)** qRT-PCR verification of the 17 gene stemness score; analysis was performed in the same manner as in a-b.

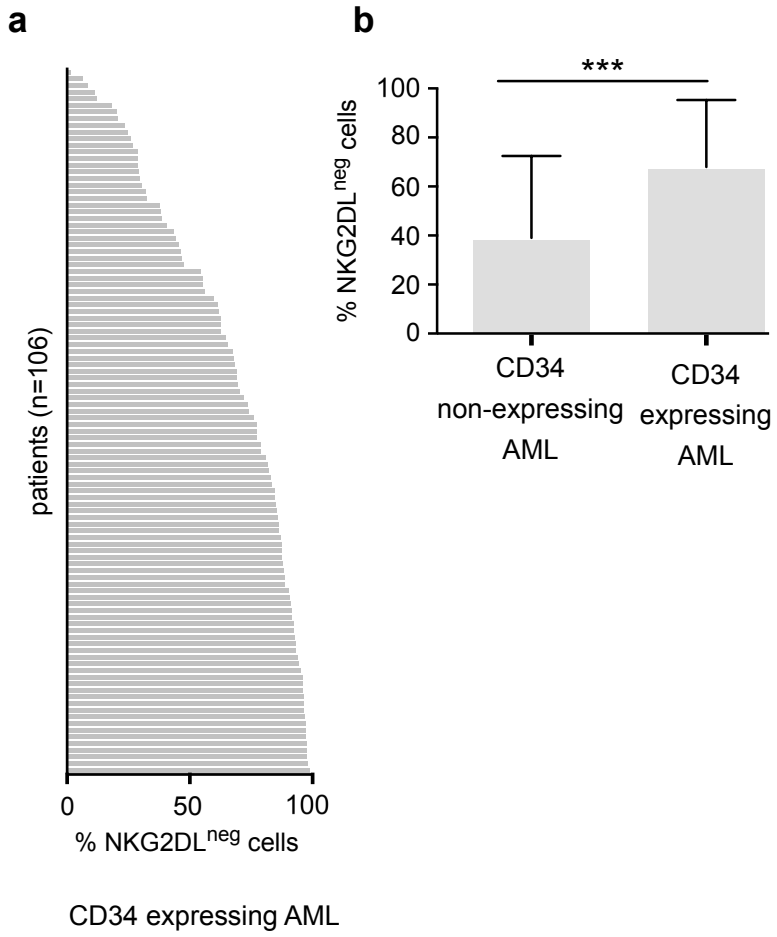

Supplementary Figure 4. NKG2DL expression in CD34 expressing compared to CD34 non-expressing AML cases. (a) Waterfall plot indicating percentages of NKG2DL^{neg} among total AML cells in individual patients. For comparison, see waterfall plot indicating percentages of NKG2DL^{neg} cells within total AML cells in CD34 expressing AML subtypes, Figure 3b. **(b)** Quantification of percentages of NKG2DL^{neg} cells among total AML cells in CD34 non-expressing versus CD34 expressing AML subtypes. A Mann-Whitney U Test was performed for statistical analysis.

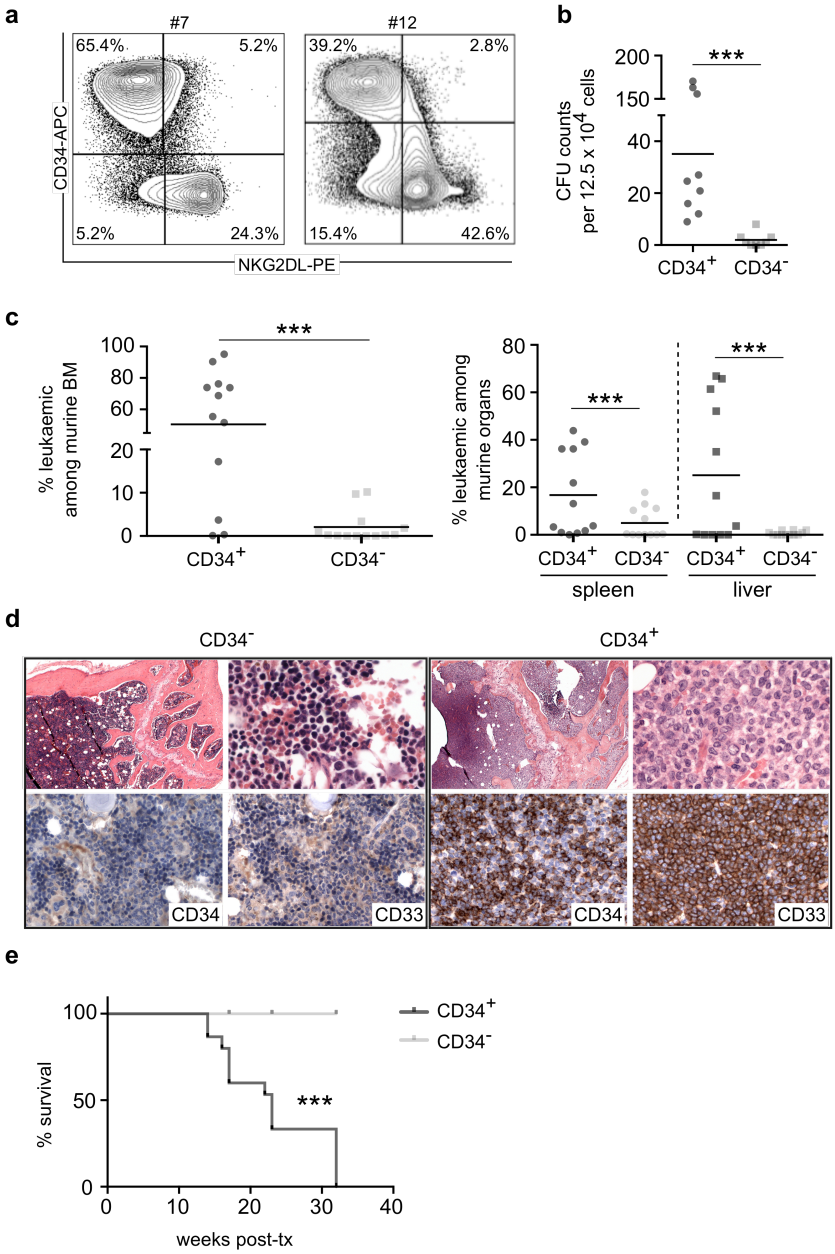

Supplementary Figure 5: Investigation of CD34⁺ and CD34⁻ AML subpopulations in CFU and *in vivo* transplantation assays. (a) Representative flow cytometry analysis and **(b-e)** analysis of sorted subpopulations in CFU (**b:** #7, #8, #12, technical triplicates) and *in vivo* xenotransplantation assays in NSG mice (#7, #8, #12; n=5 mice per AML and subpopulation) (**c:** summarized percentages of human leukaemic among murine BM, spleen and liver cells; **d:** histopathological BM analysis using antibodies that recognize human but not mouse CD33 and CD34, 630x; e: animal survival). A Mann-Whitney Test was performed for statistical analysis. Note that CD34⁺ subpopulations display lower percentages of NKG2DL^{pos} cells and have increased stemness properties.

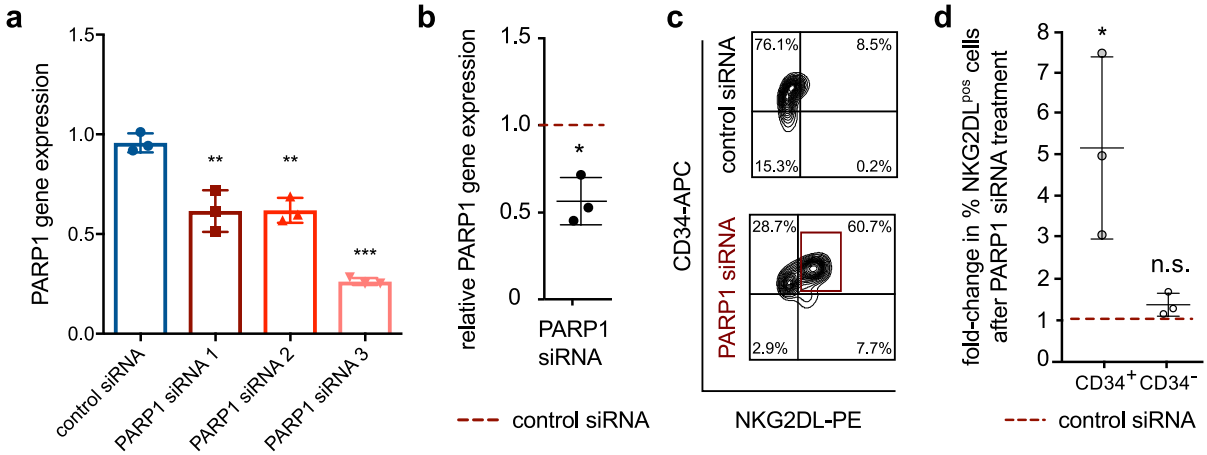

Supplementary Figure 6. PARP1 siRNA inhibition. AML cells were treated *in vitro* with individual PARP1 siRNAs, a scrambled mixture of these or scrambled non-coding PARP1 siRNAs as control. **(a-b)** qRT-PCR investigating PARP1 mRNA relative to GAPDH after 24h of treatment (**a:** single PARP1 siRNA versus scrambled control, representative data from #151, technical triplicates; **b:** scrambled mixture of PARP1 siRNAs versus scrambled control siRNAs; dots represents averages from technical triplicates performed on each patient #16, #35, #38). **(c-d)** Flow cytometry quantification of relative $CD34^{+}NKG2DL^{pos}$ and $CD34^{-}NKG2DL^{neg}$ cell percentages in cells treated with scrambled PARP1 siRNAs versus scrambled non-coding control siRNAs (**c**: representative results, #38; **d:** summarized data from #16, #35, #38, each dot represents a different patient and the result of technical triplicates performed in this patient).

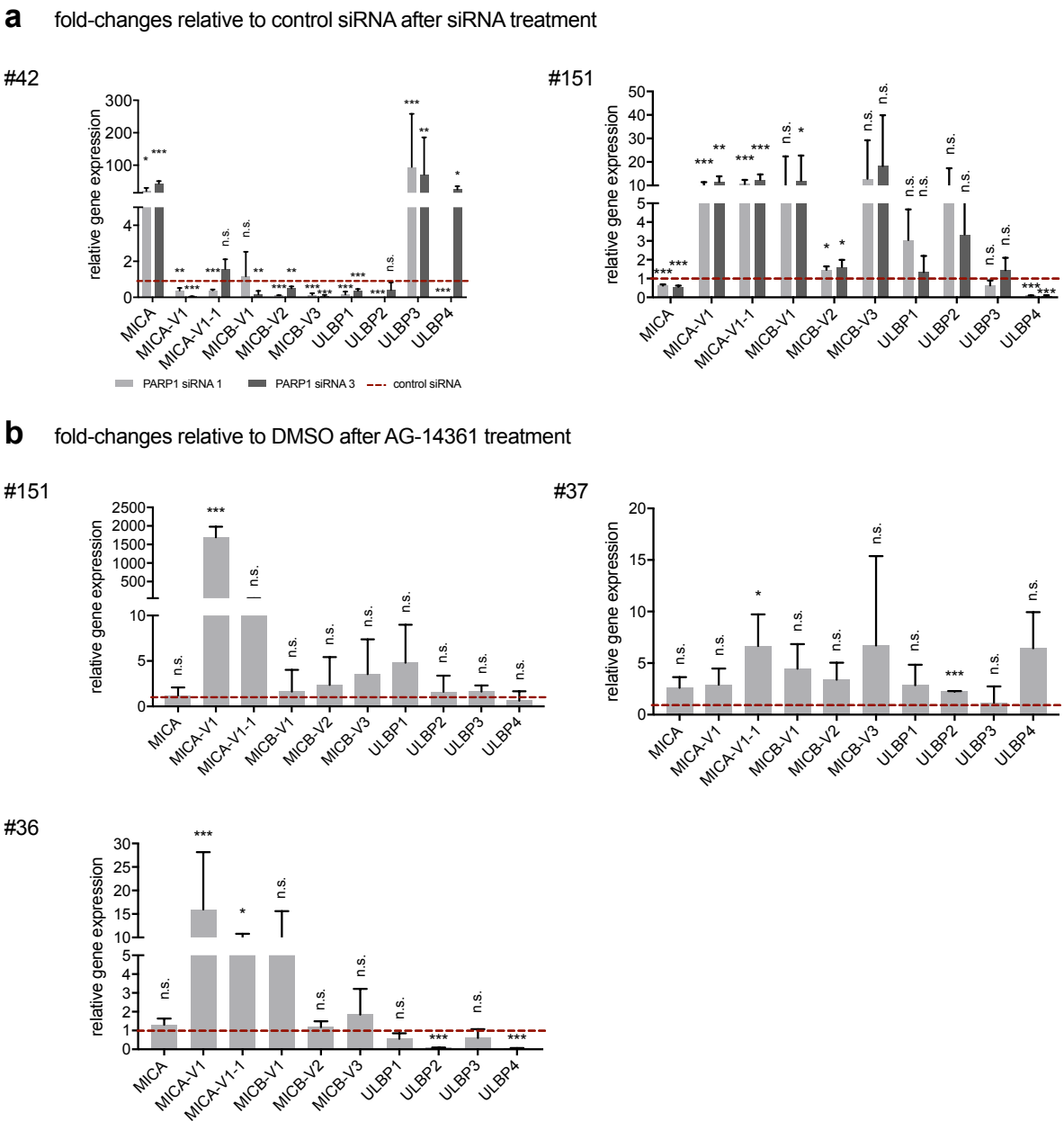

Supplementary Figure 7. NKG2DL expression after PARPi. Patient samples were treated with different PARP1 siRNAs **(a)** or AG-14361 **(b)** and corresponding controls (scrambled control siRNA or DMSO). qRT-PCR analysis of NKG2DL and their variants (MICA, MICA-V1, MICA-V1-1, MICB-V1, MICB-V2, MICB-V3, ULBP1-4) was performed 24h later. Shown are technical replicates from n=5 AML patients, as indicated. Note that heterogeneous NKG2DL are up-regulated upon PARPi in different AML cases. A Student's t-test was applied to test for statistical significance.

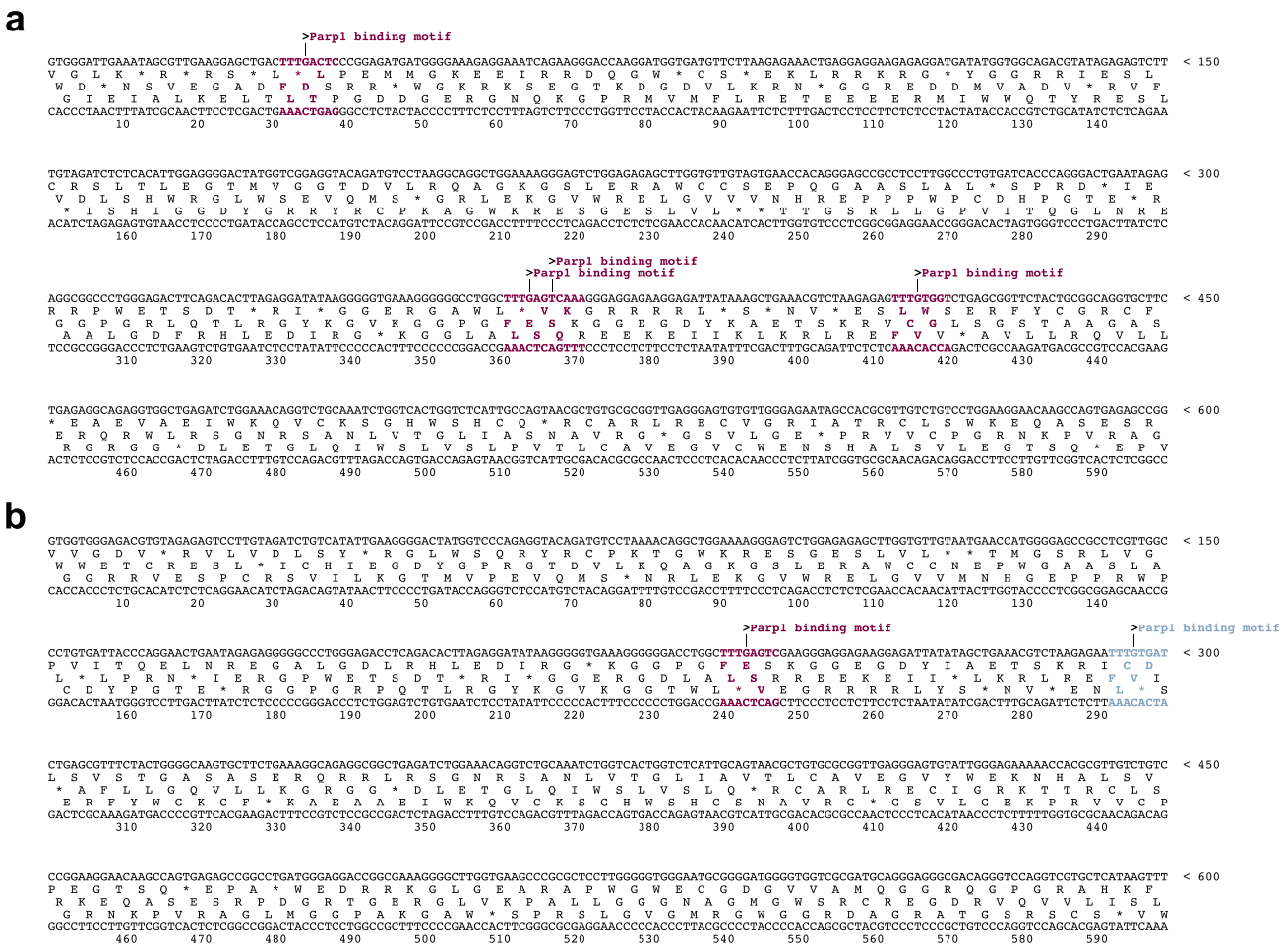

Supplementary Figure 8. ***In silico*** **analysis of PARP1 binding to the MICA (a) and the MICB promoter (b).** Shown are potential binding sites for PARP1.

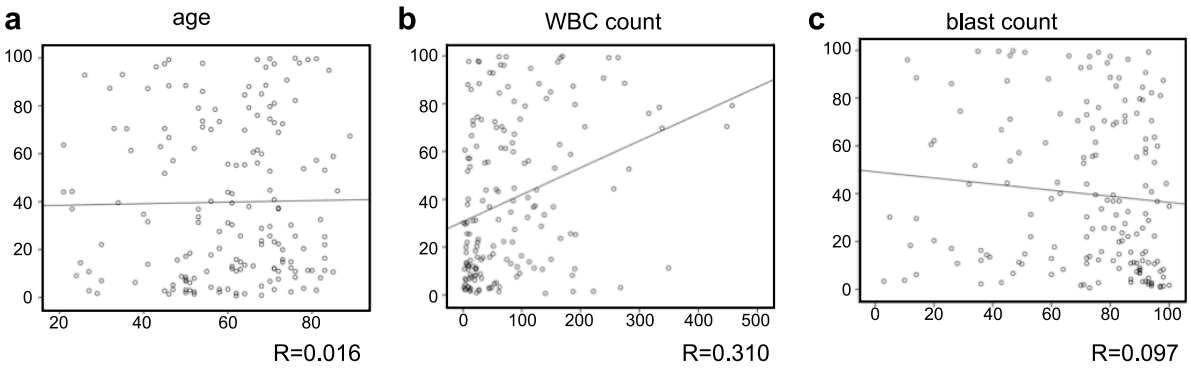

Supplementary Figure 9. Correlation of NKG2DL surface expression with (a) age, (b) white blood cell counts and (c) blast percentages at diagnosis. Shown are data from 169 out of 175 patients of our cohort; excluded were 3 patients with t(15;17) and another 3 patients in which clinical information was missing.